NATIONAL ADVISORY COMMITTEE FOR AERONAUTICS

TECHNICAL NOTE 4276

AN APPROXIMATE ANALYTICAL METHOD FOR STUDYING ENTRY INTO PLANETARY ATMOSPHERES

By Dean R. Chapman

Ames Aeronautical Laboratory
Moffett Field, Calif.

Washington
May, 1958

TABLE OF CONTENTS

NATIONAL ADVISORY COMMITTEE FOR AERONAUTICS

TECHNICAL NOTE 4276

AN APPROXIMATE ANALYTICAL METHOD FOR STUDYING ENTRY INTO PLANETARY ATMOSPHERES

By Dean R. Chapman

SUMMARY

The pair of motion equations for entry into an exponential planetary atmosphere is reduced to a single, ordinary, nonlinear differential equation of second order by disregarding two relatively small terms and by introducing a certain mathematical transformation. The reduced equation includes various terms, certain of which represent the gravity force, the centrifugal acceleration, and the lift force. If these particular terms are disregarded, the differential equation is linear and yields precisely the solution of Allen and Eggers applicable to ballistic entry at relatively steep angles of descent. If all the other terms in the basic equation are disregarded (corresponding to negligible vertical acceleration and negligible vertical component of drag force), the resulting truncated differential equation yields the solution of Sänger for equilibrium flight of glide vehicles with relatively large lift-drag ratios.

A number of solutions for lifting and nonlifting vehicles entering at various initial angles also have been obtained from the complete nonlinear equation. These solutions are universal in the sense that a single solution determines the motion and heating of a vehicle of arbitrary weight, dimensions, and shape entering an arbitrary planetary atmosphere. One solution is required for each lift-drag ratio. These solutions are used to study the deceleration, heating rate, and total heat absorbed for entry into Venus, Earth, Mars, and Jupiter. From the equations developed for heating rates, and from available information on human tolerance limits to acceleration stress, approximate conditions for minimizing the aerodynamic heating of a trimmed vehicle with constant lift-drag ratio are established for several types of manned entry. A brief study is included of the process of atmosphere braking for slowing a vehicle from near escape velocity to near satellite velocity.

INTRODUCTION

One of the many challenging problems connected with space flight occurs during the terminal phase of operation when a vehicle at near orbital velocity enters the earth's atmosphere or the atmosphere of another planet. Some important aspects of this problem are the possibly

severe decelerations for human occupants, the intense aerodynamic heating, and the tactical aspect of having satisfactory control over both the time and location of landing. The problem is made more interesting by interrelationships between these aspects which require, as always, keen understanding in order to make the best design compromises. For example, the lowest heating rates and smallest decelerations are obtained with very shallow entry paths, such as would be obtained by letting an orbit gradually decay; but the tactical aspects of fixing the time and location of a vehicle upon landing are most difficult with these very shallow re-entries. Also, the total heat absorbed during descent is greater for shallow entries than for steep ones. If descent at a steeper angle is induced by deflecting the orbit, such as by means of a retrorocket, then the total heat absorbed for laminar flow is reduced substantially, and the time and location aspects of recovery are improved, but both the deceleration and the heating rate are increased. In order to devise an efficient method of entry for a given application, it is highly desirable that a designer have available relatively simple equations for computing how each variable at his disposal affects the entry trajectory, the deceleration, and the aerodynamic heating.

For several special types of entry, analytical theories are available which provide simple equations showing clearly how each variable affects the motion and aerodynamic heating. In the case of ballistic-type entry without lift at sufficiently steep angles that the gravity and centrifugal forces can be disregarded, the analysis of Allen and Eggers (ref. 1) provides such equations. In the case of smoothly gliding-type entry at zero initial angle with a sufficiently large lift-drag ratio that the vertical acceleration and the vertical component of drag force can be disregarded, the analysis originally given by Sänger (refs. 2 and 3) would be applicable. In the case of skipping vehicles entering at sufficiently steep angles and with a sufficiently large lift-drag ratio that the gravity and centrifugal forces can be disregarded, the analysis of Eggers, Allen, and Neice (ref. 4) would apply. For more general types of entry, though, where the gravity force, centrifugal force, lift force, vertical acceleration, and vertical component of drag are all of importance, these existing analyses would not apply. Such would be the case, for example, for the entry of a satellite with a small lift-drag ratio, or for the entry of any orbiting vehicle starting with a very small initial angle. As a result, present understanding of the relatively shallow entries - which are of special interest to manned space flight - is based primarily on numerical calculations made with computing machines in connection with relatively specific vehicles (see, e.g., refs. 5, 6, and 7).

The objective of the present report is to develop an approximate analytical solution to the motion equations which is usable for engineering calculations and which is applicable to an arbitrary planetary atmosphere, to a lifting or nonlifting vehicle, and to entries along either shallow or steep descents. Such a solution could be applied to a fairly broad variety of vehicles, such as skip, glide, satellite, ballistic, or

escape vehicles undergoing the process of atmosphere braking. An additional objective is to develop a method applicable to composite types of entry, such as entering initially with zero lift, and then suddenly changing the lift and/or drag at any number of points during the descent.

During the preparation of this report an interesting report by Gazley (ref. 8) became available in which he considers the entry of a nonlifting satellite into a planetary atmosphere from a decaying orbit. He obtains an approximate analytic solution by making an arbitrary assumption about the relationship between velocity and angle of descent which is not made in the present report. As a result, his end equations for this particular type of entry are quantitatively different, though qualitatively similar to those of the present report, as discussed briefly later.

NOTATION

a resultant deceleration

A reference area for drag and lift, sq ft

C dimensional constant in heat-transfer equations (17,000 Btu $ft^{-3/2}sec^{-1}$ for numerical calculations of this report)

C_D drag coefficient, $\frac{D}{\frac{1}{2}\rho_\infty V^2 A}$

C_L lift coefficient, $\frac{L}{\frac{1}{2}\rho_\infty V^2 A}$

D drag force, lb

g gravitational acceleration, ft sec^{-2}

g_c gravitational conversion constant, 32.2 ft sec^{-2}

k_1 ratio of local heat flux to that at a stagnation point, $\frac{q}{q_s}$

k_2 average value of heat flux relative to stagnation point value, $\frac{1}{S}\int \frac{q}{q_s}\,dS$

l characteristic length of vehicle, ft

L lift force, lb

m mass of vehicle, slugs

$\overline{M}$ mean molecular weight of planetary atmosphere (consistent units with gas constant and g)

Pr Prandtl number

q convective heat-transfer rate per unit area, Btu/sq ft sec

Q total convective heat absorbed, $\iint q \, dt \, dS$, Btu

$\overline{q}$ dimensionless function proportional to heating rate ($\overline{u}^{5/2}\sqrt{Z}$ for laminar flow)

$\overline{Q}$ dimensionless function proportional to total heat absorbed $\left(\int \overline{u}^{3/2} Z^{-1/2} \cos^{-2}\varphi \, d\overline{u}\right)$

r distance from planet center, ft

R universal gas constant, or radius of curvature of vehicle surface in feet

Re Reynolds number, $\frac{\rho_\infty V l}{\mu_\infty}$

s circumferential distance traveled, ft

S surface area wetted by boundary layer, sq ft

t time, sec

T temperature (various units employed)

u circumferential velocity component normal to radius vector, ft/sec

u_c circular orbital velocity, $\sqrt{gr}$, ft/sec

$\overline{u}$ ratio, $\frac{u}{u_c}$

$\overline{u}_1$ upper limit for range and total heat absorbed (see eqs. (28) and (39b))

y altitude, ft

v vertical velocity component (along direction of radius vector), ft/sec

V resultant velocity, $\sqrt{u^2 + v^2}$

W weight of vehicle at earth's surface, mg_c, lb

Z dimensionless function of $\bar{u}$ determined by equation (21) and appropriate boundary conditions

β atmospheric density decay parameter, ft^{-1}

$\bar{\gamma}$ ratio of specific heats behind bow wave

θ angle in polar coordinates

μ coefficient of viscosity, slug $ft^{-1}sec^{-1}$

ρ density, slug ft^{-3}

φ flight-path angle relative to local horizontal direction; positive for climbing flight, negative for descent

Subscripts

o sea level

∞ free stream

s stagnation point

i initial condition

b break where $\frac{W}{C_D A}$ is discontinuously changed

$\oplus$ relative to earth

Superscripts

$'$ differentiation with respect to $\bar{u}$

$-$ mean value for exponential approximation to atmosphere density-altitude relationship, or dimensionless quantity

ANALYSIS

Assumptions and Approximations

The problem analyzed concerns that portion of the descent of a vehicle into a planetary atmosphere wherein the decelerations and the convective aerodynamic heating are dominant. Three assumptions made at the outset are:

(i) Atmosphere and planet are spherically symmetric.

(ii) Atmosphere density ρ_∞ varies exponentially with altitude.

(iii) Peripheral velocity of planet is negligible compared to the velocity of the entering vehicle.

Assumption (i) is reasonable for those planets which have only small equatorial bulges (such as Venus, Earth, and Mars), inasmuch as the severe aerodynamic heating and decelerations occur over a length of flight path which is small compared to the planet's mean radius (the order of one tenth the planet radius for nonlifting bodies). The assumption of spherical symmetry, however, would not be as reasonable for planets with relatively large equatorial bulges, such as Jupiter and Saturn. As noted later, this assumption of spherical symmetry can introduce some inaccuracy if the descent is nearly along a line of longitude and if the vehicle also happens to have a relatively large lift-drag ratio. For large lift-drag ratios the important deceleration and heating portions of the descent can be prolonged over a distance comparable to the planet's radius; hence, the nonspherical nature of the atmosphere could be important in such cases.

Assumption (ii), of an exponential atmosphere, is based upon the simple kinetic theory of an isothermal gas in a uniform gravitational field. This theory yields the well-known exponential approximation for atmospheres (see ref. 9, ch. III, for example)

$$\frac{\rho_\infty}{\rho_O} = e^{-\beta y} \tag{1}$$

where

$$\beta = \frac{\overline{M} g}{R \overline{T}} \tag{2}$$

and where $\overline{M}$ is the mean molecular weight of the planet's atmosphere, $\overline{T}$ the mean temperature, R the universal gas constant, and g the local acceleration due to gravity. It is to be noted that ρ_O represents the

intercept of the straight line which best fits a curve of $\log \rho$ versus altitude, and is not the same as the true sea level density ρ_0. From data such as presented in references 10 and 11, approximate mean values of several quantities of interest for various planets are as follows (the subscript $\oplus$ designates a value relative to the earth):

Planet	$r_\oplus$	$g_\oplus$	Gases	$\mu_\oplus$	$\overline{M}$, gm mol^{-1}	$\overline{T}$, $^\circ$K	β^{-1}, ft	$\sqrt{(\beta r)_\oplus}$
Venus	0.97	0.87	CO_2,N_2	0.8	40	270	2×10^4	1.0
Earth	1.0	1.0	N_2,O_2	1.0	29	240	2.35×10^4	1.0
Mars	.53	.38	N_2,CO_2	1.0	30	220	6×10^4	.47
Jupiter	11.0	2.63	H_2,CH_4	.5	3	170	6×10^4	2.0

The exponential approximation for the earth (with $\overline{\rho}_0 = 0.0027$ slug ft^{-3}) is compared in figure 1 with the relatively recent (1956) ARDC model of the atmosphere. It is evident that a single value for β appears to be a reasonable approximation at altitudes below about 400,000 feet (80 miles, roughly). In most cases peak decelerations and maximum aerodynamic heating occur well below this altitude. Moreover, the region of most important heating and deceleration for a given vehicle occurs only over a relatively thin strip of altitude (very roughly over a 70,000-foot strip across which the density changes by about a factor of 20). Since the analysis which follows enables the altitude of this important strip to be calculated quickly for any given vehicle, the exponential decay parameter β in each case could be selected, if desired, as corresponding to this particular altitude rather than to the mean value tabulated above. A plot of the dimensionless parameter $\sqrt{\beta r}$ as a function of altitude is shown in figure 2 for the ARDC model atmosphere. In determining $\sqrt{\beta r}$ consideration is given only to the 70,000-foot region of air immediately above a given altitude. The fluctuations in $\sqrt{\beta r}$ for this standard atmosphere below about 400,000 feet amount to the order of ± 10 percent from a mean value of 30 and are attributed primarily to the variation in temperature with altitude. Inasmuch as variations in temperature with season and with latitude (see ref. 12, for example) can fluctuate the order of ± 15 percent, the parameter $\sqrt{\beta r} \sim \overline{T}^{-1/2}$ can fluctuate about ∓ 7 percent. For most numerical calculations in this report, a constant value $\sqrt{\beta r} = 30$ is used for the earth's atmosphere corresponding to a mean atmospheric temperature of 240° K (432° R).

Assumption (iii), that the peripheral velocity of the planet is negligible compared to the velocity of the entering vehicle, would not introduce significant errors for most descents into most planetary atmospheres. For descents nearly along a line of longitude, the errors in heat transfer and deceleration would, of course, be negligible. The greatest error would occur in an equatorial descent. As a measure of this error,

we can take the ratio of the equatorial peripheral velocity u_p of the planet to the circular satellite velocity u_c. This ratio for several planets is as follows:

	u_p/u_c
Venus	[1]0.002
Earth	.06
Mars	.07
Jupiter	.29

Hence the error introduced by assuming a nonrotating atmosphere in the case of near-equatorial descents would be negligible for Venus, appreciable though not large for Earth and Mars, but probably significant for Jupiter.

In addition to these three physical assumptions, two mathematical approximations are made in the development of the subsequent analysis in order to effect major simplifications in the structure of the equations of motion. They are mentioned here for convenience:

(a) In a given increment of time, the fractional change in distance from the planet center, dr/r, is small compared to the fractional change in velocity du/u; that is, $|dr/r| << |du/u|$.

(b) For lifting vehicles, the flight-path angle φ relative to the local horizontal direction is sufficiently small that the component of lift in the horizontal direction is small compared to the drag; that is, $|(L/D)\tan\varphi| << 1$.

For nonlifting vehicles (e.g., ballistic entry), approximation (b) is automatically satisfied; approximation (a) does not specifically restrict the descent angle (0° to 90° can be analyzed for nonlifting vehicles), but it does restrict the analysis to a portion of the over-all trajectory below an upper altitude limit. Above some altitude dr/r cannot be small compared to du/u, as is shown to be the case on mathematical grounds in appendix A. Physically, this is clear from the law of conservation of angular momentum which states that in the absence of drag, $d(mur) = 0$, or $dr/r = -du/u$. Consequently, the present solution would be reasonable at least below an altitude where drag has slowed down a vehicle slightly to some point (A in sketch) where $dr/r \cong 0.1\ du/u$. It is shown in appendix B that this corresponds to the point where drag has reduced the vehicle velocity by about 0.01 of the initial velocity. Above this altitude (point A), orbit-type calculations could be applied. A method for joining the present solution to Keplerian ellipses is discussed in appendix B.

[1]This value may be a factor of ten higher due to the uncertainty in the length of the Venus day.

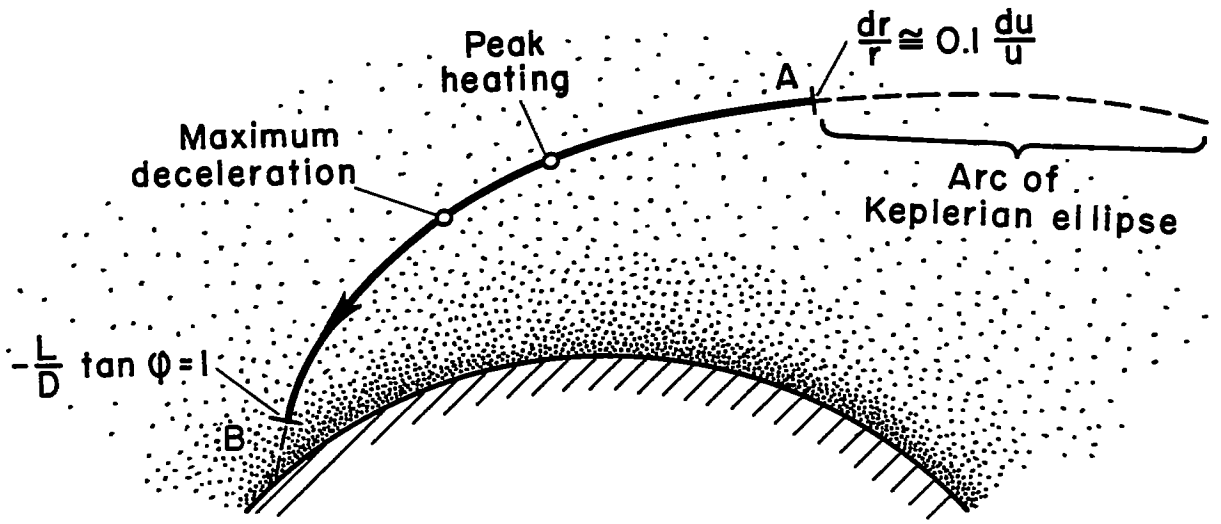

For lifting vehicles (e.g., skip or gliding entry) assumption (b) clearly restricts the analysis to small angles of descent. Even if a lifting vehicle starts entry horizontally, the angle of descent will increase as the velocity is reduced (and as the centrifugal forces are diminished) until $(L/D)\tan \varphi$ becomes unity in the terminal subsonic gliding phase. Although the solution is not valid, strictly speaking, when $(L/D)\tan|\varphi|$ is comparable to unity, a reasonable over-all trajectory would be obtained by stopping the present solution at the point where $-(L/D)\tan \varphi = 1$ (point B in above sketch), and considering that $-(L/D)\tan \varphi = 1$ thereafter. As sketched, peak heating and maximum deceleration occur well within the range (solid line) where the present solution applies.

The limitations resulting from approximations (a) and (b) are examined in appendix A, where it is shown that for vehicles entering from decaying satellite orbits, with or without positive lift, the errors introduced are only the order of a few percent insofar as aerodynamic heating and peak decelerations are concerned. Surprisingly small errors result from approximation (b), even for very large L/D ratios, because, in orbital decay or in a smooth glide, the larger the L/D the smaller the angle φ at conditions near maximum heating and peak deceleration; this keeps the product $(L/D)\tan \varphi$ small.

Various modes of entry and the portions of the trajectories of satellite, ballistic, escape, glide, and skip vehicles to which the analysis applies are sketched in figure 3.

Development of Differential Equation

Descent in a spherically symmetric atmosphere about a spherically symmetric planet would occur in a meridian plane in the absence of lateral forces. This confines the problem to one of two dimensions for which polar coordinates (r, θ) are convenient. The velocity components are (v, u), respectively, as sketched below.

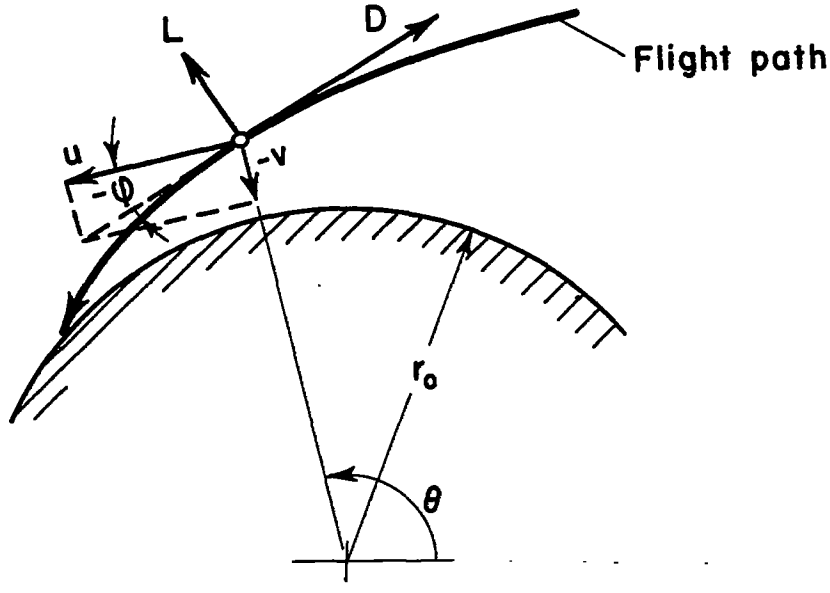

The vector acceleration in terms of the unit vectors $\vec{e}_r$ and $\vec{e}_\theta$ for polar coordinates is

$$\vec{a} = \vec{e}_r \left(\frac{dv}{dt} - \frac{u^2}{r} \right) + \vec{e}_\theta \left(\frac{du}{dt} + \frac{uv}{r} \right) \tag{3}$$

where $\vec{e}_r$ and $\vec{e}_\theta$ are the unit vectors in the r and θ directions, respectively. The local flight-path angle φ (negative for descent) is

$$\tan \varphi = \frac{v}{u} \tag{4}$$

The vector aerodynamic force

$$\vec{f} = (-mg + L \cos \varphi - D \sin \varphi)\vec{e}_r - (D \cos \varphi + L \sin \varphi)\vec{e}_\theta \tag{5}$$

must equal the mass m times the vector acceleration in the absence of thrust-type forces. Hence, equations (3), (4), and (5) yield two component equations of motion

$$-\frac{d^2y}{dt^2} = -\frac{dv}{dt} = g - \frac{u^2}{r} - \frac{L}{m}\cos\varphi + \frac{D}{m}\sin\varphi \tag{6}$$

$$\frac{du}{dt} + \frac{uv}{r} = -\frac{D}{m}\left(\cos\varphi + \frac{L}{D}\sin\varphi\right) \tag{7}$$

It is noted that g and r are local values in these equations.

We will solve this system of equations by disregarding the term uv/r in equation (7) (which, as will be evident shortly, is equivalent to assumption (a) that $|dr/r| \ll |du/u|$). This restricts the solutions to problems wherein $|uv/r| \ll |du/dt|$, but the restriction is not serious for the aerodynamic heating and deceleration aspects of entry. In the case of orbital entry, for example, maximum deceleration and heating occur at such small angles that uv/r is the order of 1 percent of du/dt (see appendix A). An alternate view of what the approximation involves can be seen as follows:

$$\frac{\left|\frac{uv}{r}\right|}{\left|\frac{du}{dt}\right|} = \frac{u\left|\frac{dr}{dt}\right|}{r\left|\frac{du}{dt}\right|} = \frac{\left|\frac{dr}{r}\right|}{\left|\frac{du}{u}\right|} \ll 1 \tag{8}$$

Consequently, the disregard of uv/r is precisely equivalent to approximation (a) mentioned earlier; namely, that the percentage change in distance from the planet center is small compared to the percentage change in velocity. We will employ this approximation several times more in the analysis. Inasmuch as du/u is relatively large only when the drag is important, it is understandable why the basic approximation $|dr/r| \ll |du/u|$ yields results applicable to regions of important deceleration and aerodynamic heating, but not to the outer regions of space where orbit-type calculations (which do not neglect the acceleration term uv/r compared to du/dt) are necessary to describe the motion of a vehicle. In these outer regions, radiant heat dominates, while convective heating and deceleration are very small.

By utilizing approximation (a) (inequality (8)), we have

$$\frac{du}{dt} = -\frac{D}{m}\cos\varphi\left(1 + \frac{L}{D}\tan\varphi\right) \tag{9}$$

so that, by introducing the drag coefficient, the exponential approximation to the atmosphere, and approximation (b) ($|(L/D)\tan\varphi| \ll 1$), and noting that $V = u/\cos\varphi$,

$$\frac{du}{dt} = -\frac{\overline{\rho}_o e^{-\beta y}}{2\left(\frac{m}{C_D A}\right)} \frac{u^2}{\cos\varphi} \tag{10}$$

We will select as an independent variable

$$\overline{u} \equiv \frac{u}{u_c} \equiv \frac{u}{\sqrt{gr}} \tag{11}$$

representing the ratio of horizontal velocity to the local circular satellite velocity. The basic approximation (8) taken together with the relation $dg/g = -2dr/r$ resulting from Newton's gravitational law enables us to disregard derivatives of both g and r relative to derivatives of either u, or $\overline{u}$; for example,

$$\frac{du}{dt} \equiv \frac{d(\sqrt{gr}\,\overline{u})}{dt} = \sqrt{gr}\,\frac{d\overline{u}}{dt} \tag{12}$$

By introduction of the drag coefficient, the motion equation (6) for an exponential atmosphere becomes

$$-\frac{1}{g}\frac{dv}{dt} = -\frac{1}{g}\frac{d^2y}{dt^2} = 1 - \overline{u}^2 + \frac{\overline{\rho}_o}{2}\frac{C_D A r \overline{u}^2 e^{-\beta y}}{m\cos^2\varphi}\left(\sin\varphi - \frac{L}{D}\cos\varphi\right) \tag{13}$$

In order to reduce the pair of motion equations (10) and (13) to a single equation, we transform to a new dimensionless dependent variable Z defined by

$$Z \equiv \frac{\overline{\rho}_o}{2\left(\frac{m}{C_D A}\right)}\sqrt{\frac{r}{\beta}}\,\overline{u}e^{-\beta y} \tag{14}$$

and employ $\overline{u}$ as the independent variable.[2] Thus, by differentiating ($Z' \equiv dZ/d\overline{u}$) and keeping in mind the basic approximation (8)

[2]The author knows of no simple way to explain a priori why this coordinate system $Z(\overline{u})$ should be introduced. It was discovered by trial and error after trying various other transformed coordinate systems which did not reduce the pair of motion equations to a single equation.

$$\frac{Z'}{\bar{u}} - \frac{Z}{\bar{u}^2} = -\frac{\bar{\rho}_o \sqrt{r\beta}}{2\left(\frac{m}{C_D A}\right)} e^{-\beta y} \frac{dy}{d\bar{u}}$$

$$= -\beta \frac{Z}{\bar{u}} \frac{dy}{dt} \frac{dt}{d\bar{u}} \tag{15}$$

We see from equations (10) and (12) that

$$\frac{d\bar{u}}{dt} = -\sqrt{g\beta} \frac{\bar{u}Z}{\cos \varphi} \tag{16}$$

so that substitution into equation (15) and noting that $dy/dt = v = \bar{u}\sqrt{gr} \tan \varphi$ yields

$$Z' - \frac{Z}{\bar{u}} = \sqrt{\frac{\beta}{g}} \frac{\cos \varphi}{\bar{u}} \frac{dy}{dt} = \sqrt{\beta r} \sin \varphi \tag{17}$$

Proceeding now by differentiation of v and $\sin \varphi$ from equation (17), there results

$$\frac{1}{g} \frac{dv}{dt} = \sqrt{\frac{r}{g}} \frac{d}{dt}\left(\frac{\bar{u} \sin \varphi}{\cos \varphi}\right) = \frac{1}{\sqrt{\beta g}} \frac{d\bar{u}}{dt}\left(\frac{\bar{u}Z''}{\cos \varphi} + \frac{\bar{u}\sqrt{\beta r} \sin^2 \varphi}{\cos^2 \varphi} \frac{d\varphi}{d\bar{u}}\right) \tag{18}$$

The term $d\varphi/d\bar{u}$ representing flight-path curvature can be expressed in several ways in terms of the Z function by noting from equations (17) and (12) that

$$\left.\begin{aligned} \bar{u} \frac{d}{d\bar{u}}\left(Z' - \frac{Z}{\bar{u}}\right) &= \bar{u}\sqrt{\beta r} \frac{d \sin \varphi}{d\bar{u}} \\ &= \bar{u}Z'' - Z' + \frac{Z}{\bar{u}} \\ &= \bar{u}Z'' - \sqrt{\beta r} \sin \varphi \end{aligned}\right\} \text{Alternate forms of terms representing flight-path curvature} \tag{19}$$

Consequently, we can substitute the first form of this equation, together with equation (16) into equation (18) to obtain

$$-\frac{1}{g}\frac{dv}{dt} = -\frac{1}{g}\frac{d^2y}{dt^2} = \frac{\bar{u}Z}{\cos^2\varphi}\left\{\bar{u}Z'' + \tan^2\varphi\left[\bar{u}\frac{d}{d\bar{u}}\left(Z' - \frac{Z}{\bar{u}}\right)\right]\right\} \quad (18a)$$

We note from equations (14) and (17) that equation (13) can be written in the form

$$-\frac{1}{g}\frac{dv}{dt} = -\frac{1}{g}\frac{d^2y}{dt^2} = 1 - \bar{u}^2 + \frac{\bar{u}Z}{\cos^2\varphi}\left(Z' - \frac{Z}{\bar{u}} - \sqrt{\beta r}\,\frac{L}{D}\cos\varphi\right) \quad (20)$$

Hence, by comparing this equation with equation (18a), and by observing from the second form of equation (19) that

$$Z' - \frac{Z}{\bar{u}} = \bar{u}Z'' - \bar{u}\frac{d}{d\bar{u}}\left(Z' - \frac{Z}{\bar{u}}\right)$$

the final equation for the Z function is obtained.

$$\bar{u}\frac{d}{d\bar{u}}\left(\frac{dZ}{d\bar{u}} - \frac{Z}{\bar{u}}\right) - \frac{1-\bar{u}^2}{\bar{u}Z}\cos^4\varphi + \sqrt{\beta r}\,\frac{L}{D}\cos^3\varphi = 0 \quad (21)$$

In this equation, $\cos\varphi = \sqrt{1 - \sin^2\varphi}$ can be expressed in terms of Z' and Z through equation (17)

$$\sqrt{\beta r}\sin\varphi = Z' - \frac{Z}{\bar{u}} \quad (17)$$

Thus, the pair of motion equations has been reduced to a single, second-order differential equation by using $\bar{u}$ as the independent variable and Z as the dependent variable.[3] For nonlifting vehicles ($L/D = 0$) the equation is applicable to large angles of descent as well as small. For lifting vehicles it is applicable for $|(L/D)\tan\varphi| \ll 1$. In all cases it is applicable when $|dr/r|/|du/u| \ll 1$. We note from equations (4) and (16) that

[3]Clearly, the same reduction would be achieved by using $g(\bar{u})$ as the independent variable and $Zh(\bar{u})$ as the dependent variable, where $g(\bar{u})$ and $h(\bar{u})$ are arbitrary functions.

$$\frac{dr/r}{du/u} = \frac{uv/r}{du/dt} = \frac{-\bar{u} \sin \varphi}{\sqrt{\beta r}\, Z} \tag{22}$$

As noted in appendix A, the ratio $|dr/r|/|du/u|$ is less than 0.1 below the altitude where drag has reduced the velocity by about 1 percent of the initial velocity.

The nonlinearity of equation (21) is due to the term $(1 - \bar{u}^2)\cos^4\varphi/\bar{u}Z$ which represents the effects of gravity and centrifugal forces in inducing a curved flight path. It is noted that the basic equation is independent of the physical characteristics C_D, W, A of the vehicle as well as independent of the sea-level characteristics $\bar{\rho}_o$ and g_o. Aerodynamic lift occurs only in the combined parameter $\sqrt{\beta r}\, L/D$. The equation has a singularity at $Z = 0$ which must be handled analytically in numerical methods. A method of solving this equation is discussed in appendix D.

It is instructive to consider the physical meaning of each of the terms in the differential equation (21). Equations (19) and (20) help in this regard.

$$\underbrace{\bar{u}Z''}_{\text{vertical acceleration}} \quad \underbrace{-\left(Z' - \frac{Z}{\bar{u}}\right)}_{\substack{\text{vertical component of drag force} \\ (\sqrt{\beta r} \sin \varphi)}} = \underbrace{\frac{1-\bar{u}^2}{\bar{u}Z}\cos^4\varphi}_{\substack{\text{gravity minus} \\ \text{centrifigal force}}} \quad \underbrace{-\sqrt{\beta r}\,\frac{L}{D}\cos^3\varphi}_{\text{lift force}} \tag{21a}$$

By understanding the physical significance of the various terms one can judge, for example, what terms to consider in obtaining special approximate solutions.

Since the basic differential equation is of second order, we need two initial conditions to complete the system. We take these at some initial velocity $\bar{u}_i$, and write as generalized initial conditions

$$Z(\bar{u}_i) \equiv Z_i \qquad Z'(\bar{u}_i) \equiv Z_i'$$

If the vehicle starts at a very high altitude where the density is negligible compared to that near peak heating, then the definition (14)

$$Z_i = \left(\frac{g_c C_D A}{2W}\sqrt{\frac{r}{\beta}}\right)\bar{u}_i \rho_i \tag{24a}$$

shows that Z_i is very small in such cases. For simplicity we take $Z_i = 0$ for entries starting at very high altitudes. The equation

$$Z_i' = \sqrt{\beta r} \sin \varphi_i + \frac{Z_i}{\bar{u}_i} \tag{24b}$$

shows that Z_i' would be equal to $\sqrt{\beta r} \sin \varphi_i$ when $Z_i = 0$. As an example, entry from a decaying satellite orbit ($\varphi_i \cong 0$ and $\bar{u}_i = 1$ in the stage of decay before appreciable aerodynamic heating begins), would be represented by the initial conditions

$$Z_i(1) = 0 \qquad Z_i'(1) = 0 \tag{25}$$

One universal Z function would be required for each value of the parameter $\sqrt{\beta r}\, L/D$ appearing in the differential equation (21).

By allowing Z_i' to take on values other than zero and allowing $\bar{u}_i$ to be either less than or greater than unity, we can obtain the corresponding Z functions for ballistic, glide, skip, or escape vehicles entering a planetary atmosphere from very high altitudes. By further allowing Z_i to be other than zero, corresponding Z functions can be obtained for entry starting from an initial altitude where the density may not be negligible compared to that near peak heating. Before presenting some solutions to equation (21), though, it is advantageous to show how the Z functions, once computed, can rapidly be used to determine a number of useful quantities in practical calculations.

Summary of Some Useful Quantities Related to the Z Function

From the Z functions, it is a relatively simple matter to obtain, for example, the horizontal component of deceleration a_θ by using equations (3), (12), and (16),

$$a_\theta \cong -\frac{du}{dt} = \frac{g\sqrt{\beta r}\, \bar{u} Z}{\cos \varphi} \tag{26}$$

or

$$-\frac{1}{g}\frac{du}{dt} \cong 30\, \bar{u} Z \quad \text{for Earth, } \varphi \text{ small}$$

Strictly speaking, g and r are local values in the outer layers of the atmosphere where the deceleration takes place. For Earth, however, these are not significantly different from their respective surface-level values. Local and surface values might be greatly different, though, for

planets such as Jupiter and Saturn which are believed to have a very deep atmosphere. The equation for the angle of descent ($\varphi < 0$ for descent) is, from equation (17),

$$\sin \varphi = \frac{Z' - (Z/\bar{u})}{\sqrt{\beta r}} \tag{27}$$

$$\cong \frac{Z' - (Z/\bar{u})}{30} \qquad \text{for Earth}$$

The circumferential distance traveled between a point where the dimensionless velocity is $\bar{u}_1$ and a point where it is $\bar{u}_2$ can be expressed in terms of Z from equation (16),

$$\frac{\Delta s}{r} = \frac{1}{r} \int_{\bar{u}_1}^{\bar{u}_2} u \frac{dt}{d\bar{u}} d\bar{u} = \frac{1}{\sqrt{\beta r}} \int_{\bar{u}_2}^{\bar{u}_1} \frac{\cos \varphi \, d\bar{u}}{Z} \tag{28}$$

or

$$\frac{\Delta s}{r} \cong \frac{1}{30} \int_{\bar{u}_2}^{\bar{u}_1} \frac{d\bar{u}}{Z} \qquad \text{for Earth, } \varphi \text{ small} \tag{29}$$

Inasmuch as the analysis is not valid in a very small neighborhood of $Z = 0$ where $\bar{u} = \bar{u}_i$, but becomes valid after drag has reduced $\bar{u}$ by less than 1 percent (as shown in appendix B), we select an upper limit such as $\bar{u}_1 = 0.995\, \bar{u}_i$ or $\bar{u}_1 = 0.99\, \bar{u}_i$ for the entry range. In a practical application, this range would have to be joined to the range of the appropriate Keplerian ellipse in order to obtain the total range. The corresponding time elapsed is obtained also with the aid of equation (16)

$$t = \int \frac{ds}{u} = \frac{1}{\sqrt{\beta g}} \int_{\bar{u}_2}^{\bar{u}_1} \frac{\cos \varphi \, d\bar{u}}{\bar{u} Z} \tag{30}$$

$$\cong 27.0 \int_{\bar{u}_2}^{\bar{u}_1} \frac{d\bar{u}}{\bar{u} Z} \qquad \text{sec for Earth, } \varphi \text{ small, } g \cong g_o$$

Another useful quantity is the density ratio, referred to the true sea-level density ($\rho_o = 0.00238$ slug ft^{-3}), which comes from the definition (14) for Z

$$\frac{\rho_\infty}{\rho_o} = \frac{2}{\rho_o}\sqrt{\frac{\beta}{r}}\left(\frac{m}{C_D A}\right)\frac{Z}{\bar{u}} \tag{31a}$$

or

$$\frac{30}{\sqrt{\beta r}}\frac{\rho_\infty}{\rho_o} = 3.7\left(\frac{W}{C_D A}\right)\frac{Z}{\bar{u}} \times 10^{-5} \quad \text{for Earth, } \frac{W}{C_D A} \text{ in lb ft}^{-2}$$

The left side of this last equation is a function only of the altitude for a given atmosphere ($\sqrt{\beta r}$ for the ARDC model atmosphere is shown in fig. 2), so that it provides for a given $Z(\bar{u})$ function the altitude-velocity relationship for any model atmosphere. The density ratio referred to the effective sea-level density ($\bar{\rho}_o = 0.0027$) which best fits the $\rho(y)$ curve is

$$e^{-\beta y} = \frac{\rho_\infty}{\bar{\rho}_o} = \frac{2}{\bar{\rho}_o}\sqrt{\frac{\beta}{r}}\left(\frac{m}{C_D A}\right)\frac{Z}{\bar{u}} \tag{31b}$$

$$= 3.2\left(\frac{W}{C_D A}\right)\frac{Z}{\bar{u}} \times 10^{-5} \quad \text{for Earth, } \frac{W}{C_D A} \text{ in lb ft}^{-2}, \sqrt{\beta r} = 30$$

The dynamic pressure is

$$\frac{1}{2}\rho_\infty V^2 = \frac{mg}{C_D A}\sqrt{\beta r}\,\frac{\bar{u}Z}{\cos^2\varphi} \tag{32}$$

$$= 30\,\bar{u}Z\left(\frac{W}{C_D A}\right) \quad \text{for Earth, } \frac{W}{C_D A} \text{ in lb ft}^{-2}, \varphi \text{ small}$$

and the free-stream Reynolds number per unit length is proportional to Z (eq. 14))

$$\frac{Re_\infty}{l} \equiv \frac{V\rho_\infty}{\mu_\infty} = \frac{2\sqrt{g\beta}}{\mu_\infty \cos\varphi}\left(\frac{m}{C_D A}\right)Z \tag{33}$$

$$\cong 7100\left(\frac{W}{C_D A}\right)Z \quad \text{for earth, } \varphi \text{ small, } \frac{W}{C_D A} \text{ in lb ft}^{-2}$$

The viscosity of air at the mean atmospheric temperature $\overline{T} = 432^{\circ}$ R is employed to obtain the constant in this last equation which is valid only for the earth's atmosphere.

It is interesting that the Reynolds numbers involved during entry from a decaying satellite orbit are relatively small. Near peak heating, for example, we will see subsequently that the value of Z ranges from about 0.17 to 0.015, for L/D ratios between 0 and 1, so the corresponding Reynolds numbers are of the order of $1000(W/C_DA)$ to $100(W/C_DA)$ per foot. These are sufficiently small for one to be optimistic about the practical possibilities of maintaining laminar flow for shallow entry from a satellite orbit. For steep entries, as for ballistic vehicles, the Z function is larger, and hence the corresponding Reynolds numbers are larger. Curves illustrating this are presented later.

Fairly simple expressions also can be obtained for the aerodynamic heating rate per unit area (q) and the total heat absorbed per unit area Q/S. Following the analysis of Lees (ref. 13), we will consider the heating rate at any point on a body to be a certain fraction

$$k_1 \equiv \frac{q}{q_s} \tag{34}$$

of the heating rate q_s at a stagnation point of radius of curvature R. The heating rate in hypersonic flow at a stagnation point, can be expressed as

$$q_s = \frac{C}{\sqrt{R}}\left(\frac{\rho_\infty}{\rho_o}\right)^n\left(\frac{\overline{u}}{\cos\varphi}\right)^m \quad \text{Btu ft}^{-2}\text{sec}^{-1} \tag{35}$$

where the constants C, n, and m depend on the type of boundary-layer flow. For laminar flow we have $n = 1/2$ and from the several references listed (with ρ_o being the true sea-level density)

Reference	C	m	Remarks
14	16,800	3.1	Intermediate enthalpy theory
13,7	19,800	3.22	Theory of Lees
15	17,600	3.15	Correlation of AVCO shock-tube experimental results

We will base all our numerical calculations on laminar flow ($n = 1/2$), and will use the value $m = 3$ for purposes of simplicity (this corresponds to a gas with viscosity proportional to $T^{1/2}$), and the value $C = 17{,}000$ Btu $\text{ft}^{-3/2}\text{sec}^{-1}$ which is adjusted to match a mean of the above results for air at velocities near peak heating ($\overline{u} \cong 0.8$). For gases other than air we use the theory of Lees (ref. 13) to obtain for hypersonic flow $C \sim \sqrt{\rho_o\mu_o}\,u_c^3\,\text{Pr}^{-2/3}[(\overline{\gamma} - 1)/\overline{\gamma}]^{1/4}$. In subsequent calculations, differences in the Prandtl number and in the ratio of specific heats for various planets are disregarded.

Proceeding from equations (35), (34), and (31) with $n = 1/2$, $m = 3$, and $C = 17{,}000$, the laminar convective heat-transfer rate can be written in terms of the Z function and the relative planetary constants ($g_\oplus = g/g_{earth}$, $\mu_\oplus = \mu/\mu_{earth}$, etc.) as

$$q = k_1 q_s = 590 \left\{ Pr^{-2/3} \mu_o^{1/2} g^{3/2} r^{5/4} \beta^{1/4} \right\}_\oplus \left[k_1 \sqrt{\frac{m}{C_D A R}} \right] \frac{\bar{q}}{\cos^3 \varphi} \quad \frac{Btu}{ft^2 sec} \tag{36}$$

where $\bar{q} \equiv \bar{u}^{5/2} Z^{1/2}$. (If the flow were turbulent $\bar{q} \sim \bar{u}^{2.2} Z^{0.8}$, approximately, and we would have different powers appearing in equation (36).) It is noted that the different variables affect the heat flux in a form represented by a series of factors; the expression in curly braces represents the effect on heat flux of the particular planetary atmosphere, the expression in brackets represents the effect of the physical characteristics of the vehicle, that is, the mass, dimensions and shape of the vehicle, and the dimensionless function $\bar{q} = \bar{u}^{5/2} Z^{1/2}$ represents the effect of the particular type of trajectory as determined by the lift-drag ratio.

Whereas equation (36) for heating rate would be useful in studying vehicles designed to operate at radiation equilibrium temperatures, an equation for the total heat absorbed during entry is of more interest for heat-sink type vehicles.

$$Q = \iint q \, dt \, dS = k_2 S \int q_s dt \tag{37}$$

where

$$k_2 \equiv \frac{1}{S} \int k_1 dS = \frac{1}{S} \int \frac{q}{q_s} dS \tag{38}$$

is the factor which takes into account the variations in heat flux over the whole surface S wetted by the boundary layer. (For a hemisphere, for example, $k_2 \cong 0.5$.) Combining equations (37), (36), and (30) yields the following equation for the heat absorbed between $\bar{u}_1$ and $\bar{u}$

$$Q = 15{,}900 \left\{ \frac{Pr^{-2/3} \mu_o^{1/2} g r^{5/4}}{\beta^{1/4}} \right\}_\oplus \left[k_2 S \sqrt{\frac{m}{C_D A R}} \right] \bar{Q} \tag{39a}$$

where

$$\bar{Q} \equiv \int_{\bar{u}}^{\bar{u}_1} \frac{\bar{u}^{3/2} d\bar{u}}{Z^{1/2} \cos^2 \varphi} \tag{39b}$$

Heat radiation from the surface is not considered in these equations. They are useful in studying vehicles incorporating heat sinks or ablation cooling under conditions when the heat radiated away is small compared to the heat absorbed; $Q = \Delta T(cm)_{sink}$ (where c is the effective specific heat of the sink material) is proportional to the heat-sink weight. We note here that the particular planetary atmosphere (g, r, β) and especially the particular trajectory $Z(\bar{u}, L/D)$ affect the heating rate q in a different fashion than the total heat absorbed Q. Examples illustrating this are presented later.

Some Approximate Analytical Z Functions Obtained From Truncated Basic Equation

By disregarding three different combinations of terms in the basic differential equation (21), three special solutions are obtained which yield results identical to previous approximate solutions. The details are described in appendix C and lead to the following approximate solutions:

Solution	Vehicle	Terms disregarded (see eq. (21a))	
$Z_I = \sqrt{\beta r}(\sin \bar{\varphi})\bar{u} \ln \frac{\bar{u}}{\bar{u}_i}$	Ballistic	Gravity, centrifugal and lift forces; $\varphi = \bar{\varphi}$ = constant	(40)
$Z_{II} = \frac{1-\bar{u}^2}{\bar{u}\sqrt{\beta r}\left(\frac{L}{D}\right)}$	Glide	Vertical acceleration and vertical component of drag force; $\cos \varphi \cong 1$	(41)
$Z_{III} = \bar{u}\left[\frac{Z_i}{\bar{u}_i} + \sqrt{\beta r}\,\varphi_i \ln \frac{\bar{u}}{\bar{u}_i} - \frac{\sqrt{\beta r}}{2}\left(\frac{L}{D}\right)\ln^2 \frac{\bar{u}}{\bar{u}_i}\right]$	Skip	Gravity and centrifugal forces; $\cos \varphi \cong 1$	(42)

The Z_I function provides an approximate solution for the motion and heating identical to the solution of Allen and Eggers (ref. 1) for ballistic entry. The Z_{II} function corresponds to equilibrium gliding flight originally discussed by Sänger (ref. 2). The corresponding aerodynamic heating problems for this type of hypersonic flight have been discussed by Eggers, Allen, and Neice (ref. 4) who also obtained a solution equivalent to the Z_{III} function for skip vehicles. As will be apparent later, the Z_I function for ballistic vehicles is quite accurate for angles of descent greater than several degrees ($\sqrt{\beta r}|\varphi_i| > 2$ approximately) and the Z_{II} function for hypersonic glide vehicles is quite accurate for L/D ratios greater than about 1 ($\sqrt{\beta r}\, L/D > 30$ approximately) provided $\varphi_i \cong 0$.

The accuracy of the Z_{III} function for skip vehicles, however, depends on both L/D and the initial angle φ_i. The conditions for applicability can be determined from an approximate solution which considers both the gravity and centrifugal forces that were neglected in obtaining Z_{III}. In appendix C the following approximate solution is developed for satellite entry ($\bar{u}_i = 1$, $Z_i = 0$) at small initial angles φ_i:

$$Z_{IV} = \bar{u}\sqrt{\beta r}\left\{\varphi_i \ln \bar{u} - \frac{L}{2D}\left[1 + \frac{1}{2\beta r \varphi_i (L/D)}\right]\ln^2 \bar{u}\right\} \tag{43}$$

By comparing with Z_{III}, we see that the gravity and centrifugal forces can be disregarded provided $2\beta r|\varphi_i(L/D)| \gg 1$. An interesting feature deduced from Z_{IV} in appendix C is that the total heat absorbed in the first skip (which is perhaps the most important) is essentially independent of both the initial angle φ_i and the velocity of exit from the skip. The heat absorbed varies as $1/\sqrt{C_L}$ and hence is a minimum for entry at $C_{L_{max}}$ (see appendix C). For flat plates in Newtonian flow this corresponds to an optimum L/D of 0.7.

Some Z Functions Obtained From Full Equation

Entry from a decaying orbit for various L/D ($\bar{u}_i = 1$, $\varphi_i = 0$).- We turn now from the special solutions obtained by truncating the full equation (21), to some solutions of the complete nonlinear equation applicable to vehicles entering from a decaying satellite orbit. As the apogee of an elliptical orbit is slowly reduced by drag (primarily exerted near the perigee), the orbit eventually becomes a near circle and then begins a gradually decaying spiral; hence, the initial angle φ_i for this type of entry is taken as zero, and the initial velocity $\bar{u}_i = 1$. The peak heating and the maximum deceleration occur at such small angles that $\cos\varphi \cong 1$. The differential equation (21) is then

$$\bar{u}\frac{d}{d\bar{u}}\left(\frac{dZ}{d\bar{u}} - \frac{Z}{\bar{u}}\right) - \frac{1 - \bar{u}^2}{\bar{u}Z} + \sqrt{\beta r}\,\frac{L}{D} = 0 \tag{44}$$

and the corresponding boundary conditions for decaying orbits are

$$Z(1) = 0 \qquad Z'(1) = 0 \tag{45}$$

This system need be solved only once for each value of the parameter $\sqrt{\beta r}(L/D)$, and the results are then applicable to any planet and to any vehicle with arbitrary shape, size, or mass. In particular, the universal Z function for $L/D = 0$ is presented in figure 4(a) ($\bar{u}Z$ is plotted since this product stays within smaller bounds than Z). Solutions of equation (44) also have been carried out for various values of $\sqrt{\beta r}(L/D)$. The

numerical method employed is described in appendix D. Curves of the Z functions and related quantities are presented in figure 4(b) for values of $\sqrt{\beta r}(L/D)$ corresponding for earth to $L/D = 0.1$, 0.25, 0.5, and 1. They are plotted in coordinates especially suited for comparison with the Z_{II} function of equation (41) representing Sänger's concept of an equilibrium hypersonic glide. Values are not shown for $L/D > 1$ since Z_{II} can be used in the velocity range of interest for these cases. This is evident from the various curves in figure 4(b). The dashed curve represents Z_{II} which is the exact solution for $L/D = \infty$. From the Z functions the various quantities of engineering interest, such as the deceleration, descent angle, range, time, density-velocity relationship, dynamic pressure, Reynolds number, heating rate, and total heat absorbed can be computed from equations (26) to (39) presented earlier.

Nonlifting entry with initial angle of descent ($\bar{u}_i = 1$, $\varphi_i < 0$).- We now consider entry when the initial descent angle is not negligible, as it is in the case of a decaying orbit, but is some finite value φ_i. Entry with an initial angle occurs in the case of a ballistic vehicle, or a satellite to which a retrorocket has been applied to divert the orbit into one which will induce the entry process. The differential equation (21) for nonlifting bodies is applicable for large as well as small angles of descent.

$$\bar{u}\frac{d}{d\bar{u}}\left(\frac{dZ}{d\bar{u}} - \frac{Z}{\bar{u}}\right) - \frac{1 - \bar{u}^2}{\bar{u}Z}\cos^4\varphi = 0 \tag{46}$$

The initial conditions are

$$Z(\bar{u}_i) = 0 \qquad Z'(\bar{u}_i) = \sqrt{\beta r}\sin\varphi_i \tag{47}$$

In this case we have a double parameter family of solutions ($\bar{u}_i$ and $\sqrt{\beta r}\sin\varphi$). Actually, we need solutions to the nonlinear equation (46) only for quite small initial angles inasmuch as the Allen-Eggers solution (eq. (40)) is applicable for moderate and large angles. This may be seen from figure 5 which presents example Z functions corresponding to the nonlinear equation for various $-\varphi_i$ up to 20° with $u_i = 0.9$ (23,400 fps, for earth). Since the ordinate is $Z/\sqrt{\beta r}(-\sin\varphi_i)$, the Allen-Eggers solution is represented by the ordinate function $\bar{u}\ln(\bar{u}_i/\bar{u})$ on this plot. It is evident that their solution, which neglects gravity and centrifugal forces, is quite accurate near peak heating ($\bar{u} \cong 0.7$) for descent angles greater than about 5°. Near maximum deceleration ($\bar{u} \cong 0.4$) the descent angle has to be somewhat larger for comparable accuracy. It is clear that, as far as peak heating and maximum deceleration are concerned, a family of solutions to the nonlinear equation need only be computed for small initial angles.

The Z functions for small initial angles and for the case of satellite entry ($\bar{u}_i = 1$) are of special practical interest. These are presented in figure 6(a) for various values of $\sqrt{\beta r}\,\varphi_i$ such that in the

earth's atmosphere $-\varphi_i = 1^\circ, 2^\circ, 3^\circ, 4^\circ$, and 6°. Rather than to plot Z itself, the quantity $30\,\bar{u}Z$ is plotted which represents for the earth the horizontal deceleration in g's. Tabulated values are presented in table I for $-\varphi_i = 0^\circ, 0.5^\circ, 1^\circ, 2^\circ, 3^\circ$, and 4°. It is noted that these values tabulated are solutions to equation (46) with the $\cos^4\varphi$ term included, and hence are applicable to terminal conditions of small $\bar{u}$ (say less than 0.1) where φ is large as well as to conditions near peak heating and maximum deceleration where φ is small. The tables of Z apply to any planet for the same initial value of $\sqrt{\beta r}\,\varphi_i$. The supplementary tables of $-\varphi_{earth}$, $(\Delta s/r)_{earth}$, and t_{earth} can be applied to other planets over the range where φ is small by regarding the tabulated values as representing $-(\sqrt{\beta r}/30)\varphi$, $(\sqrt{\beta r}/30)(\Delta s/r)$, and $27\sqrt{\beta g}\,t$, respectively (see eqs. (27), (28), and (30)).

Entry with initial angle of descent for various L/D ($\bar{u}_i = 1$, $\varphi_i < 0$).- If we now consider a vehicle with lift, we must restrict our considerations to small initial angles of descent $-\varphi_i$ and to the portion of trajectory over which $-\varphi$ remains sufficiently small that $(L/D)|\tan\varphi| \ll 1$ (assumption (b)). The basic differential equation (21), with $\cos\varphi = 1$, becomes the same as equation (44), and the initial conditions are now

$$Z(1) = 0 \qquad Z'(1) = \sqrt{\beta r}\,\varphi_i \tag{48}$$

Solutions to equation (44) with these initial conditions have been obtained for various values of $\sqrt{\beta r}\,\varphi_i$ and for various values of the parameter $\sqrt{\beta r}(L/D)$.

In figure 6 some curves representing Z functions are presented as a function of $-\varphi_i$ for earth. The various portions of this figure correspond to L/D for earth of 0.25, 0.5, 0.7, and 1. It is evident from these figures, as might be expected, that small values of L/D and $-\varphi_i$ do not result in any significant skipping, but once the L/D is increased beyond a certain amount, or the initial descent angle is greater than a certain value, then numerous skips of sizable intensity occur during the entry trajectory. Information on the heating rates, total heat absorbed, and horizontal range during entry, has been obtained from these Z functions and is discussed later. The Z functions in figure 6 could be applied to any planet by noting that φ_i for earth is equivalent to a value $(\beta r)_\oplus^{-1/2}$ times as great on another planet, and that a given (L/D) for earth is equivalent to a value $(\beta r)_\oplus^{-1/2}$ times as great.

Atmosphere braking for various L/D ($\bar{u}_i > 1$, $\varphi_i < 0$).- In entering the atmosphere of a planet from space, the approach velocity can be comparable to escape velocity ($\bar{u}_i = \sqrt{2}$). It is uneconomical in weight to use chemical rockets for reducing the approach velocity in outer space, and it is possibly uneconomical in time to use a low-thrust space engine. Hence there is considerable interest in the braking process of making successive passes through an atmosphere in order to reduce stepwise the velocity and the eccentricity of an orbit to near circular conditions ($\bar{u}_i \cong 1$).

In analyzing the atmosphere braking process, cos φ can safely be replaced by unity, so the basic differential equation (21) becomes once again the same as equation (44), but the initial conditions are now

$$Z(\bar{u}_i) = 0 \qquad Z'(\bar{u}_i) = \sqrt{\beta r}\,\varphi_i$$

where $\bar{u}_i > 1$. By arbitrarily selecting various values for the angle of entry φ_i, various solutions are obtained corresponding to single passes through the atmosphere at various altitudes from the surface. It might be more convenient in describing a single pass to select as the arbitrary parameter the velocity $\bar{u}_{ex}$ at the exit of the pass, or $30(\bar{u}Z')_{max}$, which, for the earth, would be the maximum deceleration in g's experienced during this pass, and would be independent of W/C_DA.

In figure 7, four Z functions are presented for nonlifting vehicles which start the braking process with essentially escape velocity ($\bar{u}_i = 1.4$) but with different values of maximum deceleration in the first pass. The short-dash curve (a) corresponds to a maximum deceleration in the first pass of $30(\bar{u}Z)_{max} = 0.46$. It is seen that, starting with this initial pass (and with no further control exercised on the vehicle) six passes would occur before the seventh pass completed the entry process. The long-dash curve (b) in figure 7 corresponds to $30(\bar{u}Z)_{max} = 1.65$ for the first pass. In this case only two passes occur before the third pass completes the entry. The other two curves (c) and (d) in figure 7 correspond to conditions wherein the first pass is the only one, inasmuch as it is made sufficiently close to the planet surface to complete entry without ever emerging from the atmosphere.

In computing the Z function for a successive pass, the initial angle was assumed to be the same as the exit angle of the previous pass. The exit angle was taken at the point where $dr/r = du/u$. Further discussion of these Z functions, and the results of other such functions computed for atmosphere braking are presented later.

RESULTS AND DISCUSSION

From the various Z functions presented, it is relatively easy to study the influence on entry motion of several variables of practical interest. For example, we could study the effect of lift-drag ratio on deceleration and aerodynamic heating, or the effect of a small error in initial angle of descent on the range over which the re-entry process takes place. Before considering such topics, however, it is desirable to discuss two preliminary items. First, we compare some results from the present approximate analysis for an exponential atmosphere with more exact machine calculations for a standard atmosphere. This serves to provide a feeling for the accuracy of the present analysis, and also to show how any of the subsequent results readily can be corrected, if

desired, for atmospheric temperature variations. Second, we discuss the relative deceleration and aerodynamic heating of various planetary atmospheres. This provides multiplication factors which enable any of the subsequent results for the earth's atmosphere to be quickly converted to results for other planetary atmospheres.

Comparison of Present Analysis With Other Calculations

An insight into the approximate accuracy to be expected from the present analysis can be obtained by comparison with machine calculations of the pair of motion equations for specific vehicles. Differences between the present analysis and more exact calculations can arise inasmuch as the present analysis makes certain assumptions about the trajectory (that is, $|dr/r| \ll |du/u|$ and $|(L/D)\tan\varphi| \ll 1$) and about the atmosphere ($\rho_\infty \sim e^{-\beta y}$) which need not be made in numerical machine calculations. The a posteriori check of the trajectory assumptions, as presented in appendix A, shows that insofar as convective heating and peak decelerations are concerned, only a few percent difference should be expected for vehicles entering from a satellite orbit. A check of the assumption of an exponential atmosphere can be obtained by comparing with numerical calculations for some standard atmosphere. In figure 8 a comparison is made of the present analysis with numerical calculations from the pair of motion equations using the ARDC model atmosphere. These numerical calculations were made by M. W. Rubesin and G. Goodwin using equations equivalent to (6) and (7) without discarding any terms. The curves in figure 8(a) show close agreement of both the altitude and the descent angle as a function of velocity. The curves in figure 8(b) show similar agreement of the circumferential distance traveled ($\Delta s/r$), and of the maximum deceleration (within 6 percent). This small difference in maximum deceleration is believed due primarily to the departure of the ARDC atmosphere in certain altitude regions from the idealized exponential atmosphere of constant β ($1/23{,}500$ ft^{-1}).

As noted earlier, the present analytical method can readily be applied using semilocal values of $\sqrt{\beta r}$ if it is desired to make corrections to the results in order that they more closely represent some standard atmosphere. Corrections also can be made to allow for atmospheric seasonal variations, or for variations with the earth's latitude. In this sense, analytical results for an exponential atmosphere are actually more general for global application than numerical results for any single standard atmosphere. This can be seen from the results which follow. Let us consider the maximum deceleration for entry from a decaying orbit. This occurs at a velocity near $\bar{u} = 0.43$ at which point $Z \cong 0.64$ (fig. 4(a)). The approximate altitude at which maximum deceleration occurs is obtained by substituting either into equation (31a) to yield $(\rho_\infty/\rho_o)_{\max du/dt} = 5.5(W/C_DA)\times10^{-5}$, or into equation (31b) to yield

$$y_{max\ du/dt} = 23{,}500\left(9.96 - \ln\frac{W}{C_DA}\right) \quad \text{ft} \tag{49}$$

and is seen to depend on W/C_DA. Since $\sqrt{\beta r}$ for the ARDC model atmosphere depends weakly on altitude, as shown in figure 2, the maximum deceleration $\sqrt{\beta r}(\overline{uZ})_{max} = 0.278\sqrt{\beta r}$ in a standard atmosphere also will depend weakly on altitude, and hence weakly on W/C_DA. The resulting values of $-a_{max}/g$ are shown by the solid curve in figure 9, for (W/C_DA) values ranging from 0.01 to 1000 lb/ft. They agree very well with the points shown which represent numerical integrations (Rubesin-Goodwin) of the complete equations for the ARDC model atmosphere.

If desired, similar corrections for atmospheric variations also could be made to other quantities computed for a mean value $\sqrt{\beta r} = 30$. Thus, the distance traveled varies as $(\beta r)^{-1/2}$ (eq. (28)), and the convective heating rate varies as $(\beta r)^{1/4}$ (eq.(36)). It is noted that the fluctuations in $\sqrt{\beta r}$ with altitude, as plotted in figure 2 correspond very closely to the fluctuations in $\overline{T}^{-1/2}$, as should be expected, since $\beta = Mg/R\overline{T}$. Hence any variations in mean atmospheric temperature, such as seasonal variations or longitudinal variations, can just as readily be corrected for as variations with altitude.

Gazley (ref. 8) has developed an approximate theory for the case of orbital decay with $L/D = 0$ by assuming $\overline{u\varphi}$ is constant. This arbitrary restriction yields results for orbital decay without lift that are qualitatively similar to the present analysis, but quantitatively dissimilar. For example, the density-velocity relationship near peak heating ($\overline{u} \cong 0.8$) differs by a factor of roughly 2. For higher velocities the discrepancy rapidly increases, and for lower velocities it decreases. The peak deceleration occurs at lower velocities and is not greatly affected by Gazley's assumption. For the earth ($\sqrt{\beta r} = 30$) he obtains a maximum of 9.6 g at $\overline{u} = 0.54$, whereas the present analysis, which does not make any assumptions about the $u(\varphi)$ relationship, yields 8.3 g at $\overline{u} = 0.43$.

Relative Deceleration, Heating, and Reynolds Numbers For Entry Into Various Planetary Atmospheres

For a given size and shape of vehicle the deceleration, laminar heating rate, total heat absorbed, and Reynolds number vary, according to equations (26), (36), (39), and (33), respectively, as

$$\left.\begin{aligned} a &\sim g\sqrt{\beta r}\,Z \\ q &\sim Pr^{-2/3}\mu_o^{1/2}g^{3/2}r^{5/4}\beta^{1/4}Z^{1/2} \\ Q &\sim Pr^{-2/3}\mu_o^{1/2}gr^{5/4}\beta^{-1/4}Z^{-1/2} \\ Re &\sim g^{1/2}\beta^{1/2}\mu_o^{-1}Z \end{aligned}\right\} \tag{50}$$

In the case of nonlifting entry from a decaying orbit (zero initial angle of descent), the characteristics of the planetary atmosphere ($\sqrt{\beta r}$) do not enter the differential equation or the initial conditions ($Z_i = 0$, $Z_i' = 0$); hence Z can be disregarded in computing the relative values of the above quantities for various planets. In the more general case of entry from high altitude ($Z_i = 0$) with fixed values of $\sqrt{\beta r}\,\varphi_i$ and $\sqrt{\beta r}(L/D)$, the Z function still would be the same for all planets. Neglecting differences in Prandtl number and ratio of specific heats, we have for several planets the following relative values applicable to nonlifting entry from decaying orbits, or to any other type of entry where the values of $\sqrt{\beta r}\,\varphi_i$ and $\sqrt{\beta r}(L/D)$ are fixed:

	$(du/dt)_\oplus$ relative deceleration, $(g\sqrt{\beta r})_\oplus$	$q_\oplus$ relative heating rate, $(\mu_o^{1/2} g^{3/2} r^{5/4} \beta^{1/4})_\oplus$	$Q_\oplus$ relative total heat absorbed, $(\mu_o^{1/2} g r^{5/4} \beta^{-1/4})_\oplus$	$Re_\oplus$ relative Reynolds number, $(g^{1/2} \beta^{1/2} \mu_o^{-1})_\oplus$
Venus	0.9	0.7	0.8	1.
Earth	1.00	1.00	1.00	1.00
Mars	.2	.09	.2	.4
Jupiter	5.	50.	50.	2.

It is to be remembered that, in the case of a vehicle with lift, in order to have the same Z function, a given L/D ratio on earth is equivalent to an L/D ratio $(\beta r)_\oplus^{-1/2}$ times as great on a planet other than earth, and that a given φ_i on earth also is equivalent to a φ_i value $(\beta r)_\oplus^{-1/2}$ times as great on another planet. This equivalence, together with the above table, enables any result for earth to be converted to a result for each of the other planets.

In the special case of entry at a constant angle φ_i, the atmospheric characteristics enter the initial conditions on Z ($Z_i' = \sqrt{\beta r} \sin \varphi_i$). Since equation (40) shows that $Z \sim \sqrt{\beta r}$ for this type of re-entry, we include this in the expressions (50) to obtain the following relative values applicable only to ballistic entry (L/D = 0) at constant φ:

	$(du/dt)_\oplus$ relative deceleration, $(g\beta r)_\oplus$	$q_\oplus$ relative heating rate, $(\mu_o^{1/2} g^{3/2} r^{3/2} \beta^{1/2})_\oplus$	$Q_\oplus$ relative total heat absorbed, $(\mu_o^{1/2} g r)_\oplus$	$Re_\oplus$ relative Reynolds number, $(g^{1/2} \beta r^{1/2} \mu_o^{-1})_\oplus$
Venus	0.9	0.7	0.7	1.
Earth	1.00	1.00	1.00	1.00
Mars	.09	.06	.2	.2
Jupiter	11.	70.	20.	4.

These relative values for ballistic entry are exactly the same, of course, as would be obtained directly from the theory of reference 1 and are applicable for initial angles greater than about 5°. The previous table would apply for $\varphi_i = 0^\circ$. For nonlifting entry with φ_i the order of a few degrees, the relative values for various planets would be intermediate to the above two tables.

We see that entry into the atmosphere of Venus involves only slightly less deceleration and heating than does entry into the earth's atmosphere, whereas entry into Mars involves much less deceleration and heating, and entry into Jupiter, much more. The Reynolds numbers, however, are not as greatly different for the various planets.

Effect of Lift on Deceleration, Heating Rate, and Total Heat Absorbed During Entry From Decaying Orbits

From the relative values of deceleration and heating for various planets, together with the Z functions already presented, certain quantities of practical interest readily can be computed. The remainder of this report concerns such application of the Z functions for the various types of entry. In the present section we discuss first lifting entry from decaying orbits ($\bar{u}_i = 1$, $\varphi_i = 0$).

Deceleration.- A plot of the horizontal deceleration du/dt in g's for the earth's atmosphere (equal to 30 $\bar{u}Z$) is presented in figure 10 as a function of the dimensionless velocity $\bar{u}$ for various lift-drag ratios. The powerful effect of L/D ratios the order of only a few tenths is evident from this figure. It is also evident that the maximum deceleration occurs near a velocity of $\bar{u} \cong 0.4$. These curves are independent of the shape, size, and mass of the vehicle. The resultant deceleration is taken as $a = \sqrt{(du/dt)^2 + [(dv/dt) - (u^2/r) + g]^2}$. For no motion this expression reduces to g, the gravitational constant of the planet. By substituting equations (16) and (20) we have

$$\frac{a}{g} = \frac{\sqrt{\beta r}\ \bar{u}Z}{\cos \varphi} \sqrt{1 + \left(\tan \varphi - \frac{L}{D}\right)^2} \tag{51}$$

which, for small angles ($|\varphi| \ll L/D$, $\cos \varphi \cong 1$, $\tan^2 \varphi \ll 1$) yields

$$\left(\frac{a}{g}\right)_{max} \cong \sqrt{\beta r}(\bar{u}Z)_{max} \sqrt{1 + (L/D)^2}$$

A plot of this approximation for the maximum resultant deceleration is shown in figure 11 for the several planets considered. Once again the strong influence of the L/D ratio near L/D = 0 is evident. Also

evident are the relatively low decelerations for Mars compared to earth and Venus, and the relatively high values for Jupiter.

From the viewpoint of human tolerance to acceleration stress, it is not only the peak deceleration which must be considered, but also the orientation of the body, the duration of stress, and the rate of onset of deceleration. Numerous experiments with the human centrifuge have shown that human tolerance is greatest in transverse orientation; that is, with either chest-to-back or back-to-chest loading. Centrifuge experiments (see, e.g., ref. 16 and the references quoted therein) also have shown that the magnitude of acceleration is relatively more important than the duration, in the sense that if the acceleration is increased 10 percent, the tolerable duration is decreased by a factor of about 2. Thus, a method believed to be conservative for calculating the effective duration Δt during entry is to assume that the maximum deceleration acts over the entire time it would take for this deceleration to slow the vehicle from orbital velocity to rest. Curves of maximum deceleration versus duration computed in this manner are presented in figure 12 for various planetary atmospheres and for various L/D ratios. Included in this figure is a boundary representing human tolerance in the transverse orientation for conditions of rapid onset of acceleration (ref. 16 and references quoted therein). This boundary also is conservative inasmuch as entry decelerations are built up relatively slowly under which conditions, according to the centrifuge experiments of reference 17, the body circulation builds up a reflex action of effectiveness comparable to that provided by a G-suit. The conservative limits determined from this figure are indicated in figure 11. It is evident from both figures 11 and 12 that the decelerations for orbital entry into the earth's atmosphere are well within human tolerance even for nonlifting bodies. For Mars, human tolerance is sufficient to permit entry at sizable angles of descent or with negative lifting devices. Manned entry into Jupiter, however, would require a positive lifting body, or some other device in order to maintain the decelerations within human tolerance.

Heating rate.- In examining the effect of lift on convection aerodynamic heating of entering vehicles, we can use the same Z functions as employed in studying the decelerations. We note first that for many vehicles, the values of Reynolds number near peak heating are sufficiently low that one would expect a considerable extent of laminar flow, yet sufficiently high to be in continuum-gas flow rather than free-molecule flow. A plot of Re/l at peak heating is presented in figure 13 as a function of W/C_DA for entry from orbital decay into the earth's atmosphere. A vehicle on a large parachute would correspond to W/C_DA the order of 0.1 lb/ft^2, and, with $L/D = 0$, to Re of about 10^2 ft^{-1}. For such conditions the peak heating, which occurs at a Mach number $M_\infty \cong 20$, would be near the slip-flow regime ($Re/M_\infty \cong 1$). A reasonably blunt metallic structure would correspond to W/C_DA values the order of 10 to 100 lb/ft^2, and to values of Re/l the order of 10^3 to 10^5. Such values are well within the continuum regime, yet low enough to be associated with laminar

flow. The curves in figure 13 are for earth but can be applied to other planets by multiplying the ordinate by the value of the relative Reynolds number already tabulated for several planets.

For a given atmosphere the laminar heating rate is proportional to

$$\sqrt{\frac{W}{C_D A}}\,\bar{q} \equiv \sqrt{\frac{W}{C_D A}}\left(\bar{u}^{5/2} Z^{1/2}\right)$$

A plot of the dimensionless heating rate $\bar{q}$ as a function of $\bar{u}$ is presented in figure 14 for entry from decaying orbits. The maximum value occurs at a velocity $\bar{u}$ of about 0.8 and is a function only of the parameter $\sqrt{\beta r}(L/D)$ as follows:

$\sqrt{\beta r}(L/D)$	$(L/D)_{Earth}$	$\bar{q}_{max}$	$\bar{q}_{max}^{1/4}$
-15	-0.5	0.375	0.783
-7.5	-.25	.302	.741
-3	-.1	.253	.709
0	0	.218	.683
3	.1	.184	.656
7.5	.25	.138	.610
15	.5	.098	.560
30	1.0	.070	.514

For L/D ratios greater than 1 the asymptotic solution $Z_{II} = \dfrac{(1 - \bar{u}^2)}{\sqrt{\beta r}\,\bar{u}(L/D)}$ can be used to yield $\bar{q}_{max} = \dfrac{2}{3\sqrt{3\sqrt{\beta r}(L/D)}}$ as noted in appendix C.

We will consider that the vehicle dimensions and weight (R, A, and W) are fixed, and will study the influence of vehicle shape (C_D and L/D). Under these conditions the maximum heating rate is proportional to $\bar{q}_{max}/\sqrt{C_D}$. The effect of lift-drag ratio on maximum heating rate (which occurs at a $\bar{u}$ of roughly 0.8) is illustrated in figure 15 for entry from decaying orbits. The quantities plotted have been normalized to unity for $L/D = 0$, and can be applied directly to any planet, as can the curves in figure 14, by recalling that a given L/D for Earth is equivalent to a value $(\beta r)_{\oplus}^{1/2}$ times as much for a planet other than Earth. If the L/D ratio could be increased indefinitely without changing the drag coefficient such as by using reaction lift, then the maximum laminar heating rate would be proportional to the dotted line in figure 15 representing $\bar{q}_{max}$ and would decrease indefinitely with an increase in L/D

(asymptotically as $(L/D)^{-1/2}$ for L/D greater than about 0.5). Physically this decrease arises because the greater the lift, the less rapid the vehicle descends, so that the heating occurs at higher altitudes where the density is lower. On a practical device which uses aerodynamic lift, however, the L/D ratio cannot be increased much without making the vehicle more slender and decreasing C_D; a decrease in C_D increases the heating rate ($\sim 1/\sqrt{C_D}$) because it results in less slowing down, thereby causing the peak heating to occur at lower altitudes where the density is higher. As a result, there is an optimum L/D ratio for minimizing the heating rate which, for the three families of shapes indicated in figure 15, is near the range of L/D between about 0.5 and 1. For the family of half-cones and half-paraboloids, the L/D ratio was changed by changing the fineness ratio while maintaining the flat tops parallel to the stream direction. For the family of flat plates the L/D ratio was changed by changing the angle of attack. In all cases, C_D and L/D were computed for Newtonian flow. The optimum L/D ratio is seen to depend somewhat on the particular aerodynamic shape, since L/D and C_D are coupled somewhat differently for different shapes. It is evident that the net benefit to be gained by using aerodynamic lift amounts to about a factor of 2 in reducing the maximum rate of aerodynamic heating at a stagnation point.

Inasmuch as the optimum L/D ratios for minimizing the maximum heating rate are greater than about 0.5, they are in the range where the Z_{II} function for orbital decay is a good approximation near peak heating (see fig. 4(b)). From equations (36) and (41) we see that for a given planet and given radius at a stagnation point,

$$q \sim \sqrt{\frac{W}{C_D A}}\,\bar{q} \sim \sqrt{\frac{W}{C_D A}}\,\bar{u}^{5/2}\sqrt{\frac{1-\bar{u}^2}{\bar{u}(L/D)}}$$

since $L/D = C_L/C_D$,

$$q_{max} \sim \sqrt{\frac{W}{C_L A}} \tag{54}$$

and we see that the various minima in figure 15 each correspond to entering at $C_{L_{max}}$. The peak heating always occurs at a dimensionless velocity $\bar{u} = \sqrt{2/3} = 0.82$. For flat plates in Newtonian flow $C_{L_{max}} = 0.77$ at an a angle of attack of 55°, for which $L/D = 0.71$. As noted in appendix C, these conditions also turn out to represent optimum ones for minimizing the total heat absorbed for skipping-type entry, because in this case also $\bar{q}$ and $\bar{Q}$ vary as $(L/D)^{-1/2}$.

Surface temperature for radiation equilibrium.- The stagnation surface temperature experienced during entry of a structure having relatively small heat capacity (e.g., a thin skin) is calculated by equating the

radiation heating rate to the convective heating rate. For entry from decaying orbits we may set $\cos \varphi = 1$, inasmuch as φ near peak heating varies from -2.6° to -0.2° as L/D varies from 0 to 1. We have

$$\epsilon\sigma T_{w_s}^4 = q_s = 590 \sqrt{\frac{m}{C_D A R}}\, \bar{q} \quad \text{Btu ft}^{-2}\text{sec}^{-1} \tag{55}$$

where ϵ is the surface radiative emissivity, R the radius of curvature, and $\sigma = 0.48\times10^{-12}$ Btu $ft^{-2}sec^{-1}$ $^\circ R^{-4}$ is the Stefan-Boltzmann constant. By substituting the value of g_c for Earth there results (for T_w in $^\circ R$, R in ft, W/C_DA in lb ft^{-2}),

$$T_{w_s}\epsilon^{1/4}R^{1/8} = 3840 \left(\frac{W}{C_D A}\right)^{1/8} \bar{q}^{1/4} \tag{56}$$

where $\bar{q}$ for laminar flow is equal to $\bar{u}^{5/2}Z^{1/2}$. The maximum value $\bar{q}_{max}^{1/4}$ is listed in the preceding table for entry from decaying orbits. Other types of entry would require the use of other Z functions, but equation (56) would remain unchanged. For a planet other than Earth, the radiation-equilibrium temperature calculated from the above equation for Earth would have to be multiplied by the 1/4-root of a quantity already tabulated; namely, the relative rate of heating $\bar{q}_\oplus$ for that planet. The relative radiation-equilibrium temperature factors $T_{w_\oplus} = q_\oplus^{1/4}$ are:

	$T_{w_\oplus}$
Venus	0.91
Earth	1.00
Mars	.55
Jupiter	2.7

A graph of the maximum temperature parameter $T_{w_s}\epsilon^{1/4}R^{1/8}$ for entry from decaying orbits is presented in figure 16 as a function of W/C_DA (W in Earth weight). It is noted that the numerical calculations for nonlifting satellites descending in the Earth's atmosphere, as reported by Kemp and Riddell (ref. 6) and by Gazley and Masson (ref. 5), agree well with the analytical variation represented by the present analysis.

The curves for T_{w_s} in figure 16 could be applied to other planets for any given value of $\sqrt{\beta r}(L/D)$ by multiplying the ordinate by the quantity $T_{w_\oplus}$ tabulated above. Since L/D is a more convenient variable than $\sqrt{\beta r}(L/D)$, however, a separate plot of the parameter $T_{w_s}\epsilon^{1/4}/(W/C_DAR)^{1/8}$ (which represents the maximum surface temperature that is experienced during entry for radiation equilibrium at a stagnation point of radius of curvature R) is presented in figure 17 as a function of L/D for several planets. The coupling between C_D and L/D is taken as that for the family of half-paraboloids. The others would not be

greatly different, as may be seen from the curves in figure 15. We can deduce from figure 17, for example, that a nonlifting body with $\epsilon = 0.9$, and $W/C_DAR = 1$ lb ft^{-3} (e.g., R = 1 ft and $W/C_DA = 1$ lb ft^{-2} or R = 10 ft and $W/C_DA = 10$ lb ft^{-2}) would experience during entry from orbital decay a maximum stagnation temperature of approximately 1000° F for Mars, 2000° F for Venus, 2200° F for Earth, and 6800° F for Jupiter.

Total heat absorbed.- It is emphasized that the effect of lift-drag ratio on the total heat absorbed Q is quite different from the effect just discussed on the heating rate q. The use of lift prevents a vehicle with a given drag coefficient from descending as rapidly as a nonlifting one, thus leading to lower heating rates at higher altitudes, but the lift also prolongs the descent markedly. This prolongation dominates over the reduced rate of heating, to lead to a net increase in total heat absorbed with increasing L/D. That the total heat absorbed must increase with an increase in L/D, may be clearly seen from the general equation

$$Q = \frac{C_F'}{2C_D}\left(\frac{S}{A}\right)\left(\frac{1}{2}mV^2\right) \tag{57}$$

developed by Allen and Eggers in reference 1. For a given C_D, an increase in L/D does not change the kinetic energy loss, but it does increase the effective laminar skin-friction coefficient C_F' inasmuch as the corresponding increase in altitude results in the heat being taken aboard at lower Reynolds numbers where C_F' is higher.

The quantitative magnitude of the increase in Q with an increase in L/D may be deduced from equation (39) for Q (which neglects the heat radiated from the surface). For a given atmosphere (given Pr, μ, g, r, β) and a given size and weight (A, R, W), Q for laminar flow and $\cos\varphi \cong 1$ is proportional to the quantity

$$\frac{\bar{Q}}{\sqrt{C_D}} = \frac{1}{\sqrt{C_D}}\int_{\bar{u}}^{\bar{u}_1}\frac{\bar{u}^{3/2}d\bar{u}}{Z^{1/2}}$$

where $\bar{Q}$ is a function of L/D and is very insensitive to the lower limit $\bar{u}$ down to which the integration is carried (providing $\bar{u}$ is small). For convenience in evaluating $\bar{Q}$ from the Z functions, we select an arbitrary upper limit $\bar{u}_1 = 0.99$. The following values for $\bar{Q}$ are obtained for entry from decaying orbits:

$\sqrt{\beta r}(L/D)$	$(L/D)_{Earth}$	for $\bar{u}_1 = 0.99$ $\bar{Q}$
-30	-1.0	0.75
-15	-.5	.93
-7.5	-.25	1.09
-3	-.1	1.23
0	0	1.36
3	.1	1.54
7.5	.25	1.90
15	.5	2.53
30	1.0	3.54

For L/D ratios greater than 1 the asymptotic Z_{II} function can be used to yield $\bar{Q}_{II} = 0.62(\beta r)^{1/4}\sqrt{L/D}$ for the heat absorbed between $\bar{u}_1 = 0.99$ and $\bar{u} \cong 0$. (See appendix C for a more general expression for $\bar{Q}_{II}$.)

The effect of lift-drag ratio on the total convective heat absorbed (disregarding radiation from the surface) during entry into the earth's atmosphere from decaying orbits is plotted in figure 18. These curves are normalized to unity for L/D = 0. In contradistinction to the effect on q, an increase in L/D by itself is seen to always increase $\bar{Q}$, and hence Q, as anticipated from equation (57). When the coupling between L/D and C_D is considered, an optimum occurs at negative L/D ratios, near the range -0.7 to -0.5. In view of the fact that these negative L/D ratios result in high decelerations (fig. 11) they would not be feasible for a manned entry into the earth's atmosphere; the practical optimum for a heat-sink vehicle would be near L/D = 0.

In figure 19 curves are presented of the total heat absorbed per unit area during entry into various planets from decaying orbits. Radiation from the surface is disregarded for these curves. They represent the family of half-paraboloids, but the other families would not be significantly different. As would be expected, the minimum for each planet occurs at a negative L/D ratio. For Mars the decelerations are not excessive for L/D near -0.5 (see fig. 11) but the reduction in total heat absorbed compared to a nonlifting vehicle is only about 10 percent.

Nonlifting Entry From Deflected Orbits

In the discussions thus far we have considered only the trajectories resulting from decaying orbits wherein the initial descent angle is essentially zero. This type of entry leads to relatively shallow angles of descent with relatively low heating rates, but provides very little control over the time of entry and the location of impact. One method commonly envisioned to fix the time of entry, and greatly improve the accuracy of landing in a predetermined area, is to induce entry by

suddenly deflecting an orbit so as to enter at some initial flight path angle φ_i. A retrorocket force, for example, or a rocket force applied in the direction toward the planet center will initiate such entry. Induced entry of this type, however, results in greater decelerations and can affect the aerodynamic heating problem either adversely or favorably.

A curve is presented in figure 20(a) showing the effect of initial angle φ_i on the maximum deceleration experienced during entry of nonlifting vehicles into the earth's atmosphere. Also shown for comparison is the approximate limit of human tolerance (for rapid onset with transverse orientation), and a dotted curve corresponding to the Allen-Eggers theory for φ = constant = φ_i. This theory for $\bar{u}_i = 1$ can be used for descent angles greater than about 4° or 5°. Above about $-\varphi_i = 3^\circ$ the decelerations exceed human tolerance, so that some method of deceleration alleviation, such as provided by lift, or by increasing the value of W/C_DA during descent, would have to be employed for manned vehicles entering at these larger angles of descent. The curve of $(d\bar{u}/dt)_{max}$ in Earth g's can be applied to any planet by regarding the abscissa scale as being $-(\sqrt{\beta r})_\oplus \varphi_i$ and then multiplying the ordinate scale by $(g\sqrt{\beta r})_\oplus$.

The effect of initial angle on maximum laminar heating rate and on the total laminar heat absorbed is shown in figure 20(b). As would be expected, the steeper the descent the greater the heating rate. The total heat absorbed, however, is less for the steeper descents because the shorter duration more than compensates for the greater laminar heating rates. Equation (57) shows that this must be the case, since entry at larger angles results in the heat being taken aboard at lower altitudes where the laminar skin-friction coefficients are small. If the flow were turbulent the corresponding reduction in C_F' and hence in $\bar{Q}$ with an increase in descent angle would be less. The curves in figure 20(b) approach the curves developed from the Z_I function corresponding to the solution of Allen and Eggers (see eqs. (C3) and (C4) of appendix C). In order to be consistent with the other values of $\bar{Q}$ representing the heat absorbed from $\bar{u} = 0.99$ to $\bar{u} \cong 0$, a calculated factor 0.84 has been applied to equation (C4) which represents the heat absorbed from $\bar{u} = 1$ to $\bar{u} = 0$. It is seen from figure 20(b) that the Allen-Eggers solution for heat transfer in this case ($\bar{u}_i = 1$) is quite accurate for descent angles greater than about 2°. The curves in figure 20(b) can be applied to other planets by regarding the abscissa as a scale for the quantity $-(\sqrt{\beta r})_\oplus \varphi_i$.

In the figure 20(c) a curve is presented showing the strong influence of initial descent angle on entry range for Earth. Two incremental ranges are shown: a solid line curve for the distance between the point where $\bar{u} = 0.995$ and the impact point ($\bar{u} = 0$), and a dashed-line curve for the distance between $\bar{u} = 0.99$ and impact. From the slope of the solid-line curve we obtain the lower curve shown of average miss distance for an error in φ_i of 0.5°. It is to be remembered that this miss distance curve does not consider the essentially dragless portion of a deflected orbit from the point of orbit deflection to the point where $\bar{u} = 0.995$, and hence it is indicative of only the entry portion of the practical

problem of estimating miss distance. The curve illustrates, however, the advantage of using a small initial descent angle in order to greatly improve the ability to determine impact point.

A further contribution to miss distance which can be studied with the present equations is that due to atmospheric variations in temperature with either season or latitude. Equation (28) shows that $\Delta s \sim (\sqrt{\beta r})^{-1}$, so that a ±15-percent seasonal variation in temperature would correspond to a ∓7-percent variation in $\sqrt{\beta r}$ and in Δs. For small initial angles, say $\varphi_i = -1^\circ$, the range during entry from $\bar{u} = 0.995$ to impact is roughly 1000 miles according to figure 20(c), and hence the impact point would vary ±70 miles. The entry range would be greater in summer than in winter.

A graph of the Reynolds number per foot at peak heating for nonlifting entry into the earth's atmosphere with $\bar{V}_i = 1$ is presented in figure 21 for $-\varphi_i = 0^\circ$, 5°, 10°, 20°, 40°, and 90°. The $-\varphi_i = 0^\circ$ curve is based on the Z function of figure 4(a). All others are based on the Z_I function corresponding to the Allen-Eggers solution. Entry at other values of $\bar{V}_i$, according to this solution, results in values of Re proportional to $\bar{V}_i$.

Lifting Entry From Deflected Orbits

If a vehicle with $L/D > 0$ enters the atmosphere from a deflected orbit at a sufficiently large initial angle of descent, the entry trajectory is comprised of one or more skips. This is to be expected on physical grounds and is evident from the Z functions already presented in figures 6(b) to 6(e). During the first portion of descent, a vehicle undergoing a sizable skip will, at the bottom of the skip, decelerate and take on heat at a lower altitude than a vehicle at the same velocity which glides in smoothly from a decaying orbit ($\varphi_i = 0$). For large initial angles of descent, then, we might expect a skipping vehicle entering from a deflected orbit to experience greater decelerations, higher heating rates, and shorter entry range than a gliding vehicle entering from a decaying orbit. On the other hand, since the skipping vehicle takes on most of its heat at a lower altitude (where the skin-friction coefficients are lower) we would expect from equation (57) that the skipping vehicle would absorb less total heat during entry than the orbiting-decay vehicle. Calculations from the Z functions of figures 6(b) to 6(e) show these various expectations to be the case for initial descent angles $-(\varphi_i)_{\text{Earth}}$ greater than about 1°. This is illustrated in figure 22(a) for maximum laminar heating rate, in figure 22(b) for total laminar heat absorbed, and in figure 22(c) for entry range. The expected increase in deceleration is already evident from figures 6(b) to 6(e) which show $30\ \bar{u}Z \sim du/dt$ as the ordinate.

If a vehicle with $L/D > 0$ enters the atmosphere from a deflected orbit at a very small initial angle of descent, so that the trajectory

might be described more appropriately as a rippling descent rather than a skipping one, then the peak deceleration and maximum heating rates can actually be slightly smaller than for the same vehicle gliding in from a decaying orbit. What happens in such cases may be seen, for example, in figure 6(c) by comparing the curves for $-\varphi_i = 1^\circ$ and $-\varphi_i = 0^\circ$. The rippling entry ($-\varphi_i = 1^\circ$) has one maximum on each side of the maximum for $-\varphi_i = 0^\circ$ representing orbital-decay entry. These two maxima in deceleration for $-\varphi_i = 1^\circ$ are slightly less than the single maximum for $-\varphi_i = 0^\circ$. A similar situation can exist for the maxima in heating rate. As a result, the curves in figure 22(a) for the dimensionless maximum heating rate $\bar{q}_{max}$ for lifting vehicles entering from deflected orbits show slight waviness and sometimes slight reductions below the values for $-\varphi_i = 0$ when the initial descent angle is less than about $1/2^\circ$ to 1°. Consequently, we can say that, in principle, a rippling-type descent from a deflected orbit can have lower maximum heating rates than a gliding descent, but for practical purposes, there is no significant difference between the two.

Composite Entry

It may be desirable to combine lifting and nonlifting entry in order to achieve some advantages of both types. For landing maneuverability it obviously is advantageous to employ a lifting vehicle. The total heat absorbed by a lifting vehicle, however, is much higher than for a nonlifting vehicle (fig. 18). The optimum use of aerodynamic lift reduces the maximum heating rate only to about one-half that of a nonlifting vehicle of the same W/A. Nonlifting vehicles can more easily be constructed with much lighter W/A ratios by employing, for example, a large, light drag device (for example, a parachute). The larger the device, the smaller is the heating rate ($q \sim 1/\sqrt{A\bar{l}} \sim \bar{l}^{-3/2}$), the smaller the entry Reynolds numbers ($Re \sim (W/C_DA)\bar{l} \sim \bar{l}^{-1}$), and the better the possibilities are of maintaining laminar flow. Nonlifting vehicles with shuttlecock stability are advantageous also from the viewpoint of minimum control requirements during entry. Hence, an evident composite type of entry, which combines some of the desirable features of lifting and nonlifting trajectories, would be to enter first without lift but with a small W/C_DA provided by a drag device; then, when the velocity is reduced to a certain value $\bar{u}_b$ the device is jettisoned or retracted, leaving a lifting vehicle of larger W/C_DA for the remainder of the descent.

A practical compromise is required in selecting $\bar{u}_b$, because the drag device should be jettisoned as soon as possible from the viewpoint of achieving maximum maneuvering range, but as late as possible from the viewpoint of achieving major reductions in heating rate. For the initial nonlifting portion of descent let the drag-weight parameter be $(W/C_DA)_0$ and the Z function be Z_0. For the subsequent portion let the corresponding quantities be $(W/C_DA)_1$ and Z_1. Since the altitude y and the

angle of descent φ are continuous at the break velocity $\bar{u}_b$, we have two conditions from equations (14) and (17)

$$(Z_1)_b \sqrt{\left(\frac{W}{C_D A}\right)_1} = (Z_o)_b \sqrt{\left(\frac{W}{C_D A}\right)_o} \tag{58}$$

$$\left(Z_1' - \frac{Z_1}{\bar{u}}\right)_b = \left(Z_o' - \frac{Z_o}{\bar{u}}\right)_b \tag{59}$$

for determining the initial conditions $Z_{1_i} \equiv Z_{1_b}$ and $Z_{1_i}' \equiv Z_{1_b}'$ for the second portion of descent. Hence the Z_1 function can be determined approximately from equation (C13) of appendix C by substituting $\bar{u}_i = \bar{u}_b$, $Z_i = Z_{1_b}$, $\sin \varphi_i = \varphi_b$, and $\cos \bar{\varphi} = 1$. The maximum heating rate occurs near the bottom of the first dip after the break, and can be obtained from equation (C24) in appendix C with the same substitutions. The total heat absorbed in this dip can be obtained from equation (C25).

As an example let us consider the case of a large drag device ($(W/C_D A)_1 \gg (W/C_D A)_o$) jettisoned at a velocity $\bar{u}_b$ during entry from a decaying orbit. In order to minimize the peak heating after jettisoning, as well as minimize the total heat absorbed during the skip, a value $L/D \cong 0.7$ is selected. Curves showing the resulting values for maximum heating rate $\bar{q}_m$ after jettisoning, and total heat absorbed $\bar{Q}_1$ during the first skip, are presented in figure 23 as a function of the break velocity $\bar{u}_b$. We see that a large drag device carried down to $\bar{u}_b = 0.4$, for example, would have a maximum heating rate about 1/4 of that for the same vehicle with no drag device.

It may be noted that the deceleration history for a drag device jettisoned at $\bar{u}_b = 0.4$, for example, is essentially the same as the acceleration history investigated in the human centrifuge tests of reference 18. The select individuals for these centrifuge tests did not blackout (or grayout, or even get dizzy) during the runs. They were able to perform continually simple dual control operations even when the acceleration dropped suddenly from about 8g to about 2g.

Comparison of Several Types of Entry With $\bar{u}_i = 1$

It is interesting to compare the relative magnitude of aerodynamic heating for the several types of entry discussed. The dimensionless maximum heating rate $\bar{q}_m$ and the dimensionless total heat absorbed $\bar{Q}$ are used for this comparison. They would be proportional to the actual

heating rate and the total heat absorbed for vehicles of the same size and W/C_DA. The table which follows summarizes these quantities for seven different types of entry, all starting with $\bar{u}_i = 1$.

Type of entry	L/D	$\bar{q}_{max}$	for $\frac{\bar{Q}}{\bar{u}_i} = 0.99$
Near optimum glide, for minimum q_{max} ($\varphi_i = 0$)	0.7	0.084	3.0
Near optimum ripple for minimum q_{max} ($-\varphi_i = 0.5^\circ$)	.7	.083	2.9
Near optimum glide, for minimum Q ($\varphi_i = 0$)	-.5	.78	.93
Near optimum first skip for minimum Q	.7	.15($-\varphi_i = 2^\circ$)	.90
Nonlifting ($\varphi_i = 0$)	0	.22	1.4
Nonlifting, from deflected orbit with $-\varphi_i = 2^\circ$	0	.27	.93
Composite, large drag device jettisoned at $\bar{u}_b = 0.4$	0 for $\bar{u} > 0.4$ 0.7 for $\bar{u} < 0.4$	.02	.16

In comparing these values it should be remembered that the actual quantities of interest for a given W/A are $q_{max}/\sqrt{C_D}$ and $\bar{Q}/\sqrt{C_D}$, and that nonlifting vehicles are placed at a small disadvantage in the table because they presumably can be designed with somewhat higher values of C_D than lifting vehicles. It is noted that the total heat absorbed in the case of the skip vehicle, corresponds only to the first skip. Presumably this is all that should be considered if the vehicle is designed, as suggested by Ferri (ref. 7), to radiate essentially all of the heat absorbed after each skip.

Atmosphere Braking

During entry of a planet's atmosphere from space at near escape velocity, possibly severe deceleration and heating problems can occur during the process of passing through an outer segment of the atmosphere. The closer a pass is made to a planet surface, the greater is the braking action, the greater the deceleration, and the greater the rate of aerodynamic heating. The Z functions for four different entry histories of nonlifting vehicles starting with escape velocity ($\bar{u}_i = 1.4$) have already

been presented in figure 7. These functions apply to any planet. They are based on the assumption that after the initial pass no further control of the vehicle is exercised.

Entry (a) is initiated with $30(\bar{u}Z)_{max} = 0.46$ during the first pass (0.46 g maximum deceleration for earth) and corresponds to a dimensionless peak heating rate of $\bar{q}_{max} = 0.24$ at $\bar{u} = 1.38$. The successive peaks correspond to $\bar{q}_{max}$ progressively less, while the seventh pass, which starts from $\bar{u} = 1.08$ and completes the entry, corresponds to $\bar{q}_{max} = 0.20$. As might be expected this is not far from the value 0.22 corresponding to orbital decay from $\bar{u}_i = 1$ with $L/D = 0$. Since $\bar{q}_{max}$ is a measure of the maximum temperature experienced by a radiation-cooled vehicle, it follows that entry of such a vehicle could be completed on the seventh pass, without the temperature during any of the atmosphere braking passes exceeding appreciably that experienced during orbital decay.

Entry (b) in figure 7 is initiated with $30(\bar{u}Z)_{max} = 1.65$ in the first pass during which an amount of heat is absorbed corresponding to $\bar{Q} = 1.5$. This heat could be radiated to space before the second pass is made in which an additional amount $\bar{Q} = 1.4$ is absorbed. The third pass starts from $\bar{u} = 1.09$ and completes the entry with $\bar{Q} = 1.7$. These values are not far from the value $\bar{Q} = 1.4$ corresponding to orbital decay with $L/D = 0$. Since $\bar{Q}$ is a measure of the total heat absorbed by a heat-sink vehicle, it follows that such a vehicle could complete an entry on the third pass without absorbing much more heat during each of the two atmosphere braking passes than that absorbed during orbital decay.

Entries (c) and (d) in figure 7 are completed in a single pass and both lose an amount of kinetic energy $(1/2)m(1.4\sqrt{gr})^2 = mgr$. They absorb a quantity of heat corresponding to $\bar{Q} = 2.9$ and $\bar{Q} = 2.1$, respectively, and experience maximum heating rates corresponding to $\bar{q}_{max} = 0.58$ and $\bar{q}_{max} = 0.73$, respectively. The total laminar heat absorbed by (d) is less than (c), even though the maximum heating rate is greater, because entry (d) corresponds to a closer pass to the planet surface for which the heat is taken aboard, on the average, at lower altitudes where the friction coefficients are lower (see eq. (57)).

In addition to the four Z functions just discussed, a number of Z functions (not presented) have been computed for lifting vehicles undergoing single atmosphere braking passes in which the entering velocity is $\bar{u}_i$ and the exit velocity is $\bar{u}_{ex}$. Results are presented in figure 24 for $\bar{u}_i = 1.4$ and in figure 25 for $\bar{u}_i = 1.2$. In each figure curves are presented for the maximum value of horizontal deceleration $30(\bar{u}Z)_{max}$, the dimensionless maximum laminar heating rate $\bar{q}_{max}$, and the dimensionless laminar heat absorbed $\bar{Q}$ during the single pass. The curves are labeled as to the L/D values corresponding to earth; they also can be applied to other planets by recalling that a given value of L/D on Earth is equivalent to a value $(\beta r)_{\oplus}^{-1/2}$ times as much on another planet.

An interesting feature of these results for single atmosphere brakings is that for a given loss in kinetic energy (given $\bar{u}_{ex}$), they exhibit the opposite variation with L/D from that previously found for orbital decay. Thus, an increase in L/D decreases the maximum deceleration for orbital decay but increases it for atmosphere braking; an increase in L/D decreases the heating rate $\bar{q}_{max}$ for orbital decay but increases it for atmosphere braking; an increase in L/D increases the heat absorbed $\bar{Q}$ for orbital decay but decreases it for atmosphere braking. From a mathematical viewpoint the reason for this contrasting behavior is that the gravity minus centrifugal force term $(1 - \bar{u}^2)/\bar{u}Z$ in the basic differential equation changes algebraic sign at $\bar{u} = 1$. From a physical viewpoint, the effect of L/D on atmosphere braking can be understood by noting that in order to lose the same amount of kinetic energy, a lifting vehicle must pass closer to the surface than a nonlifting one. Hence at the lower altitude the deceleration and rate of heating of the lifting vehicle are greater, while the friction coefficients are smaller and hence the heat absorbed for a given loss in kinetic energy is smaller (see eq. (57)).

A plot of the maximum surface temperature parameter $T_{w_s}\epsilon^{1/4}/(W/C_DAR)^{1/8}$ as a function of the maximum deceleration in Earth g's is presented in figure 26 for atmosphere braking in various planets with L/D = 0. These curves are for a single pass starting with $\bar{u}_i = 1.4$. It is seen that in the earth's atmosphere, for example, the maximum deceleration that can be experienced in a single pass and still enable the vehicle to exit from the atmosphere at some velocity $\bar{u}_{ex} > 1$, is about 3.5g. If the nonlifting vehicle attempts to decelerate more than this by passing closer to the surface, then before it exits from the atmosphere, the velocity is reduced to $\bar{u} = 1$ at some point within the atmosphere and the vehicle completes entry in a single pass experiencing at least 7.2g deceleration in the process. Any pass still closer to the surface only increases further the maximum deceleration and temperature. When the maximum deceleration during a single pass jumps discontinuously from 3.5g to 7.2g, the corresponding maximum temperature does not jump because the maximum temperature already has been experienced before $\bar{u} = 1$ was reached. The limiting maximum deceleration for atmosphere braking in Mars is seen to be much less (0.7 Earth g), and for Jupiter much more than for Earth.

A companion plot to figure 26, only for the laminar heat absorbed per unit area in a single pass, is presented in figure 27. These curves also are for L/D = 0 and $\bar{u}_i = 1.4$. In this case, the heat absorbed increases discontinuously when the maximum deceleration increases discontinuously (from 3.5g to 7.2g for Earth) because of the additional loss in kinetic energy. Any pass still closer to the surface increases the deceleration but decreases the laminar heat absorbed. This decrease exists because, for a given loss in kinetic energy, any pass taking on its heat at lower altitudes will have smaller laminar friction coefficients, and hence less total heat absorbed (see eq. (57)).

CONCLUDING REMARKS

An approximate analytical solution for the motion and aerodynamic heating of a lifting vehicle entering a planetary atmosphere has been obtained by disregarding two relatively small terms in the complete motion equations, and then introducing a mathematical transformation which reduces the pair of motion equations to a single, ordinary, nonlinear differential equation. Relatively few solutions to this differential equation provide quite general results inasmuch as the basic equation is independent of the physical characteristics of a vehicle, as well as independent of the sea-level characteristics of an atmosphere. The solutions apply to any exponential planetary atmosphere.

Certain asymptotic solutions in closed form result from a process of truncating various combinations of terms from the basic nonlinear differential equation. The aggregate of terms represents vertical acceleration, vertical component of drag force, gravity force, centrifugal force, and aerodynamic lift force. This truncation procedure yields an asymptotic solution for ballistic vehicles entering at relatively steep angles of descent (which solution is identical to that of Allen and Eggers), an asymptotic solution for glide vehicles of relatively large lift-drag ratio, and a solution for skip vehicles.

Comparison of the present solution for an idealized exponential atmosphere with digital computing-machine results for a standard atmosphere reveals differences the order of about ±10 percent. These relatively small differences are due primarily to the variations in atmospheric temperature with altitude in the standard atmosphere. The present analytic solution enables corrections readily to be made in order to yield results applicable to any standard atmosphere, or to an atmosphere which has variations in temperature with season or with latitude.

Maximum deceleration during entry into an exponential atmosphere from a decaying orbit does not depend on the vehicle weight, shape, or dimensions; it occurs at a velocity of about 0.4 of orbital velocity, and is much less for lift-drag ratios as small as a few tenths than for a lift-drag ratio of zero. Even for nonlifting vehicles, though, the decelerations are within human tolerance for Earth and Venus, and far below for Mars. Manned entry into Jupiter would require a lifting vehicle in order to avoid excessive decelerations.

For vehicles entering from a decaying orbit with aerodynamic lift, the maximum heating rate depends strongly on the vehicle weight, shape, and dimensions through the parameter W/C_DA; maximum heating occurs at a velocity of about 0.8 of orbital velocity, and, for any given loading W/A, is minimum for entry at $C_{L_{max}}$. This corresponds for common shapes to optimum L/D ratios between about 0.5 and 1.0. Because of the

coupling between C_D and L/D for any aerodynamic shape, the use of a near optimum L/D can reduce the maximum heating rate to no more than about one-half that for a nonlifting vehicle.

The laminar heating rate varies directly as $\sqrt{W/C_DA}$; hence, by using a drag device to increase markedly C_DA, such as a drag parachute or flare, much larger reductions in heating rate are possible than through the use of a trimmed lifting vehicle.

The total heat absorbed during entry from a decaying orbit increases rapidly with lift-drag ratio for vehicles with positive lift. It is a minimum for lift-drag ratios near about -0.5, but these negative lifts result in excessive decelerations for manned entry into the earth's atmosphere; hence the practical optimum for minimizing the total heat absorbed in orbital-decay entry of a manned vehicle is near a lift-drag ratio of zero. The total laminar heat absorbed, like the laminar heating rate, varies directly as $\sqrt{W/C_DA}$.

By inducing entry at a sizable initial angle of descent, the total heat absorbed for laminar convection can be reduced substantially. The limit of human tolerance to deceleration stress is closely approached for nonlifting vehicles entering the earth's atmosphere at an initial descent angle of about 3°, under which conditions the total heat absorbed is 0.6 of that for a decaying orbit having zero initial angle of descent, while the decelerations and the maximum heating rate are correspondingly increased. However, if a vehicle with small aerodynamic lift (say, $L/D \leq 0.7$, approximately) enters with a small initial angle, the trajectory is a rippling descent which can have a slightly lower maximum heating rate as well as smaller total heat absorbed than for gliding entry from a decaying orbit.

The total heat absorbed during the first skip of a lifting vehicle entering at a sizable initial angle of descent, is essentially independent of both the angle of descent and the velocity of exit from the skip. It is a minimum for entry at $C_{L_{max}}$ (lift-drag ratios near 0.7). For a given W/C_DA, this minimum total heat absorbed during the first skip is roughly the same as that absorbed during the entry of a nonlifting vehicle entering at an initial angle of descent of about 2°.

In the process of atmosphere braking for stepwise slowing a space vehicle from near escape velocity to circular orbital velocity, the effects of L/D on peak deceleration, on maximum heating rate, and on total heat absorbed are the opposite to the corresponding effects in the process of orbital-decay entry. For example, an increase in L/D with a given C_D increases the maximum heating rate in atmosphere braking, but decreases it in orbital decay. For nonlifting vehicles starting with escape velocity and employing atmosphere braking, entry to a planet surface can be completed on the third pass without the total heat absorbed

in any pass exceeding that absorbed for orbital decay, and can be completed on the seventh pass without the maximum rate of heating exceeding that for orbital decay.

Ames Aeronautical Laboratory
National Advisory Committee for Aeronautics
Moffett Field, Calif., Apr. 9, 1958

APPENDIX A

CHECK ON APPROXIMATIONS MADE IN ANALYSIS

The basic approximation (a) of the analysis, as represented by equation (8), can be expressed fairly simply in terms of the transformed variable Z and the angle of descent

$$\frac{|dr/r|}{|du/u|} = \frac{|\bar{u}(dy/dt)|}{|r(d\bar{u}/dt)|} = \frac{\bar{u}|\sin \varphi|}{\sqrt{\beta r}\, Z} \ll 1$$

Inasmuch as $Z/\bar{u} \sim \rho_\infty$, this shows that approximation (a) cannot be valid at very high altitudes which are represented by a small neighborhood near $\bar{u} = \bar{u}_i$ and $Z = 0$. In figures 28(a) and 28(b), curves of the ratio $(dr/r)/(du/u)$ are shown for lifting entry into the earth's atmosphere from decaying orbits and for nonlifting entry from deflected orbits with various initial angles φ_i. It is evident that in the regions near peak heating ($\bar{u} \cong 0.8$) and near peak deceleration ($\bar{u} \cong 0.3$ to 0.5) the basic approximation should introduce errors the order of only 1 percent. As a vehicle initially enters the atmosphere, however, the decelerations are very small and the errors introduced are larger. As a general rule, approximation (a) is valid for engineering calculations once the air drag has reduced the velocity by about one-half of one percent (see appendix B). Approximation (b), that $(L/D)|\tan \varphi| \ll 1$ likewise is a valid one for heat transfer and deceleration calculations of vehicles with zero or positive lift entering from decaying orbits. As figure 28(c) illustrates, approximation (b) may result in substantial errors near maximum deceleration for vehicles having negative lift, but still results in reasonably small errors near peak heating of such vehicles.

APPENDIX B

MATCHING PRESENT SOLUTION TO KEPLERIAN ELLIPSE

Let us assume that a retrorocket force, or some other force, has deflected an orbiting vehicle into a new Keplerian ellipse which, in the absence of drag, would intersect the planet surface at some angle φ_o. A "zeroth order" approximation would be to use this angle in the present solution as the initial angle φ_i for the entry. This would be sufficiently accurate for descent angles greater than a few degrees, but for very small angles of descent a more accurate matching of the present solution to the Keplerian ellipse may be desirable.

Since the present solution assumes that $|dr/r| \ll |du/u|$ whereas the conservation of angular momentum requires that $dr/r = -du/u$ outside the atmosphere, it seems reasonable to select the point of matching where the ratio $(dr/r)/(du/u)$ is some value less than unity. Let the descent angle at the point of matching be φ_m, and the velocity be $\bar{u}_m$. Let us confine our attention to a small region near matching, where the density is very low, the aerodynamic forces are very small, and the flight path is only slightly curved. We represent the Z function in this region by the approximation Z_I from equation (40) for constant angle of descent, namely,

$$Z_m \cong \sqrt{\beta r}\, \bar{u}_m \sin \varphi_m \ln(\bar{u}_m/\bar{u}_i)$$

Since $\bar{u}_m$ is only slightly less than $\bar{u}_i$ we approximate $\ln(\bar{u}_m/\bar{u}_i)$ by $(\bar{u}_m - \bar{u}_i)/\bar{u}_i$. Hence from equation (22), it follows that at the matching point the ratio $\tilde{r}_m$ of terms discarded to terms retained is

$$\tilde{r}_m \equiv \frac{dr/r}{du/u} = -\frac{\bar{u}_m \sin \varphi_m}{\sqrt{\beta r}\, Z_m} \cong \frac{\bar{u}_i}{(\beta r)(\bar{u}_i - \bar{u}_m)} \tag{B1}$$

For Earth $\beta r = 900$, so that $\tilde{r}_m = 1$ at $\bar{u}_m = 0.999\, \bar{u}_i$, $\tilde{r}_m = 0.2$ at $\bar{u}_m = 0.995\, \bar{u}_i$, and $\tilde{r}_m = 0.1$ at $\bar{u}_m = 0.99\, \bar{u}_i$. Thus, it would be reasonable to match the present solution with a Keplerian ellipse at some velocity in the range, say, $\bar{u}_m = 0.995\, \bar{u}_i$ to $\bar{u}_m = 0.99\, \bar{u}_i$. The density ρ_m at the matching altitude (from the defining equation (14) for Z and from equation (B1)) can be determined from

$$\frac{\sqrt{r/\beta}\, \rho_m}{2(m/C_D A)} = Z_m \cong \sqrt{\beta r}\, (\bar{u}_i - \bar{u}_m)(-\sin \varphi_o) \tag{B2}$$

$$\rho_m = 2\left(\frac{m}{C_D A r}\right) \frac{\bar{u}_i}{\tilde{r}_m} (-\sin \varphi_o) \tag{B3}$$

or, from ρ_m we can determine the altitude y_m and hence the corresponding value of φ_m from the Keplerian ellipse at this altitude. The value of φ_m so determined would be the value of φ_i which closely matches the present solution for the entry motion.

An equivalent way of matching would be to select first arbitrarily various altitudes $y_1, y_2, y_3, \ldots$ and corresponding densities $\rho_1, \rho_2, \rho_3, \ldots$. From the Keplerian ellipse the slightly different angles $\varphi_1, \varphi_2, \varphi_3, \ldots$ could be determined, and by substitution of these into equation (B3) in place of φ_o, the respective values $(m/C_DA)_1$, $(m/C_DA)_2, \ldots$ which would bring about proper matching for a given value of $\tilde{r}_m$ (say, 0.1) could be computed. Interpolation would yield the matching angle φ_m, and the matching altitude y_m for any desired value of m/C_DA.

APPENDIX C

DEVELOPMENT OF SOME APPROXIMATE SOLUTIONS

The first approximate solution is that for entry of a nonlifting vehicle along a spiral path which makes a constant angle $\bar{\varphi}$ with respect to the local horizontal direction. For this first special case we designate the Z function by Z_I, and see from the right members of equation (19) that

$$\frac{d}{d\bar{u}}(\sin\varphi) = 0 = \bar{u}Z_I'' - \sqrt{\beta r}\sin\bar{\varphi}$$

or, after one integration,

$$Z_I' = \sqrt{\beta r}\sin\bar{\varphi}\ln\bar{u} + \text{constant} \tag{C1}$$

The integration constant can be evaluated in terms of the initial velocity $\bar{u}_i$ and the angle $\bar{\varphi}$, to yield after one more integration for entry from high altitudes ($Z_i = 0$),

$$\frac{Z_I}{\bar{u}\sqrt{\beta r}\sin\bar{\varphi}} = \ln\frac{\bar{u}}{\bar{u}_i} = \frac{C_D A\bar{\rho}_o}{2m\beta\sin\bar{\varphi}}e^{-\beta y} \tag{C2}$$

from which it follows that the dimensionless laminar heating rate $\bar{q}_I \equiv \bar{u}^{5/2}Z_I^{1/2}$ has a maximum value

$$\bar{q}_{I_{max}} = 0.247\,\bar{u}_i^{3}(\beta r)^{1/4}\sqrt{\sin(-\bar{\varphi})} \tag{C3}$$

and the dimensionless total heat absorbed from $\bar{u} = \bar{u}_i$ to $\bar{u} = 0$ is evaluated by noting that the integral of equation (39b) is proportional to $\Gamma(1/2) = \sqrt{\pi/2}$.

$$(\bar{Q}_I) = \left(\frac{\bar{u}_i}{\cos\bar{\varphi}}\right)^2\frac{\sqrt{\pi/2}}{(\beta r)^{1/4}\sqrt{\sin(-\bar{\varphi})}} \tag{C4}$$

This solution for Z_I corresponds to setting the left members of equation (21) to zero. In order that the right members of equation (21a) also vanish, we see from equation (C2) that this special solution can be realized in two ways: (1) by maintaining a true spiral path through programming the lift with velocity in the very special way such that at all points

$$\frac{L}{D} = \frac{(1-\bar{u}^2)\cos\bar{\varphi}}{\bar{u}^2(\beta r)\sin\bar{\varphi}\ln(\bar{u}/\bar{u}_i)} \tag{C5}$$

or (2) by entering with a nonlifting vehicle along such a steep path that the gravity forces minus the centrifugal forces are negligible compared to the vertical component of drag force (this yields essentially a straight-line trajectory). Case (1) of spiral trajectories with programmed lift, is not easily realized in practice, but case (2) represents exactly the physical situation considered by Allen and Eggers (ref. 1) for their solution to the problem of ballistic entry. Hence, it should not be surprising that equation (C2) is identical to their solution. This solution for nonlifting vehicles at constant φ does not depart significantly from the complete solutions near peak heating ($\bar{u}/\bar{u}_i \cong 0.8$) except for initial descent angles less than a few degrees, and near maximum deceleration ($\bar{u}/\bar{u}_i \cong 0.4$ to 0.6) except for initial descent angles less than about 5°.

As a second special case, we consider smoothly gliding, hypersonic flight ($\bar{u}$ near 1) with a large L/D and at sufficiently small descent angles that $\cos\varphi \cong 1$ and $\sin\varphi \cong \varphi \ll L/D$. Under these conditions the left-hand terms of equation (21a) involving the normal deceleration and the vertical component of drag force can be disregarded. The right members yield for the special function Z_{II} representing balance between gravity, centrifugal, and lift forces,

$$Z_{II} = \frac{1 - \bar{u}^2}{\bar{u}\sqrt{\beta r}\,(L/D)} \tag{C6}$$

The flight-path angle is obtained from equation (17) by differentiating equation (C6)

$$-\varphi = \frac{2}{\beta r \bar{u}^2 (L/D)} \tag{C7}$$

This particular solution is the same as the solution for gliding flight orginally given by Sänger (refs. 2 and 3) for which the aerodynamic heating problems have been studied by Eggers, Allen, and Neice (ref. 4). This special solution is quite good for L/D ratios greater than about 1 (for Earth) and hence is adequate for most glide vehicle analysis. It cannot be applied, however, to entries with other than zero initial angle, inasmuch as extremely small initial angles of descent will result in a skipping trajectory for which the vertical acceleration term is not small compared to the lift force. For this gliding solution Z_{II} the maximum heating rate proportional to $\bar{q}_{max} = (\bar{u}^{5/2} Z^{1/2})_{max}$ occurs at $\bar{u} = \sqrt{2/3}$ with

$$(\bar{q}_{II})_{max} = \frac{2}{3\sqrt{3}\,(\beta r)^{1/4}\sqrt{L/D}} \tag{C8}$$

the dimensionless function proportional to the total heat absorbed is

$$\overline{Q}_{II} = (\beta r)^{1/4}\sqrt{\frac{L}{D}}\int_0^{\overline{u}_i}\frac{\overline{u}^2 d\overline{u}}{\sqrt{1-\overline{u}^2}} = \frac{(\beta r)^{1/4}}{2}\sqrt{\frac{L}{D}}\left(\sin^{-1}\overline{u}_i - \overline{u}_i\sqrt{1-\overline{u}_i^2}\right) \tag{C9}$$

and the range function is

$$\frac{\Delta s_{II}}{r} = \frac{L}{D}\int_0^{\overline{u}_i}\frac{\overline{u}\,d\overline{u}}{1-\overline{u}^2} = \frac{L}{2D}\ln\frac{1}{1-\overline{u}_i^2} \tag{C10}$$

as obtained in reference 4.

As a third special case, we consider entry with lift along a trajectory wherein the gravity minus centrifugal force is relatively small (see eq. (21a)). A skip vehicle, for example, would fall in this category. In this case the flight path is determined primarily by a balance between the normal acceleration term $\overline{u}Z'$, the lift term $\sqrt{\beta r}(L/D)\cos^3\varphi$, and the vertical drag component. The trajectory is, by assumption, influenced only secondarily by the gravity minus centrifugal force term $(1-\overline{u}^2)\cos^4\varphi/(\overline{u}Z)$; hence we may render the basic differential equation linear by supposing that Z in the denominator of this nonlinear term be approximated a priori by some Z function obtained either by neglecting this nonlinear term or obtained in some other way such as by expanding Z about $\overline{u}_i$. By writing $\cos\overline{\varphi}$ as the "average" value of $\cos\varphi$ for the flight path according to the theorem of the mean, we have, after one quadrature,

$$\frac{dZ}{d\overline{u}} - \frac{Z}{\overline{u}} = \cos^4\overline{\varphi}\int_{\overline{u}_i}^{\overline{u}}\frac{1-\overline{u}^2}{\overline{u}^2 Z}\,d\overline{u} - \cos^3\overline{\varphi}\sqrt{\beta r}\,\frac{L}{D}\ln\frac{\overline{u}}{\overline{u}_i} + \text{constant} \tag{C11}$$

at $\overline{u} = \overline{u}_i$; equation (17) shows that $(dZ/d\overline{u}) - (Z/\overline{u}) = \sqrt{\beta r}\sin\varphi_i$ hence the descent angle is given by

$$\sqrt{\beta r}\,(\sin\varphi - \sin\varphi_i) = \cos^4\overline{\varphi}\int_{\overline{u}_i}^{\overline{u}}\frac{1-\overline{u}^2}{\overline{u}^2 Z}\,d\overline{u} - \cos^3\overline{\varphi}\,\frac{L}{D}\sqrt{\beta r}\ln\frac{\overline{u}}{\overline{u}_i} \tag{C12}$$

and the Z function is obtained by solving the first-order differential equation (C11), noting that $1/\overline{u}$ is an integrating factor,

$$\frac{Z}{\overline{u}} = \frac{Z_i}{\overline{u}_i} + \cos^4\overline{\varphi}\int_{\overline{u}_i}^{\overline{u}}\frac{d\overline{u}}{\overline{u}}\int_{\overline{u}_i}^{\overline{u}}\frac{(1-\overline{u}^2)d\overline{u}}{\overline{u}^2 Z} + \sqrt{\beta r}\sin\varphi_i\ln\frac{\overline{u}}{\overline{u}_i} - \frac{\cos^3\overline{\varphi}}{2}\left(\frac{L}{D}\right)\sqrt{\beta r}\ln^2\frac{\overline{u}}{\overline{u}_i} \tag{C13}$$

By disregarding the gravity minus centrifugal force integral, we obtain a special function Z_{III} representing balance between normal acceleration, vertical drag component, and lift force,

$$\frac{Z_{III}}{\bar{u}} = \frac{Z_i}{\bar{u}_i} + \sqrt{\beta r}\left[\sin\varphi_i \ln\frac{\bar{u}}{\bar{u}_i} - \frac{\cos^3\bar{\varphi}}{2}\left(\frac{L}{D}\right)\ln^2\frac{\bar{u}}{\bar{u}_i}\right] \tag{C14}$$

and

$$\sin\varphi = \sin\varphi_i - \cos^3\bar{\varphi}\left(\frac{L}{D}\right)\ln\frac{\bar{u}}{\bar{u}_i} \tag{C15}$$

These last two equations for $L/D = 0$ reduce to equation (C2). If desired, we could substitute Z_{III} (or some other initial estimate of Z) into the denominator of the integrand in equation (C13), thus obtaining a correction term for the gravity minus centrifugal force term. The success of such a method would depend upon the accuracy and simplicity of the initial estimate.

To illustrate one application of the special solution Z_{III} given by equation (C14), we consider the first skip only of a lifting vehicle entering the atmosphere at a small angle φ_i ($\cos\varphi_i \cong 1$) and at orbital velocity ($\bar{u}_i = 1$). The first skip is generally the most severe from the heat-transfer viewpoint. We have for $Z_i = 0$,

$$\frac{Z_{III}}{\bar{u}} = \sqrt{\beta r}\left(\varphi_i \ln\bar{u} - \frac{L}{2D}\ln^2\bar{u}\right) \tag{C16}$$

which can be substituted into the integrand of equation (C13) to yield an expression for the gravity minus centrifugal force term. We notice first, though, that by definition $(Z_{III}/\bar{u}) \sim \rho_\infty$ returns to its small initial value Z_i whenever the vehicle returns to the initial altitude ρ_{∞_i}. At the end of the first skip the velocity is reduced to some value $\bar{u}_{III_e}$ such that

$$\ln(\bar{u}_{III})_e = \frac{2\varphi_i}{L/D}$$

in accordance with the results of reference 4. This is the velocity at the end of the dip. Since we are considering small angles only, $-2\varphi_i/(L/D) \cong 1 - \bar{u}_{III_e}$, and we may substitute $\ln\bar{u} \cong \bar{u} - 1$ in equation (C16) for the purpose of evaluating the double integral of equation (C13) representing the gravity minus centrifugal forces. This yields a new Z function

$$\frac{Z_{IV}}{\bar{u}} = \frac{(1-\bar{u})^2}{4\sqrt{\beta r}\,(-\varphi_i)} + \frac{Z_{III}}{\bar{u}} \tag{C17}$$

$$\cong Z_i + \sqrt{\beta r}\left[\varphi_i \ln\bar{u} - \left(\frac{L}{2D} + \frac{1}{4\beta r\varphi_i}\right)\ln^2\bar{u}\right]$$

The velocity at the end of the dip is given by

$$\ln \bar{u}_e = \frac{2\varphi_i}{(L/D) + (1/2\beta r\varphi_i)} \tag{C18}$$

Since $\beta r = 900$ for Earth, the correction term $1/(4\beta r\varphi_i)$ can often be disregarded. The path angle is obtained from equation (C15)

$$\varphi = \varphi_i - \left(\frac{L}{D}\right)\ln \bar{u} \tag{C19}$$

so we see that

$$\varphi_e = \varphi_i - \frac{L}{D}\ln \bar{u}_e = -\varphi_i \frac{1 - \frac{1}{2(L/D)\beta r\varphi_i}}{1 + \frac{1}{2(L/D)\beta r\varphi_i}} \tag{C20}$$

If $2(L/D)\beta r\varphi_i \gg 1$ these equations reduce to results previously obtained by Eggers, Allen, and Neice (ref. 4). In particular, for relatively large values of $(L/D)\varphi_i$, the angle leaving the dip is equal but opposite to the initial angle φ_i of entry, as noted in reference 4. After a skip, a period of weightlessness follows at an essentially constant velocity $\bar{u}_e$ under conditions where the vertical acceleration $(dv/dt) = g - (\bar{u}_e^2/r)$ is constant; hence the duration of weightlessness $\Delta t = 2v_e/(dv/dt)$ is

$$\Delta t = \frac{2\bar{u}_e(\varphi_e)}{g(1 - \bar{u}_e^2)} \tag{C21}$$

After this period, a second entry occurs at nearly the same angle as the first entry, only at the reduced velocity $\bar{u}_e$. The maximum laminar-heating rate occurs near, but not at the bottom of the dip ($\varphi = 0$) at which point the velocity $\bar{u}_m$ is given by $\ln \bar{u}_m = \varphi_i/(L/D)$. By substituting this into equation (C16) the approximate maximum laminar heating rate is then represented by

$$\bar{q}_m = (\bar{u}_m^{5/2} Z_m^{1/2}) = (\beta r)^{1/4} e^{\frac{3\varphi_i}{L/D}} \frac{(-\varphi_i)}{\sqrt{2L/D}} \tag{C22}$$

$$\cong \frac{(\beta r)^{1/4}(-\varphi_i)}{\sqrt{2L/D}} \qquad \text{for } -\varphi_i \ll \frac{L}{D}$$

An interesting result concerns the total heat absorbed in a single skip starting from satellite velocity ($\bar{u}_i = 1$). The total heat absorbed is obtained from equation (39) together with

$$\bar{Q} = \int_{\bar{u}_e}^{1} \frac{\bar{u}^{3/2}\,d\bar{u}}{\sqrt{Z}} = \frac{\sqrt{2}}{(\beta r)^{1/4}\sqrt{L/D}} \int_{\bar{u}_e}^{1} \frac{\bar{u}\,d\bar{u}}{\sqrt{\ln \bar{u}\left(\frac{2\varphi_i}{L/D} - \ln \bar{u}\right)}}$$

By employing the same approximation $\ln \bar{u} \cong -1 + \bar{u}$ the integral can be evaluated.

$$\bar{Q} = \frac{\sqrt{2}}{(\beta r)^{1/4}\sqrt{L/D}}\,\pi\left(1 + \frac{\varphi_i}{L/D}\right) \tag{C23}$$

This is essentially independent of φ_i, since $\varphi_i/(L/D)$ for many skip vehicles would be small.

$$\bar{Q} \cong \frac{\sqrt{2}\,\pi}{(\beta r)^{1/4}\sqrt{L/D}} \qquad \text{for } -\varphi_i \ll \frac{L}{D}$$

Although the maximum heating rate in a skip is proportional to the initial angle of descent φ_i, the total heat absorbed is essentially independent of both the initial angle φ_i and the exit velocity $\bar{u}_e$ of the skip. Since $Q \sim \bar{Q}/\sqrt{C_D}$, we see that $Q \sim 1/\sqrt{C_L}$, which means that the least heat is absorbed by skipping at $C_{L_{max}}$. For inclined flat surfaces in hypersonic flow, simple Newtonian theory yields $C_{L_{max}} = 0.77$ at an angle of attack of 55°, at which angle $L/D = 0.71$. Hence

$$(\bar{Q})_{\min Q} = \sqrt{2}\,\pi/(\beta r)^{1/4}\sqrt{0.71} = 0.96$$

This value is compared elsewhere in the DISCUSSION with corresponding values of $\bar{Q}$ for other types of entry.

If a skip vehicle does not enter initially at orbital velocity, but at some different value $\bar{u}_i$, then the corresponding equations with gravity and centrifugal forces neglected indicate the bottom of the dip to be at a velocity $\bar{u}_m$ given by $\ln(\bar{u}_m/\bar{u}_i) = \varphi_i/(L/D)$. At this point the heating rate is represented by

$$\bar{q}_m = (\beta r)^{1/4}\bar{u}_i^{\,3} e^{\frac{3\varphi_i}{L/D}} \frac{(-\varphi_i)}{\sqrt{2L/D}} \tag{C24}$$

The exit of the skip occurs at a velocity $\bar{u}_e$ given by

$$\ln(\bar{u}_e/\bar{u}_i) = 2\varphi_i/(L/D)$$

The dimensionless total heat absorbed is approximately

$$\bar{Q} \cong \frac{\sqrt{2}\,\pi\bar{u}_i^{\,2}}{(\beta r)^{1/4}\sqrt{L/D}} \tag{C25}$$

APPENDIX D

INTEGRATION OF BASIC NONLINEAR EQUATION

Many numerical methods could be used to compute stepwise a Z function from a nonlinear equation such as

$$\bar{u}Z'' - Z' + \frac{Z}{\bar{u}} = \frac{1 - \bar{u}^2}{\bar{u}Z} \cos^4\varphi - \sqrt{\beta r}\,\frac{L}{D}\cos^6\varphi \qquad \text{(D1a)}$$

where $Z' - \frac{Z}{\bar{u}} = \sqrt{\beta r}\sin\varphi$. A study has not been made of the best way to integrate such an equation, or of whether or not an alternate form of this equation, such as

$$\bar{u}\,\frac{d}{d\bar{u}}\left(\bar{u}\,\frac{dF}{d\bar{u}}\right) = \frac{1}{F}\left(\frac{1}{\bar{u}^2} - 1\right)\cos^4\varphi - \sqrt{\beta r}\,\frac{L}{D}\cos^3\varphi \qquad \text{(D1b)}$$

where $F \equiv Z/\bar{u}$ and $\bar{u}F' = \sqrt{\beta r}\sin\varphi$, may be preferable for purposes of integration. The particular method employed, while probably not extremely accurate, is simple in the sense that it involves merely the repetition of a large number of identical operations. Suppose we know at some initial point $\bar{u}_n$ the values of Z_n and Z_n'. Then from the differential equation we have for the second derivative (with $\cos\varphi$ set equal to unity for purposes of simplicity in illustrating the method),

$$Z_n'' = \frac{1}{\bar{u}_n}\left(Z_n' - \frac{Z_n}{\bar{u}_n} + \frac{1 - \bar{u}_n^2}{\bar{u}_n Z_n} - \sqrt{\beta r}\,\frac{L}{D}\right) \qquad \text{(D2)}$$

and for the third derivative

$$Z_n''' = \frac{1}{\bar{u}_n}\left[\frac{1}{\bar{u}_n}\left(Z_n' - \frac{Z_n}{\bar{u}_n}\right) - \frac{1 - \bar{u}_n^2}{\bar{u}_n}\,\frac{Z_n'}{Z_n^2} - \frac{1 + \bar{u}_n^2}{\bar{u}_n^2 Z_n}\right] \qquad \text{(D3)}$$

Hence a Taylor expansion for Z_{n+1} and Z_{n+1}' at the next point $\bar{u}_{n+1}$ yields

$$Z_{n+1} = Z_n + Z_n'\Delta\bar{u} + Z_n''\,\frac{(\Delta\bar{u})^2}{2} + Z_n'''\,\frac{(\Delta\bar{u})^3}{6}$$

$$Z_{n+1}' = Z_n' + Z_n''\Delta u + Z_n'''\,\frac{(\Delta\bar{u})^2}{2}$$

while the above equations (D2) and (D3) yield Z_{n+1}'' and Z_{n+1}''' when n is replaced by n+1 in the formulas. Thus the process can be continued. For most cases the Z functions are fairly smooth, and the inclusion of Z''' is unnecessary in the above procedure if sufficiently small $\Delta\bar{u}$ are used. For the present calculations Z''' was omitted; $\Delta\bar{u} = 0.001$ was employed for $\bar{u}_i = 1$, and $\Delta\bar{u} = 0.002$ for $\bar{u}_i = 1.4$ and $\bar{u}_i = 1.2$. For skip vehicles, the Z function can vary quite rapidly and the inclusion of Z''' presumably would enable larger increments $\Delta\bar{u}$ to be used.

This particular procedure requires a knowledge of nonzero values Z_o and Z_o' at some initial point $\bar{u}_o$. Hence the first step is taken analytically. For decaying orbits an analytical representation in the vicinity of $\bar{u} \cong 1$, where $(1 - \bar{u}^2)/\bar{u} \cong 2(1 - \bar{u})$, is

$$Z_o = 2\sqrt{\frac{2}{3}}\,(1 - \bar{u}_o)^{3/2} \tag{D4}$$

$$Z_o' = -\sqrt{6}\,(1 - \bar{u}_o)^{1/2} \tag{D5}$$

since these yield $Z_o'' = 2(1 - \bar{u}_o)/Z_o$ and correspond to values of both Z_o' and $Z_o/\bar{u}_o$ small compared to Z_o'' (see eq. (D1)). Equations (D4) and (D5) would apply to a lifting vehicle provided $(1 - \bar{u}_o)$ is selected small enough so that $\sqrt{\beta r}\,\frac{L}{D} \ll (1 - \bar{u}_o)^{-1/2}$. If the L/D ratio is large, we can use the Z_{II} function to obtain

$$Z_o = \frac{1 - \bar{u}_o^2}{\sqrt{\beta r}\,(L/D)\bar{u}_o} \tag{D6}$$

$$Z_o' = -\frac{1 + \bar{u}_o^2}{\sqrt{\beta r}\,(L/D)\bar{u}_o^2} \tag{D7}$$

For re-entry with an initial angle φ_i at initial velocity u_i we can use the Z_{III} function for the first step,

$$Z_o = \sqrt{\beta r}\,\bar{u}_o\left[\sin\varphi_i \ln\frac{\bar{u}}{\bar{u}_i} - \frac{\cos^3\varphi_i}{2}\left(\frac{L}{D}\right)\ln^2\frac{\bar{u}}{\bar{u}_i}\right] \tag{D8}$$

$$Z_o' = \sqrt{\beta r}\,\sin\varphi_i + \frac{Z_o}{\bar{u}_o} \tag{D9}$$

REFERENCES

1. Allen, H. Julian, and Eggers, A. J., Jr.: A Study of the Motion and Aerodynamic Heating of Missiles Entering the Earth's Atmosphere at High Supersonic Speeds. NACA TN 4047, 1957.

2. Sänger, Eugen: Raketen-Flugtechnik. R. Oldenbourg (Berlin), 1933.

3. Sänger, E., and Bredt, J.: A Rocket Drive for Long Range Bombers. Deutsche Luftfahrtforschung UM 3538 (1944). Translation CGD-32, Tech. Information Branch, BUAER, Navy Department.

4. Eggers, Alfred J., Jr., Allen, H. Julian, and Neice, Stanford E.: A Comparative Analysis of the Performance of Long-Range Hypervelocity Vehicles. NACA TN 4046, 1957. (Supersedes NACA RM A54L10)

5. Gazley, Carl, Jr., and Masson, David J.: A Recoverable Scientific Satellite. Rand Rep. RM-1844, 1956.

6. Kemp, N. H., and Riddell, F. R.: Heat Transfer to Satellite Vehicles Re-entering the Atmosphere. Jet Propulsion, vol. 27, no. 2, Feb. 1957, pp. 132-137.

7. Ferri, Antonio, Feldman, Lewis, and Daskin, Walter: The Use of Lift for Re-entry From Satellite Trajectories. Jet Propulsion, vol. 27, no. 11, Nov. 1957, pp. 1184-1191.

8. Gazley, Carl, Jr.: Deceleration and Heating of a Body Entering a Planetary Atmosphere From Space. Rand Rep. P-955, 1957.

9. Kennard, E. H.: Kinetic Theory of Gases. McGraw-Hill, New York, 1938.

10. Kuiper, G. P.: The Atmospheres of the Earth and Planets. Univ. of Chicago Press, 1949.

11. Struve, Otto: The Atmospheres of Jupiter and Saturn. Sky and Telescope, vol. XIII, no. 10, Aug. 1954, pp. 336-338.

12. Goody, R. M.: The Physics of the Stratosphere. Cambridge, Univ. Press, 1954.

13. Lees, Lester: Laminar Heat Transfer Over Blunt-Nosed Bodies at Hypersonic Flight Speeds. Jet Propulsion, vol. 26, no. 4, April 1956, pp. 259-269.

14. Romig, Mary F.: Stagnation Point Heat Transfer for Hypersonic Flow. Jet Propulsion, vol. 26, no. 12, Dec. 1956, pp. 1098-1101.

15. Detra, R. W., Kemp, N. H., and Riddell, F. R.: Addendum to "Heat Transfer to Satellite Vehicles Re-entering the Atmosphere." Jet Propulsion, vol. 27, no. 12, Dec. 1957, pp. 1256-1257.

16. Duane, T. D., Beckman, Edw. L., Ziegler, J. E., and Hunter, H. N.: Some Observations on Human Tolerance to Accelerative Stress. III Human Studies of Fifteen Transverse G. Jour. Aviation Medicine, vol. 26, no. 4, Aug. 1955, pp. 298-303.

17. Edelberg, Robert, Henry, James P., Maciolek, John A., Salzman, Edwin W., and Zuidema, George D.: Comparison of Human Tolerance to Accelerations of Slow and Rapid Onset. Jour. Aviation Medicine, vol. 27, no. 6, Dec. 1956, pp. 482-489.

18. Thomas, H. Preston, Edelberg, Robert, Henry, James P., Miller, J., Salzman, Edwin W., and Zuidema, George D.: Human Tolerance to Multistage Rocket Acceleration Curves. Jour. Aviation Medicine, vol. 26, no. 5, Oct. 1955, pp. 390-398.

TABLE I.- VALUES OF Z FUNCTIONS AND RELATED QUANTITIES FOR L/D = 0 AND $\bar{u}_1 = 1$

$\bar{u}$	Z	$-\varphi_{Earth}$ deg	$\bar{q}$	$\left(\frac{\Delta s}{r}\right)_{Earth}$	t_{Earth} sec	Z	$-\varphi_{Earth}$ deg	$\bar{q}$	$\left(\frac{\Delta s}{r}\right)_{Earth}$	t_{Earth} sec	Z	$-\varphi_{Earth}$ deg	$\bar{q}$	$\left(\frac{\Delta s}{r}\right)_{Earth}$	t_{Earth} sec
	$(-\varphi_1)_{Earth} = 0°$					$(-\varphi_1)_{Earth} = 0.5°$					$(-\varphi_1)_{Earth} = 1°$				
0.995	0.00038	0.33	0	0	0	0.00131	0.50	0	0	0	0.0026	1.00	0	0	0
.99	.00165	.48	.156	.169	140	.00270	.57	.113	.088	72	.0053	1.04	.080	.044	37
.98	.00467	.68	.338	.288	238	.00603	.71	.265	.169	140	.0108	1.11	.191	.088	73
.96	.01315	.96	.550	.372	309	.01457	.95	.460	.240	199	.0229	1.26	.342	.129	108
.94	.0241	1.19	.688	.409	341	.0253	1.16	.593	.274	229	.0361	1.40	.451	.152	126
.92	.0369	1.39	.792	.431	360	.0378	1.36	.695	.296	248	.0505	1.53	.537	.168	141
.90	.0515	1.57	.875	.446	374	.0519	1.53	.777	.311	262	.0660	1.67	.609	.180	152
.85	.0939	1.98	1.030	.470	396	.0934	1.94	.932	.335	284	.1092	2.01	.750	.199	170
.8	.1435	2.36	1.140	.485	411	.1421	2.33	1.042	.349	298	.1580	2.34	.853	.212	183
.75	.1991	2.73	1.223	.494	421	.1970	2.70	1.126	.359	309	.212	2.69	.933	.221	192
.7	.260	3.11	1.288	.502	429	.257	3.08	1.191	.366	317	.270	3.05	.996	.228	200
.65	.324	3.50	1.340	.507	436	.321	3.48	1.243	.372	324	.333	3.42	1.047	.233	207
.6	.392	3.91	1.381	.512	442	.389	3.89	1.285	.377	330	.398	3.83	1.088	.238	213
.55	.463	4.36	1.415	.516	448	.460	4.35	1.318	.381	336	.466	4.28	1.122	.242	218
.5	.536	4.86	1.442	.519	453	.533	4.85	1.346	.384	341	.537	4.77	1.149	.245	223
.45	.610	5.43	1.464	.522	458	.607	5.42	1.367	.387	346	.608	5.34	1.170	.248	228
.4	.684	6.09	1.481	.525	463	.681	6.08	1.385	.390	351	.680	6.00	1.188	.251	233
.35	.757	6.89	1.495	.527	468	.754	6.89	1.399	.392	356	.752	6.81	1.202	.253	238
.3	.827	7.89	1.505	.529	473	.824	7.89	1.409	.394	361	.821	7.82	1.212	.255	244
.25	.892	9.21	1.513	.531	479	.890	9.22	1.417	.396	367	.885	9.15	1.220	.257	249
.2	.949	11.09	1.519	.533	486	.947	11.10	1.423	.398	374	.942	11.04	1.226	.259	256
.15	.992	14.04	1.523	.535	493	.991	14.05	1.427	.399	382	.986	14.01	1.230	.260	264
.1	1.009	19.52	1.525	.536	504	1.009	19.53	1.429	.401	392	1.005	19.52	1.232	.262	275
.05	.958	33.3	1.527	.538	521	.958	33.3	1.431	.402	409	.956	33.3	1.234	.263	292
.025	.825	50.7	1.527	.538	537	.825	50.7	1.431	.403	425	.824	50.8	1.234	.264	307
	$(-\varphi_1)_{Earth} = 2°$					$(-\varphi_1)_{Earth} = 3°$					$(-\varphi_1)_{Earth} = 4°$				
0.995	.0052	2.00	0	0	0	.0078	3.00	0	0	0	.0105	4.00	0	0	0
.99	.0105	2.02	.057	.0222	18	.0157	3.02	.047	.0148	12	.0209	4.01	.040	.0111	9
.98	.0210	2.06	.136	.0443	37	.0313	3.04	.111	.0295	24	.0416	4.03	.097	.0222	18
.96	.0422	2.13	.246	.0663	55	.0624	3.09	.201	.0443	37	.0827	4.07	.175	.0333	28
.94	.0638	2.21	.327	.0790	66	.0934	3.15	.268	.0589	44	.1233	4.11	.233	.0398	33
.92	.0858	2.29	.393	.0880	74	.1243	3.20	.323	.0591	50	.1633	4.15	.281	.0445	38
.90	.1080	2.37	.449	.0949	80	.1550	3.26	.370	.0639	54	.203	4.19	.322	.0481	41
.85	.1651	2.59	.560	.1073	92	.231	3.41	.463	.0726	62	.300	4.31	.404	.0548	47
.8	.224	2.82	.646	.1159	100	.306	3.57	.536	.0788	68	.393	4.44	.469	.0596	52
.75	.284	3.07	.714	.1225	107	.380	3.76	.595	.0837	74	.482	4.58	.521	.0634	56
.7	.346	3.34	.769	.1278	113	.452	3.96	.643	.0877	78	.568	4.74	.564	.0666	59
.65	.409	3.64	.815	.1322	119	.523	4.20	.683	.0911	82	.649	4.93	.599	.0693	63
.6	.474	3.97	.852	.1360	124	.591	4.46	.717	.0941	86	.726	5.14	.630	.0718	66
.55	.538	4.35	.883	.1393	128	.657	4.77	.744	.0968	90	.797	5.39	.655	.0739	69
.5	.603	4.79	.908	.1422	133	.721	5.13	.767	.0992	94	.863	5.69	.676	.0759	72
.45	.668	5.30	.929	.1448	137	.781	5.56	.787	.1014	98	.922	6.06	.693	.0778	75
.4	.732	5.91	.946	.1472	142	.838	6.09	.802	.1035	102	.974	6.51	.708	.0795	79
.35	.794	6.67	.959	.1493	147	.890	6.76	.815	.1054	106	1.018	7.08	.719	.0812	82
.3	.853	7.63	.969	.1513	152	.936	7.63	.824	.1072	110	1.058	7.85	.729	.0828	86
.25	.907	8.93	.977	.1532	157	.975	8.82	.832	.1089	115	1.076	8.92	.736	.0843	91
.2	.954	10.79	.983	.1550	164	1.005	10.57	.838	.1106	121	1.086	10.52	.741	.0859	97
.15	.989	13.75	.987	.1567	172	1.021	13.42	.841	.1122	129	1.079	13.20	.745	.0874	104
.1	1.002	19.28	.989	.1583	182	1.016	18.87	.844	.1137	139	1.048	18.45	.747	.0889	114
.05	.958	33.2	.991	.1598	200	.952	32.8	.845	.1153	157	.960	32.3	.748	.0904	131
.025	.822	50.8	.991	.1605	215	.820	50.6	.845	.1160	172	.821	50.3	.749	.0911	146

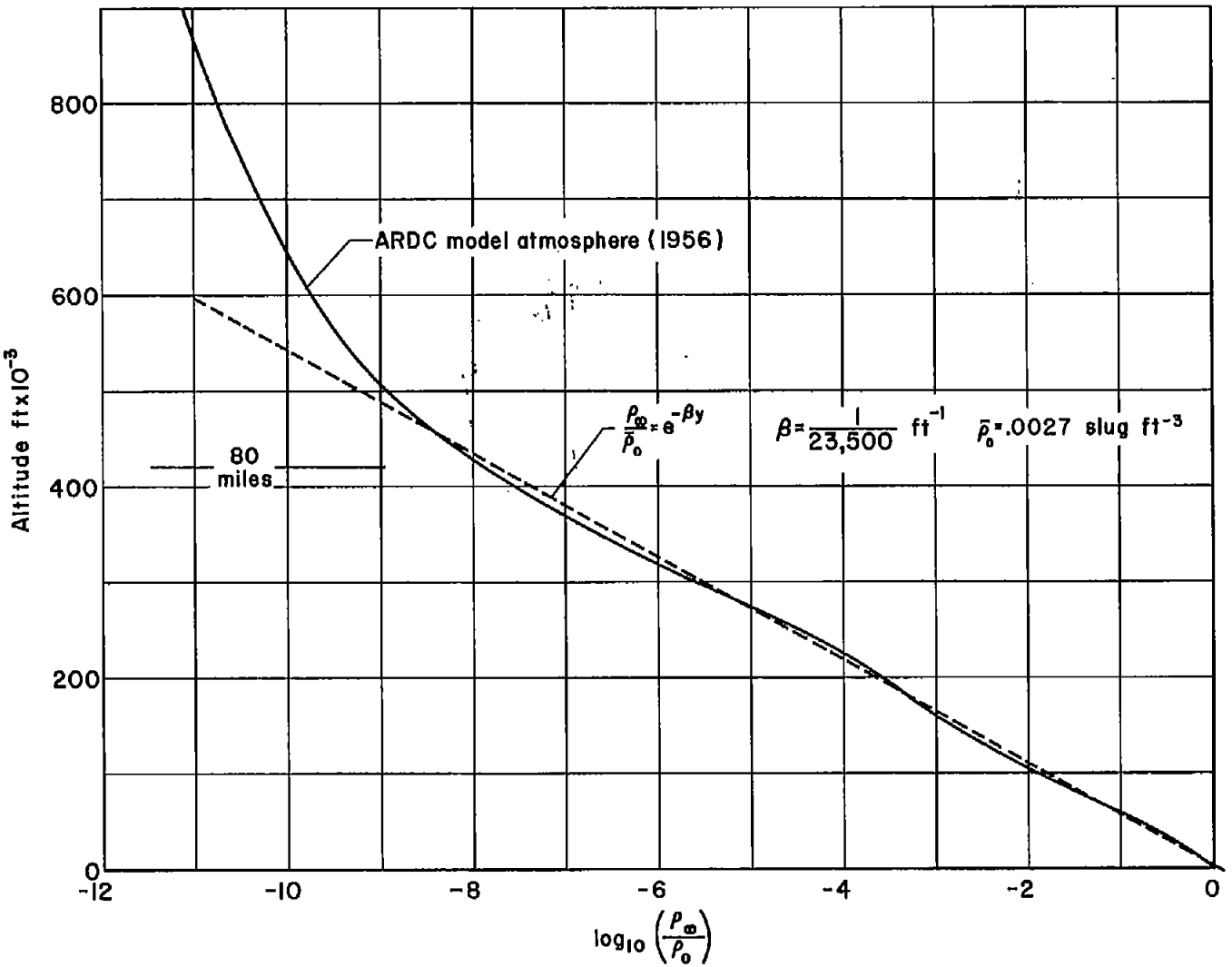

Figure 1.- Comparison of exponential approximation with ARDC model of Earth atmosphere (1956).

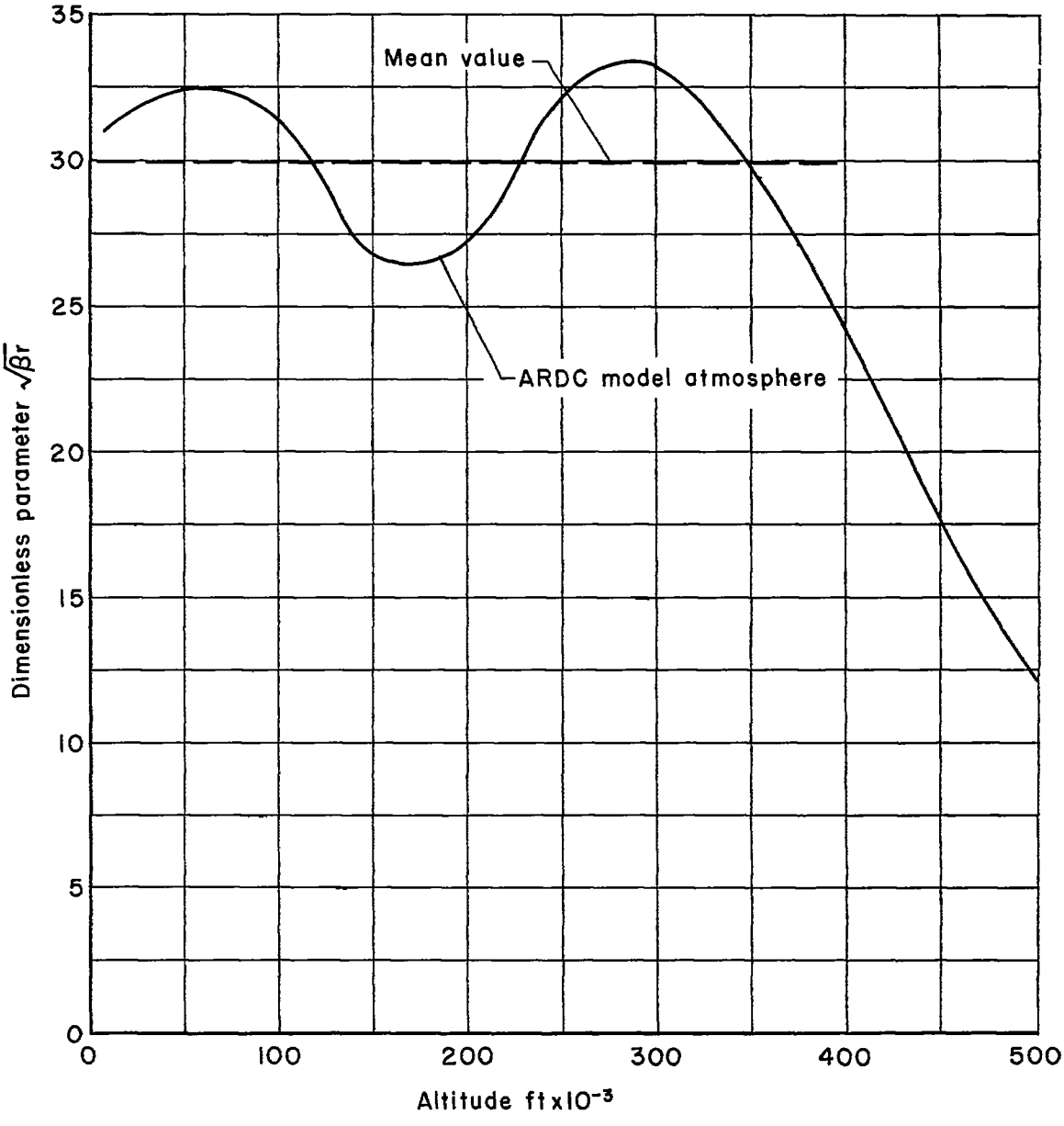

Figure 2.- Dimensionless parameter $\sqrt{\beta r}$ for ARDC model of Earth atmosphere.

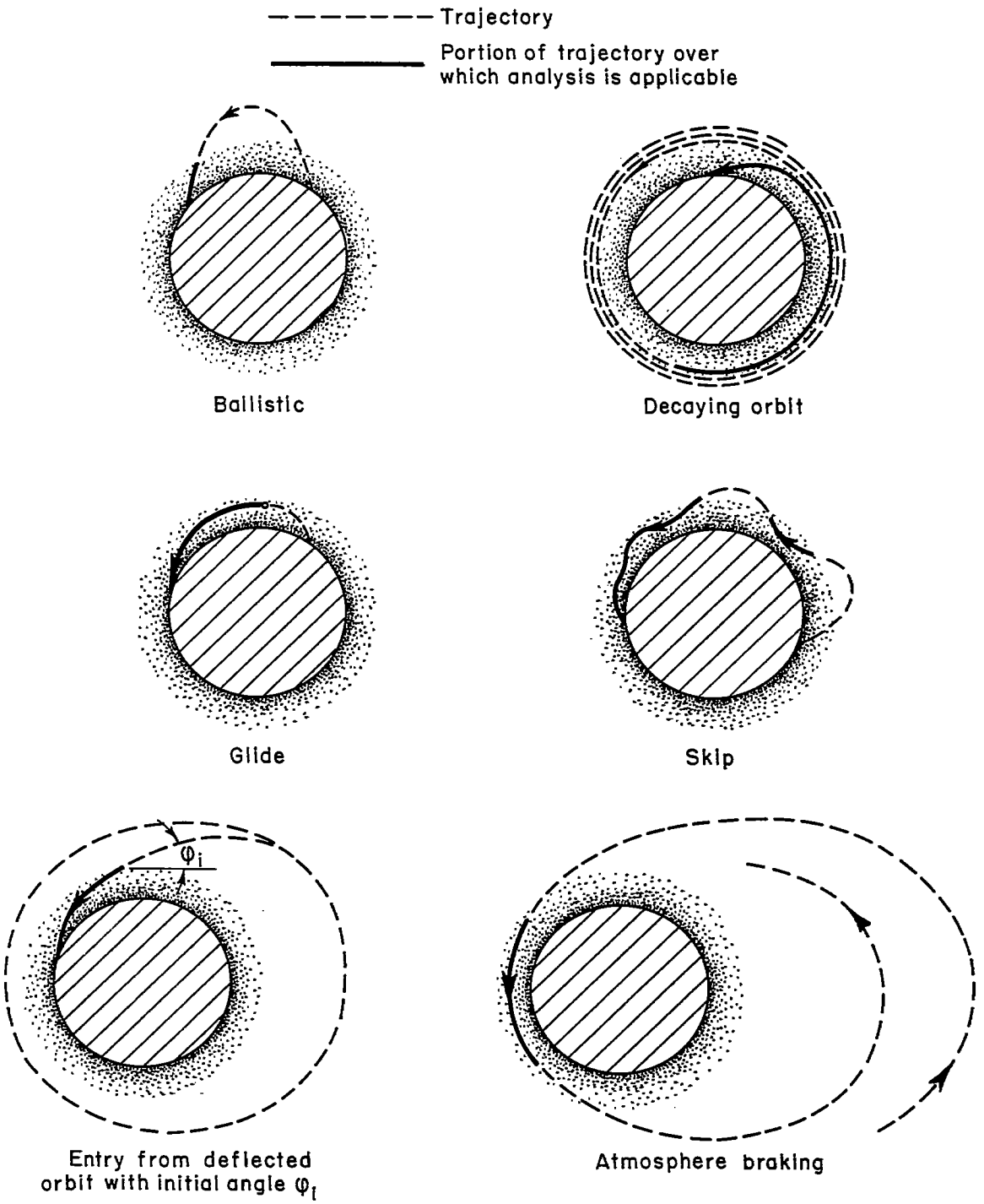

Figure 3.- Sketches of typical entry trajectories and portions to which present analysis applies.

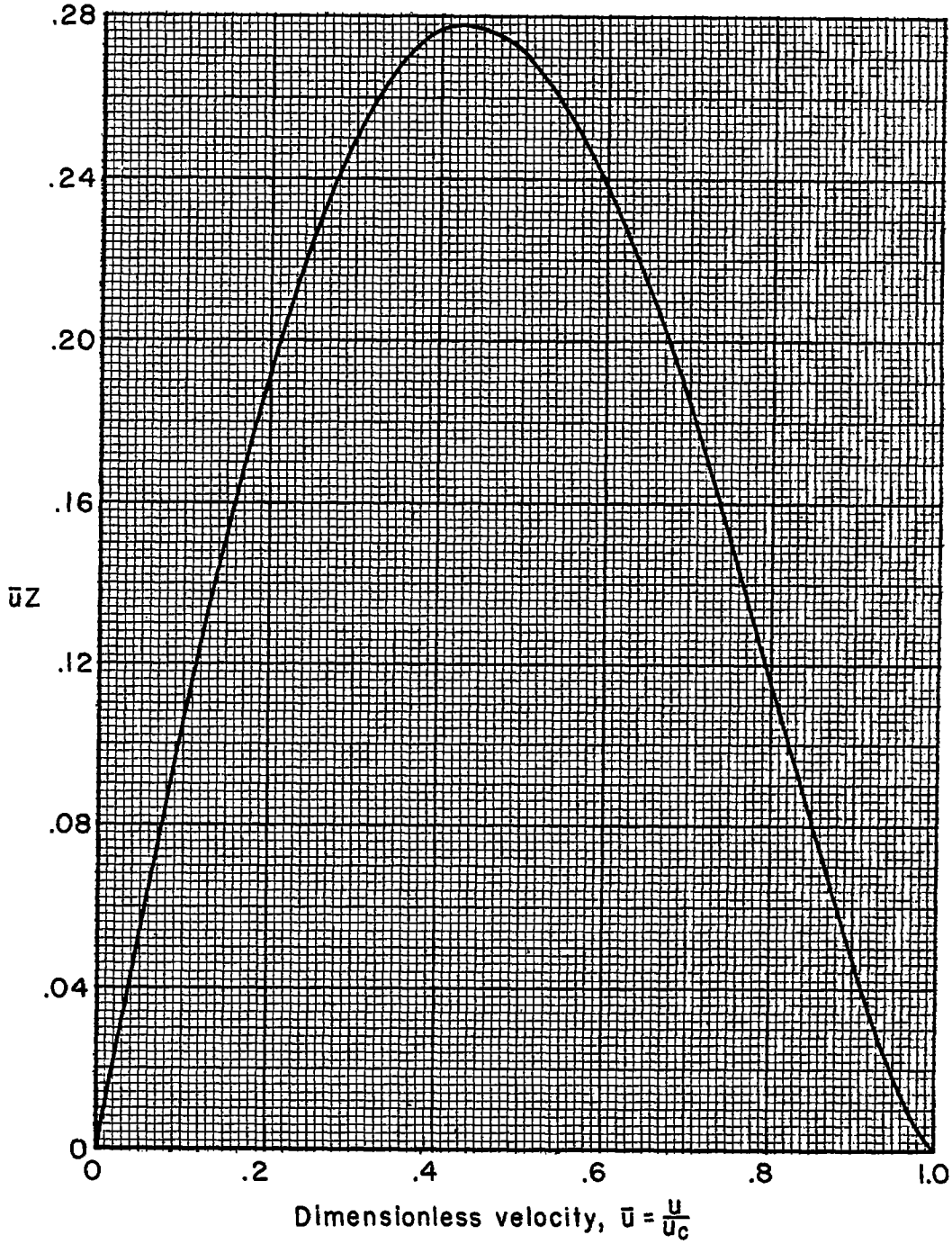

(a) Nonlifting vehicles.

Figure 4.- Values of Z functions for entry from decaying orbits into planetary atmosphere.

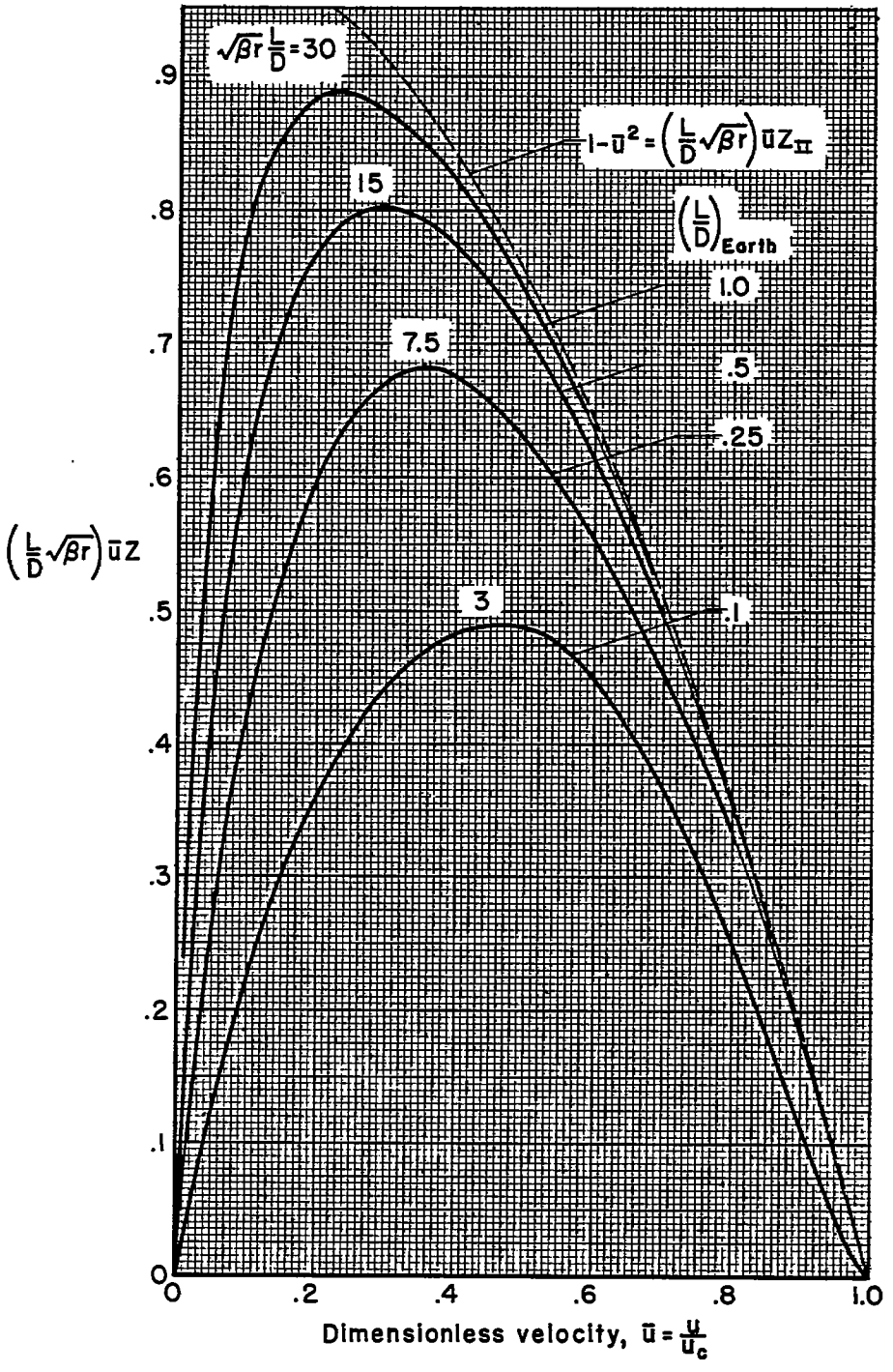

(b) Vehicles with $L/D > 0$.

Figure 4.- Concluded.

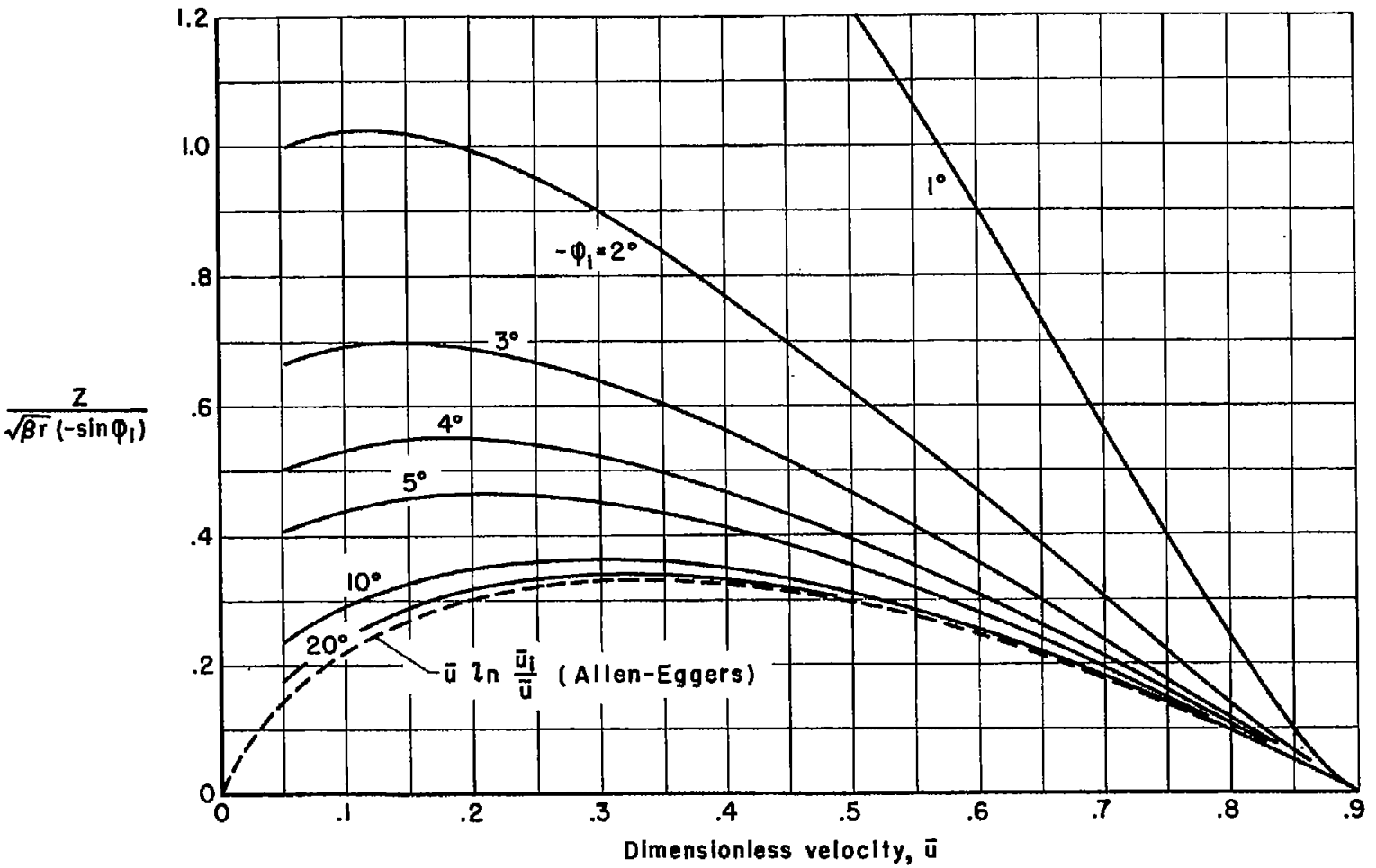

Figure 5.- Comparison of Z functions for nonlifting entry with analysis of Allen and Eggers; $\bar{u}_1 = 0.9$ (23,400 fps for earth).

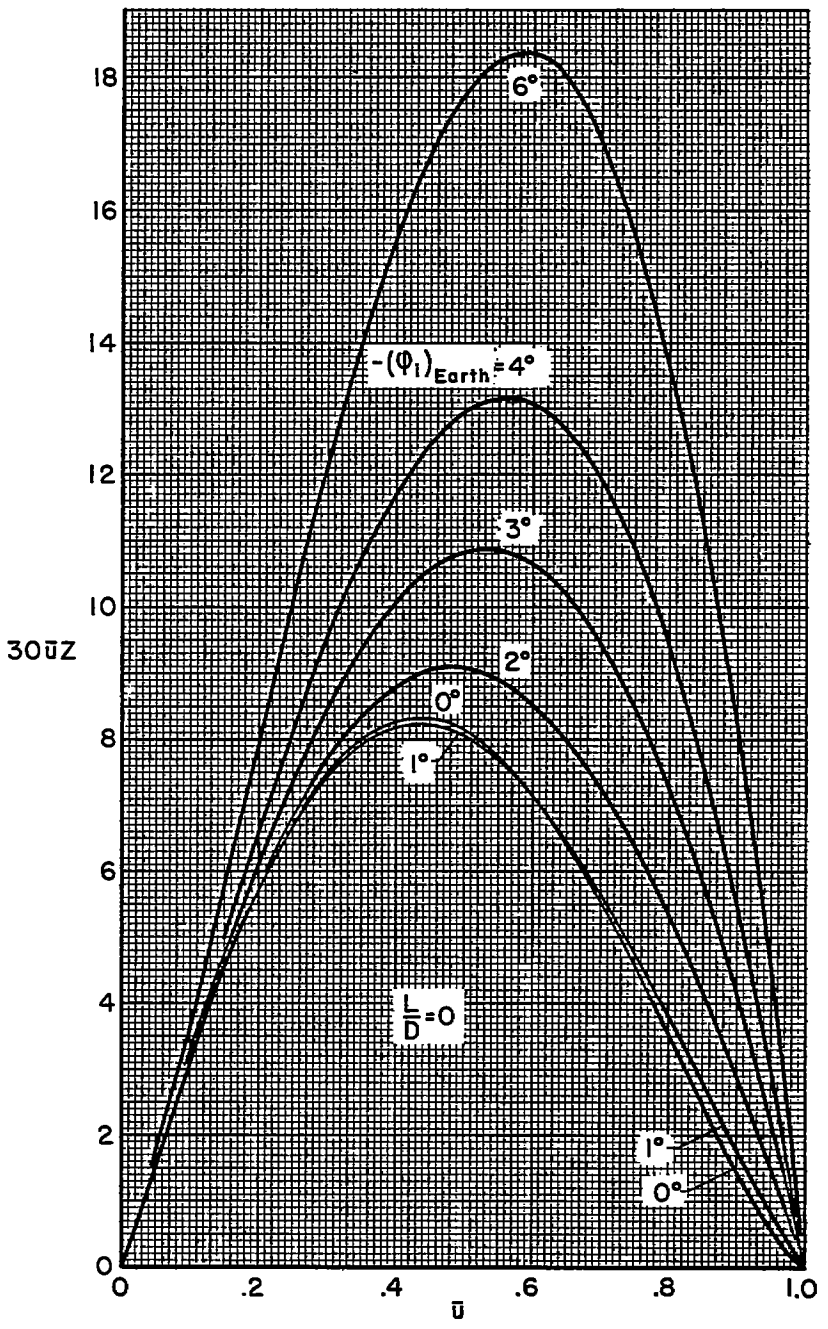

(a) Nonlifting vehicles.

Figure 6.- Values of Z functions for entry from orbital velocity at initial angles of descent; $\bar{u}_1 = 1$.

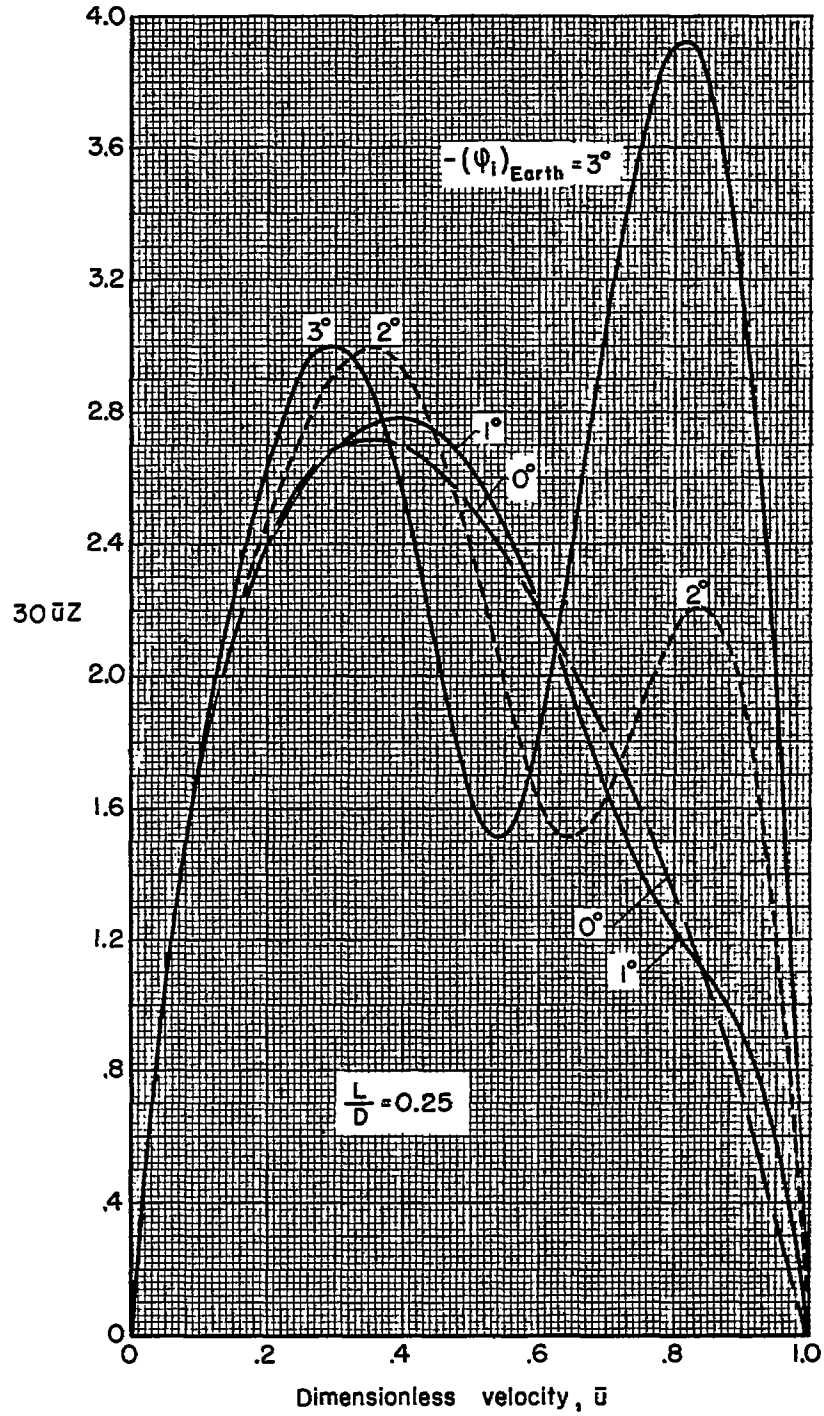

(b) Vehicles with L/D = 0.25.

Figure 6.- Continued.

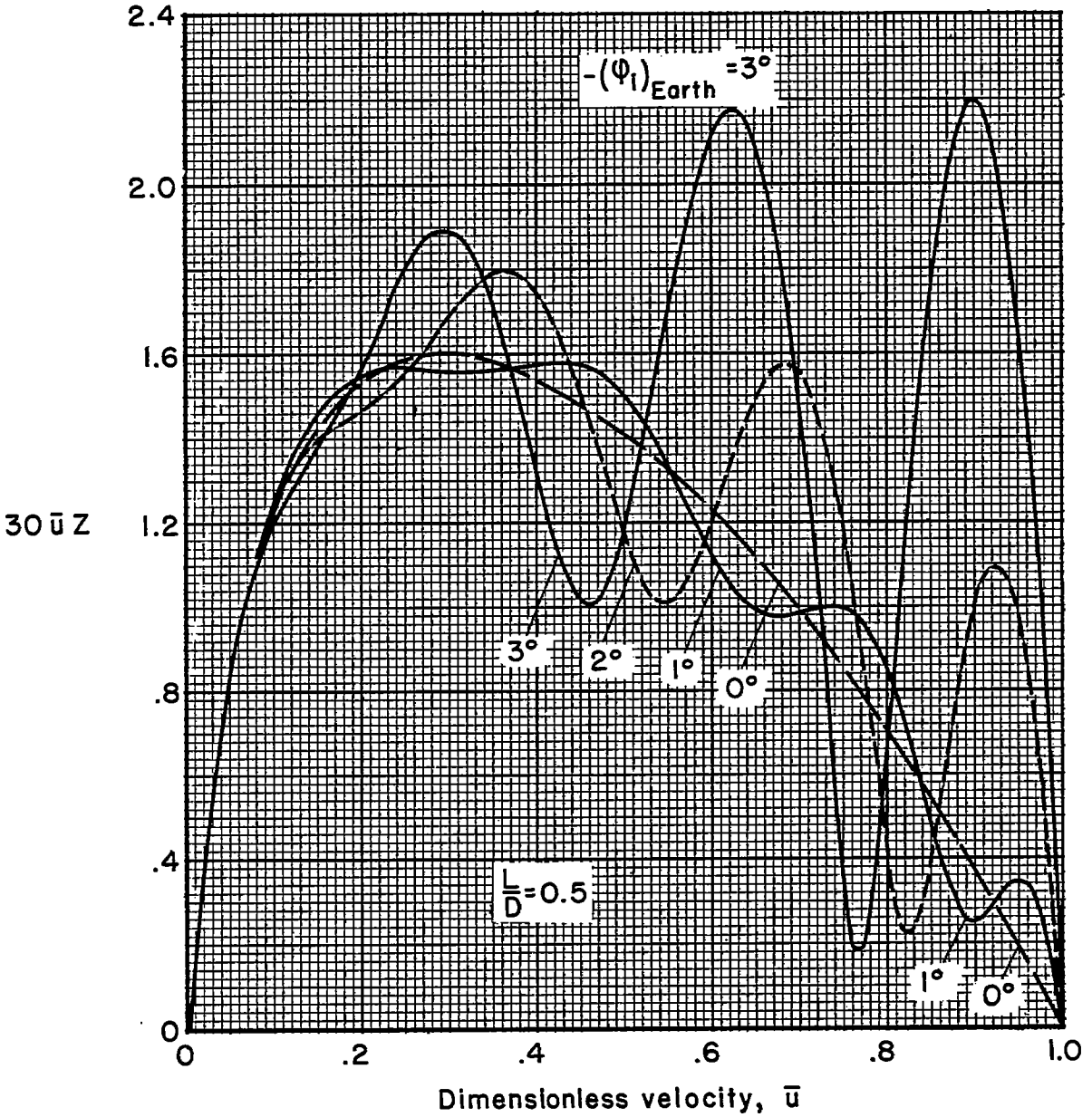

(c) Vehicles with L/D = 0.5.

Figure 6.- Continued.

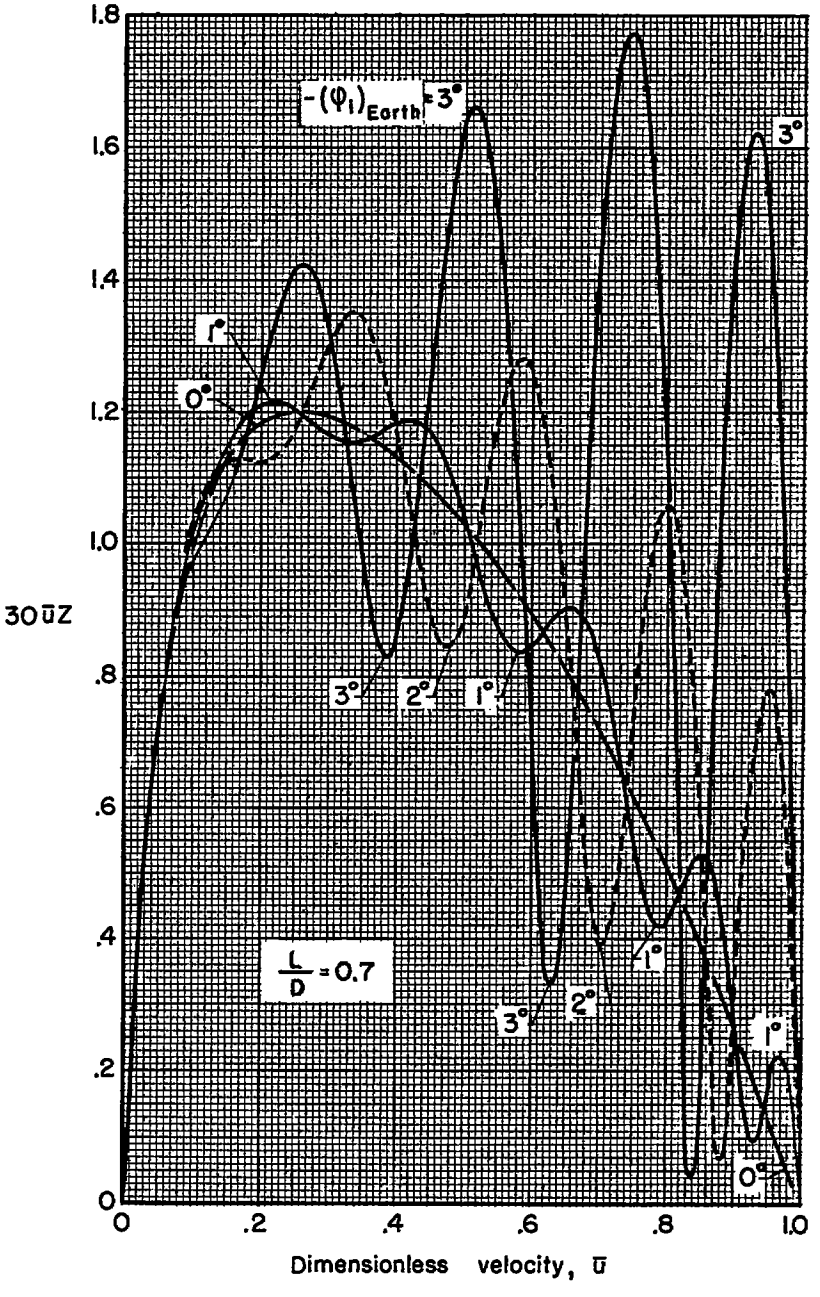

(d) Vehicles with L/D = 0.7.

Figure 6.- Continued.

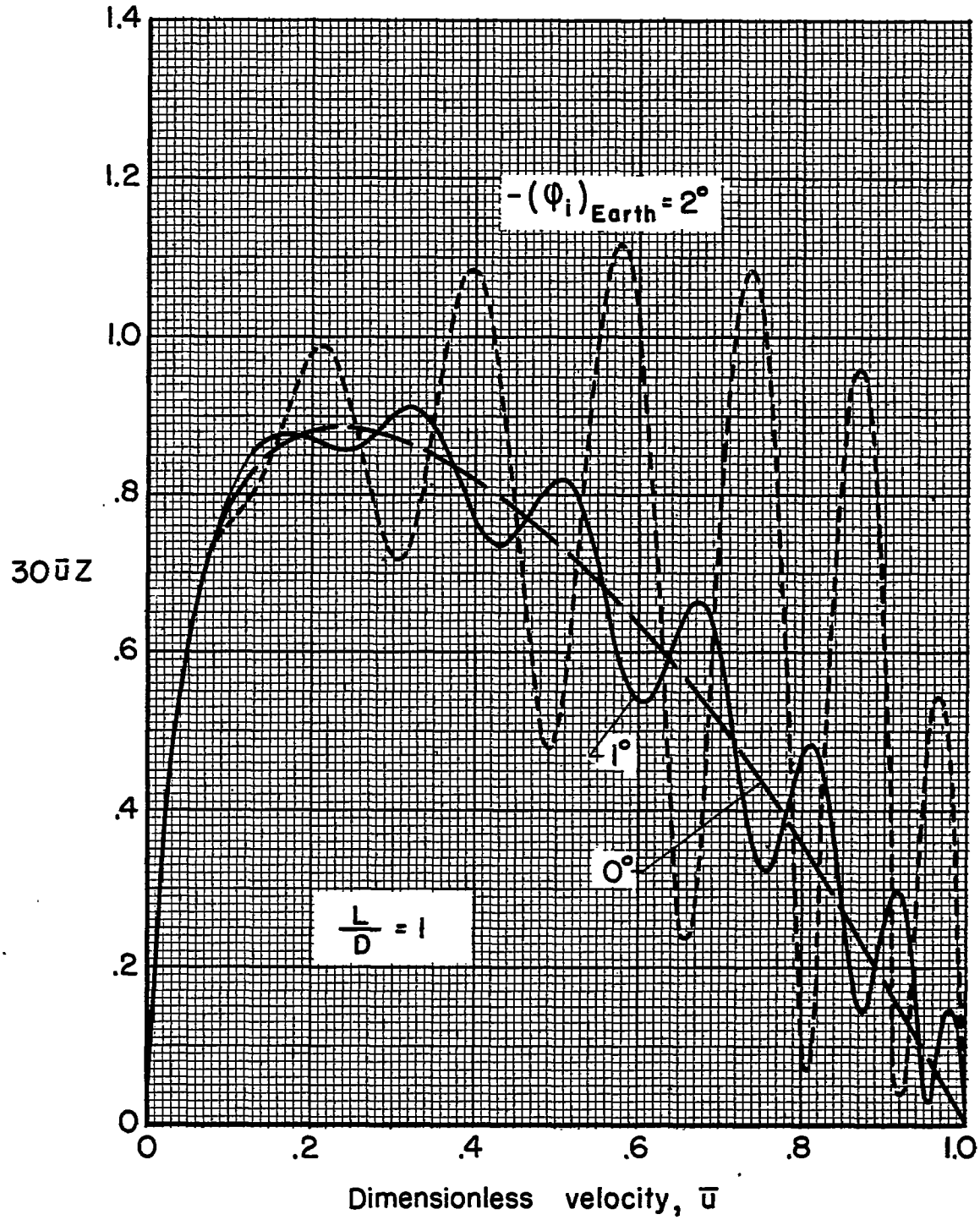

(e) Vehicles with L/D = 1.

Figure 6.- Concluded.

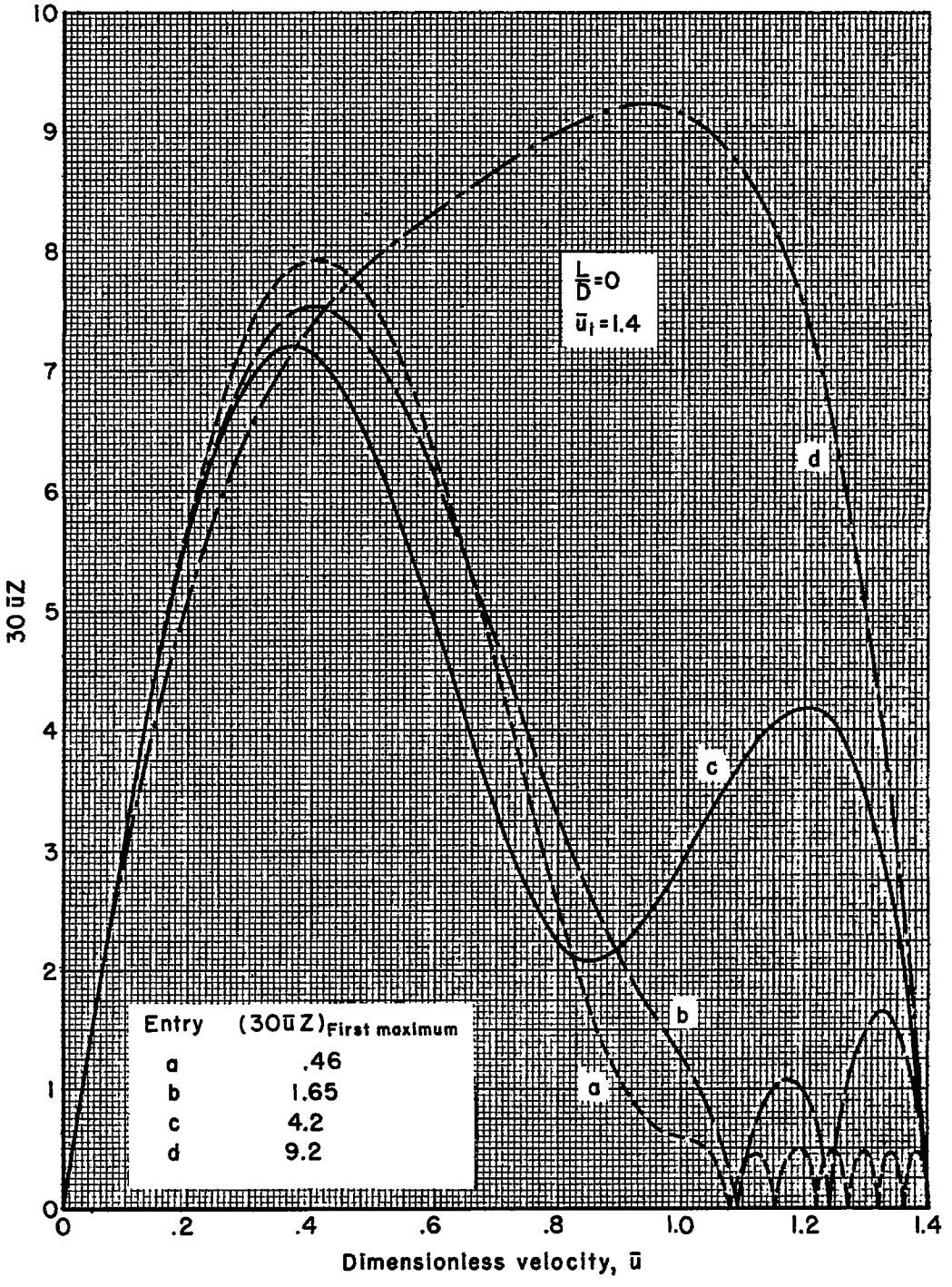

Figure 7.- Values of Z functions for atmosphere braking of nonlifting vehicles; $\bar{u}_i = 1.4$.

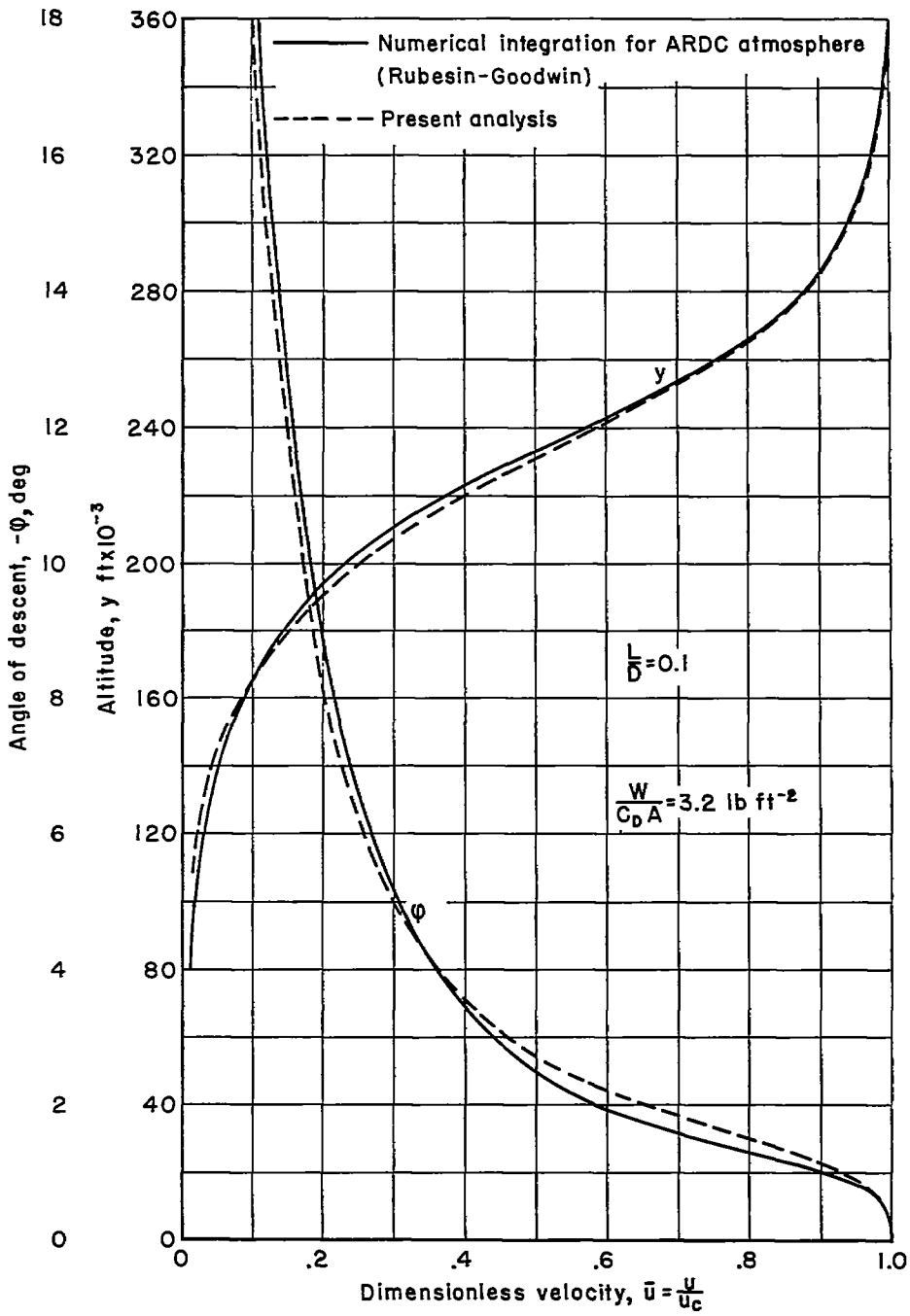

(a) Angle of descent and altitude-velocity trajectory.

Figure 8.- Comparison of present approximate analysis with more exact machine calculations for ARDC model atmosphere.

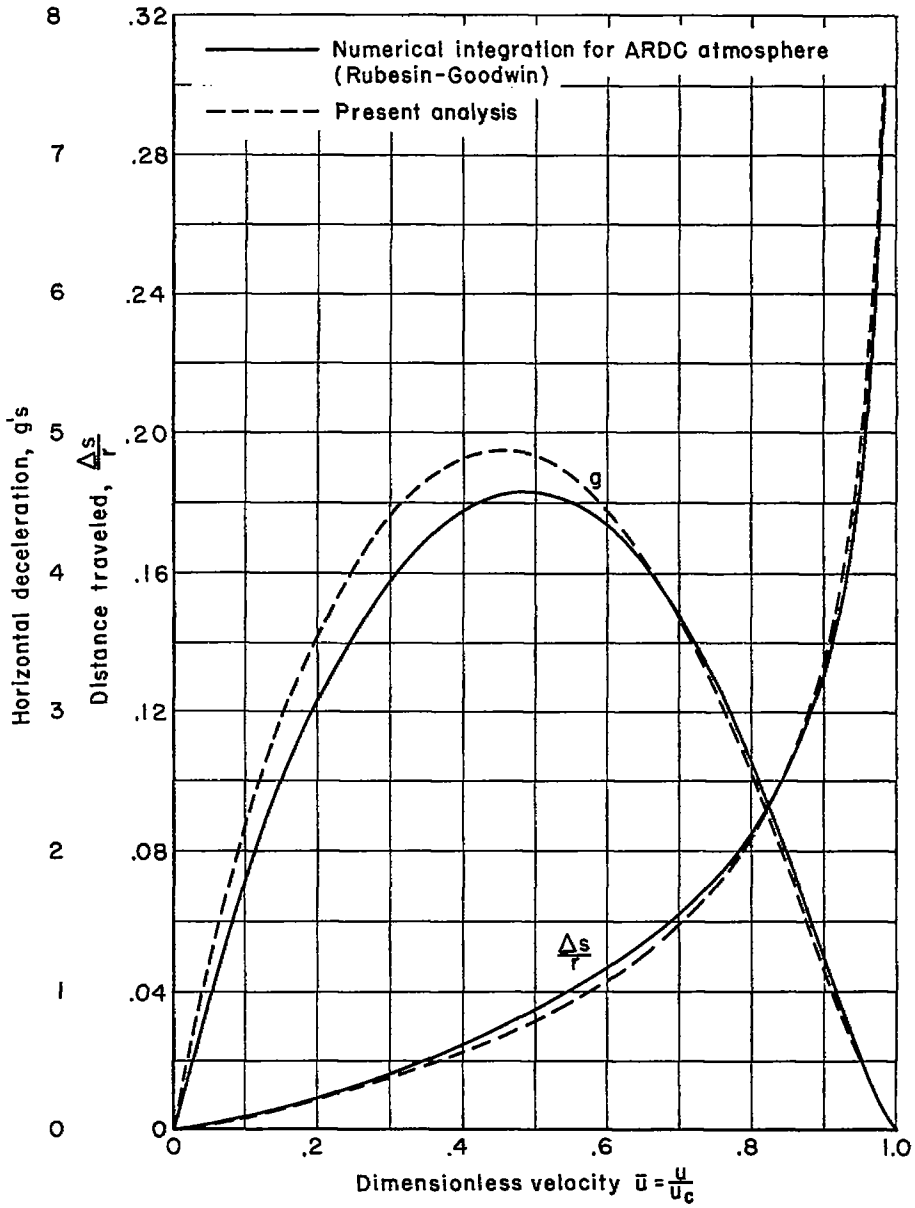

(b) Deceleration and distance traveled.

Figure 8.- Concluded.

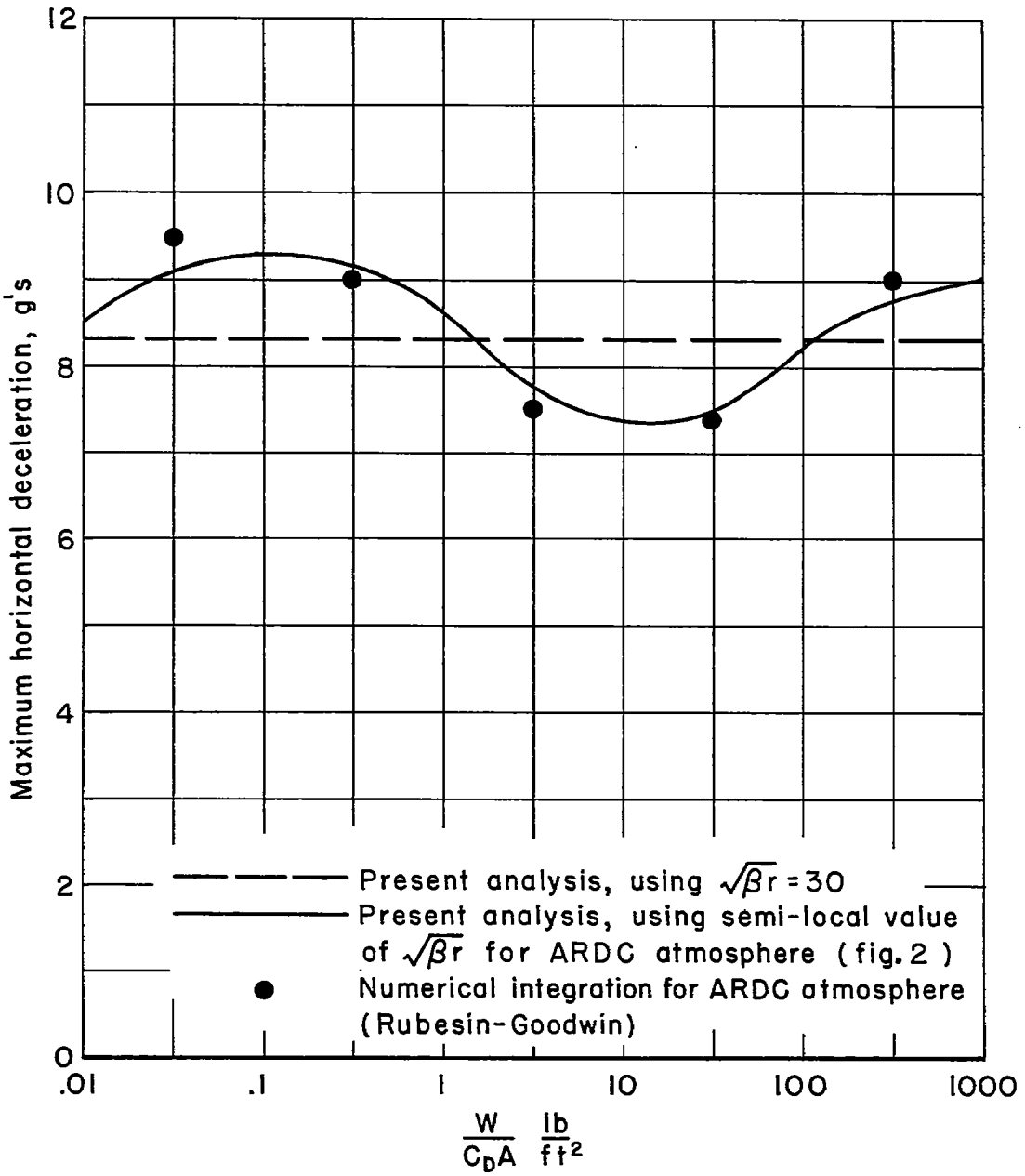

Figure 9.- Example application of present analysis to a model atmosphere, and comparison with more exact machine calculations; nonlifting entry from decaying orbit.

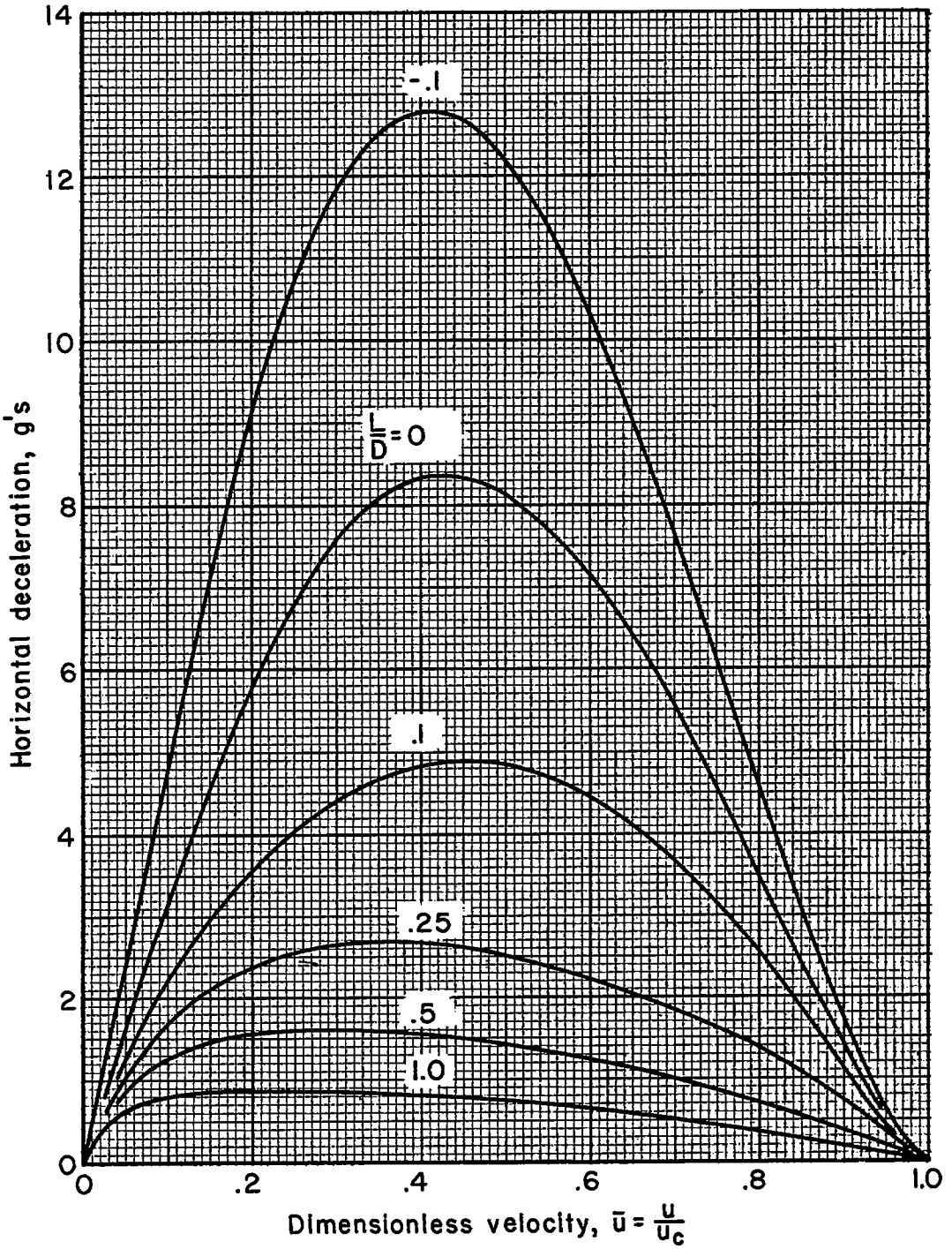

Figure 10.- Effect of lift-drag ratio on deceleration for entry into Earth atmosphere from decaying orbits.

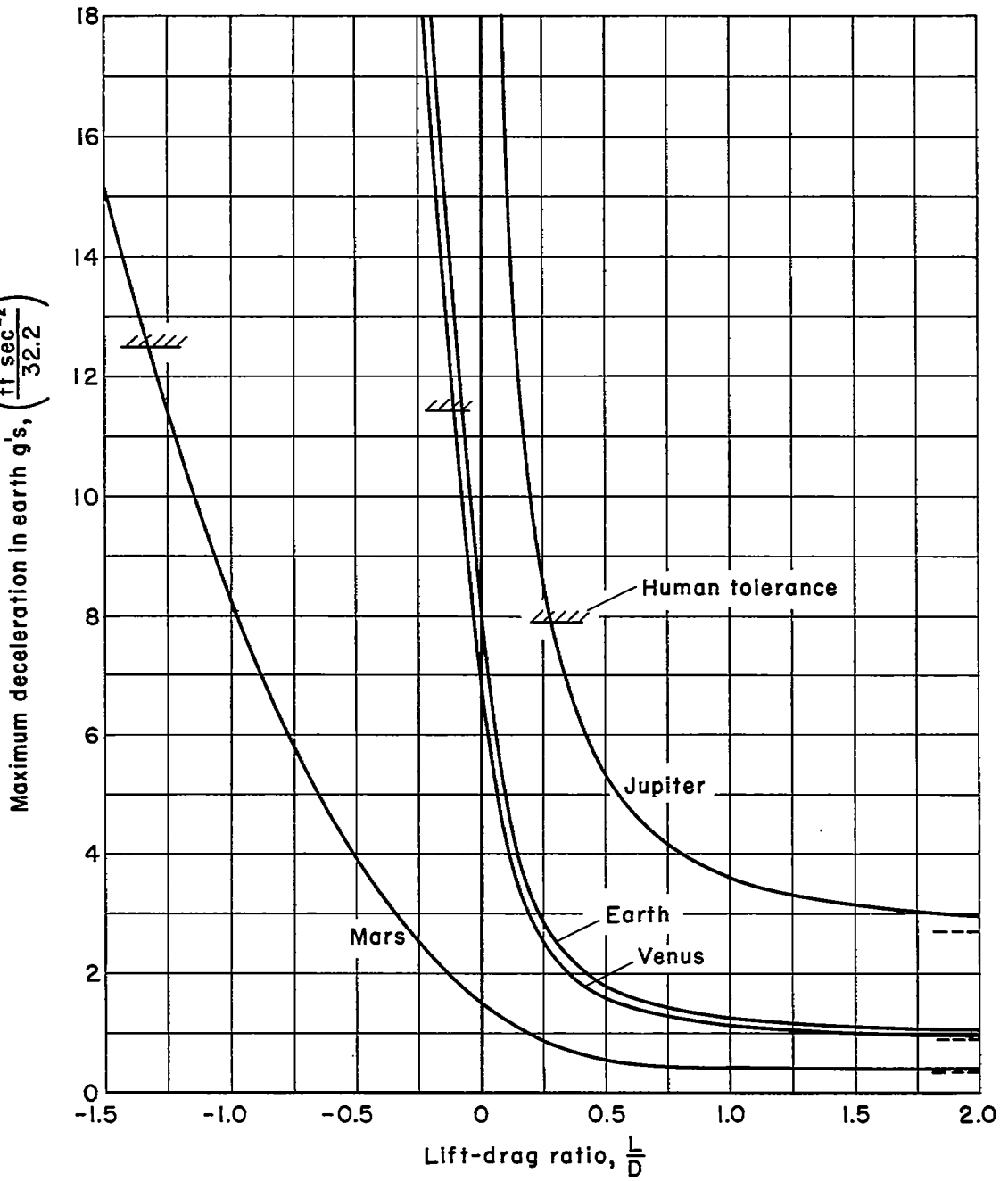

Figure 11.- Effect of lift-drag ratio on maximum deceleration for entry into various planetary atmospheres from decaying orbits.

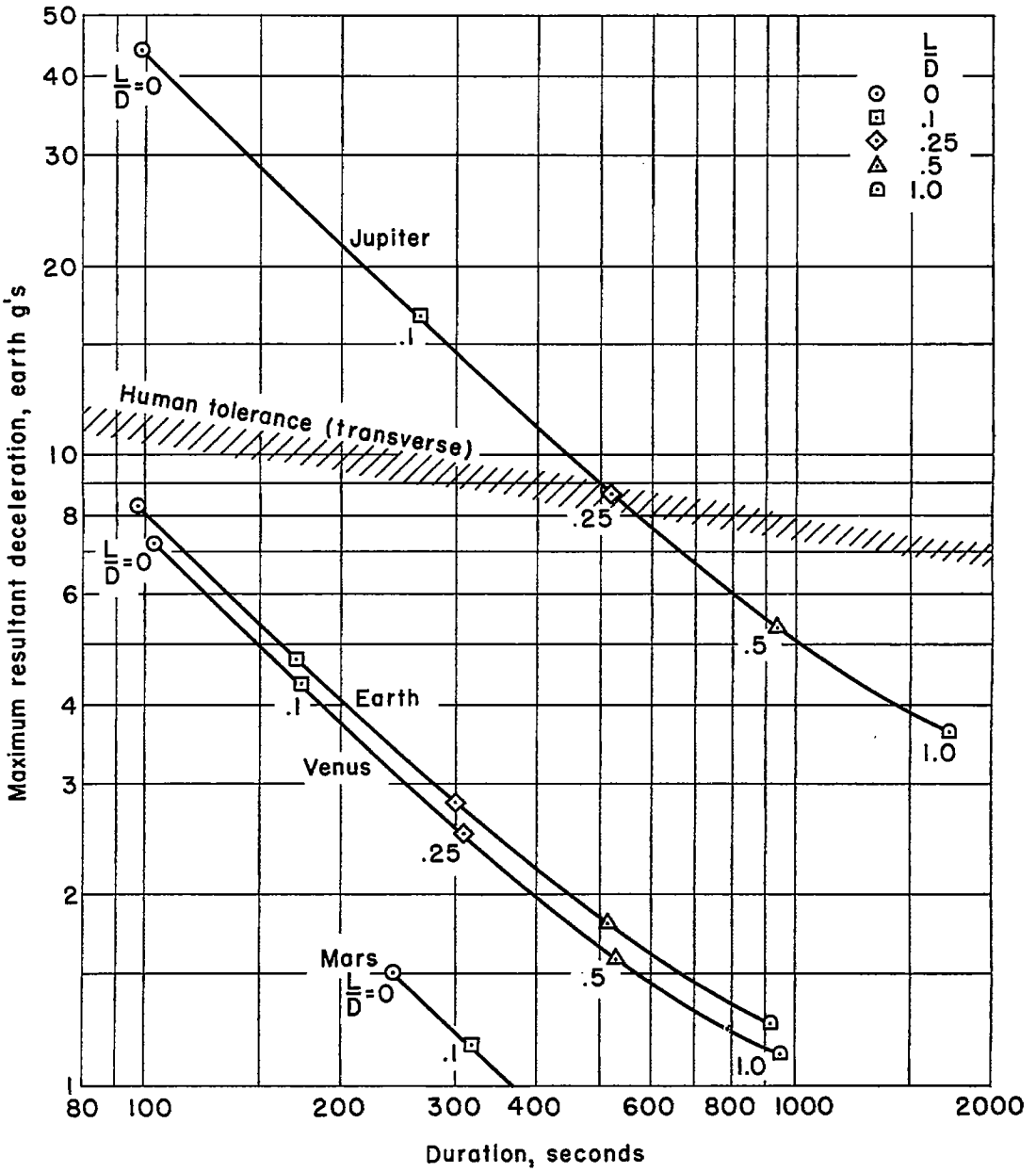

Figure 12.- Comparison of decelerations and duration for entry into various planetary atmospheres from decaying orbits.

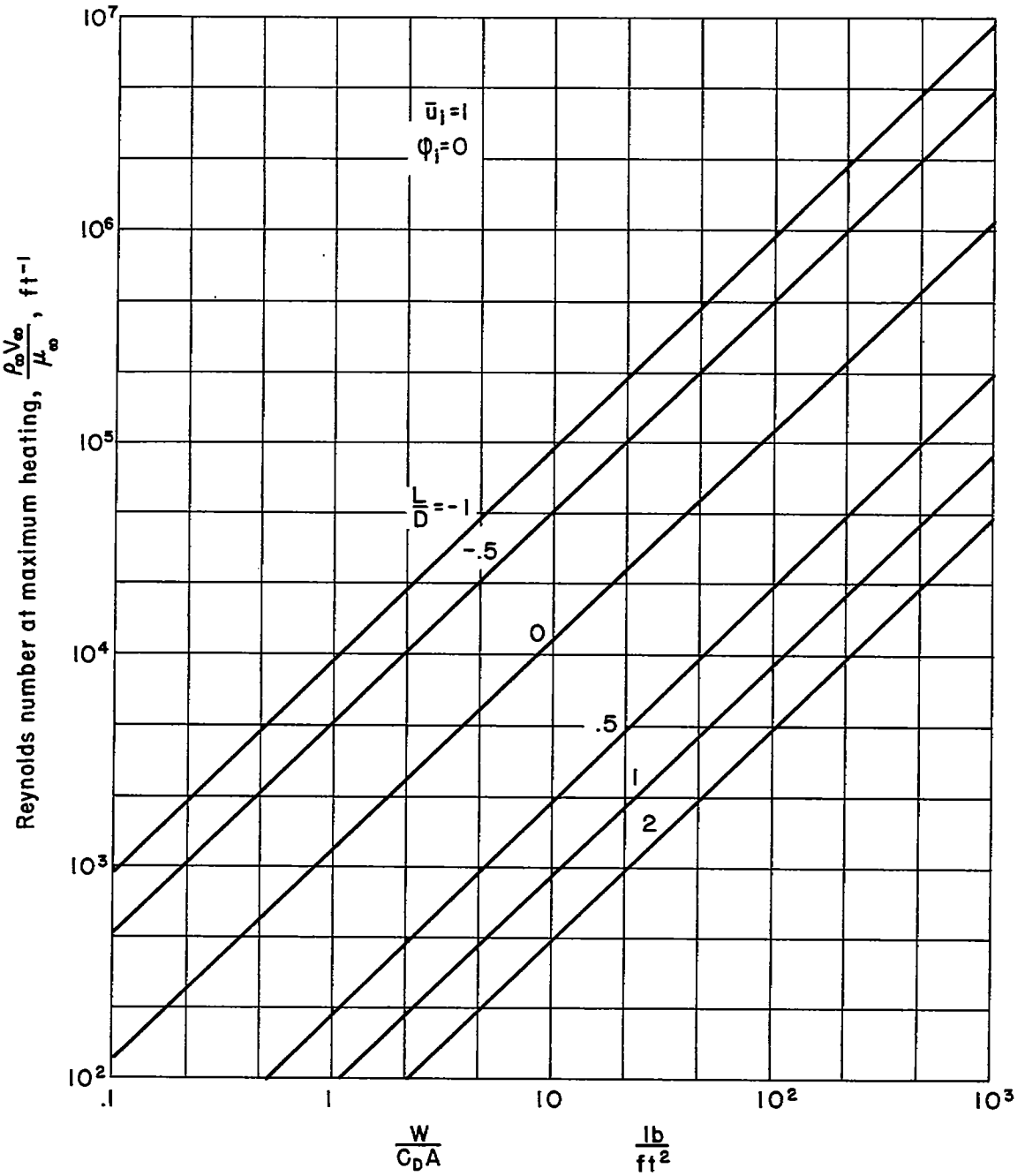

Figure 13.- Reynolds number at peak heating for entry from decaying orbits into Earth atmosphere.

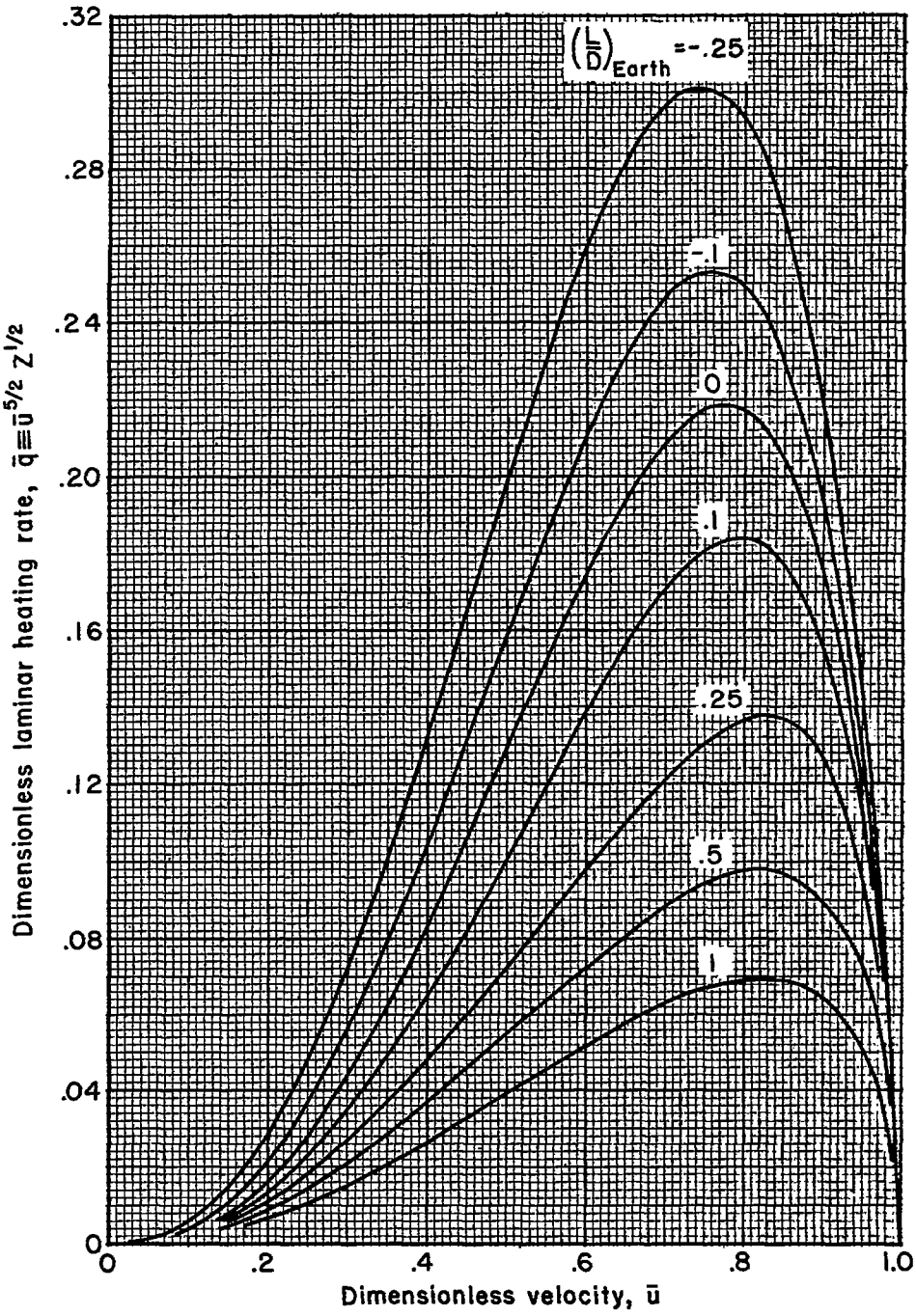

Figure 14.- Effect of lift-drag ratio on laminar heating rate for entry from decaying orbits.

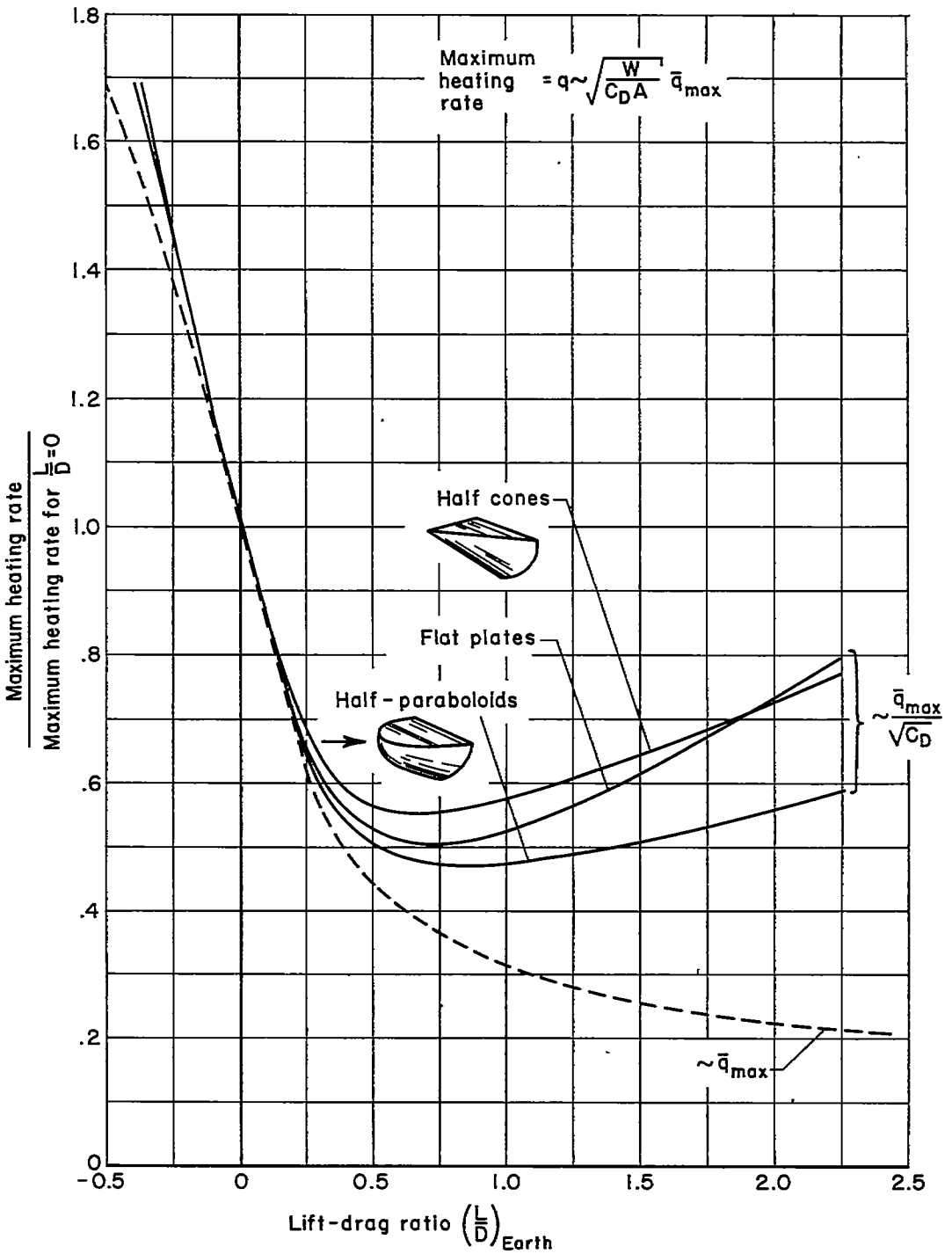

Figure 15.- Effect of lift-drag ratio on maximum laminar heating rate at stagnation point for entry from decaying orbits.

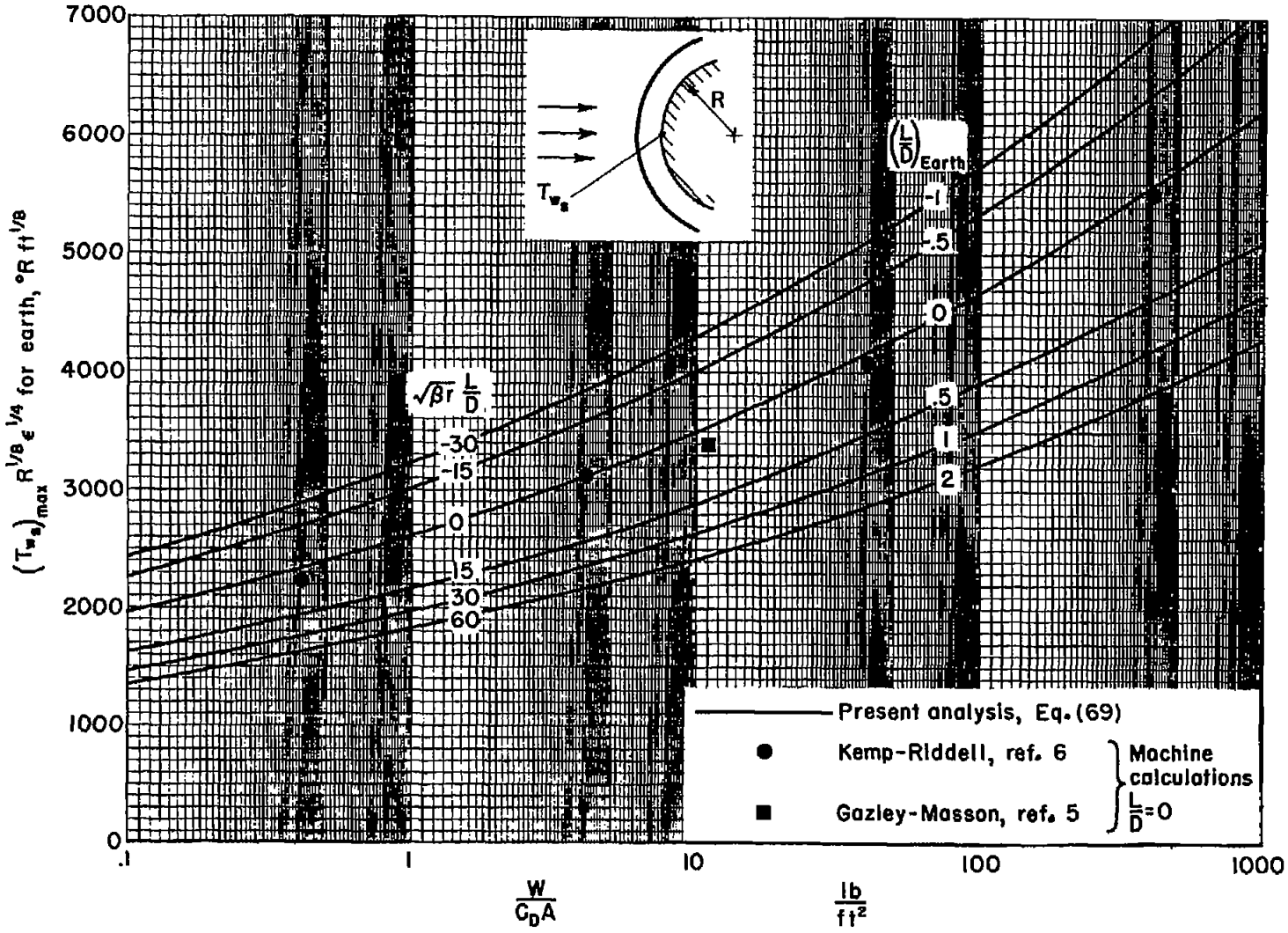

Figure 16.- Maximum radiation-equilibrium temperature at laminar stagnation point for entry from decaying orbits into Earth atmosphere.

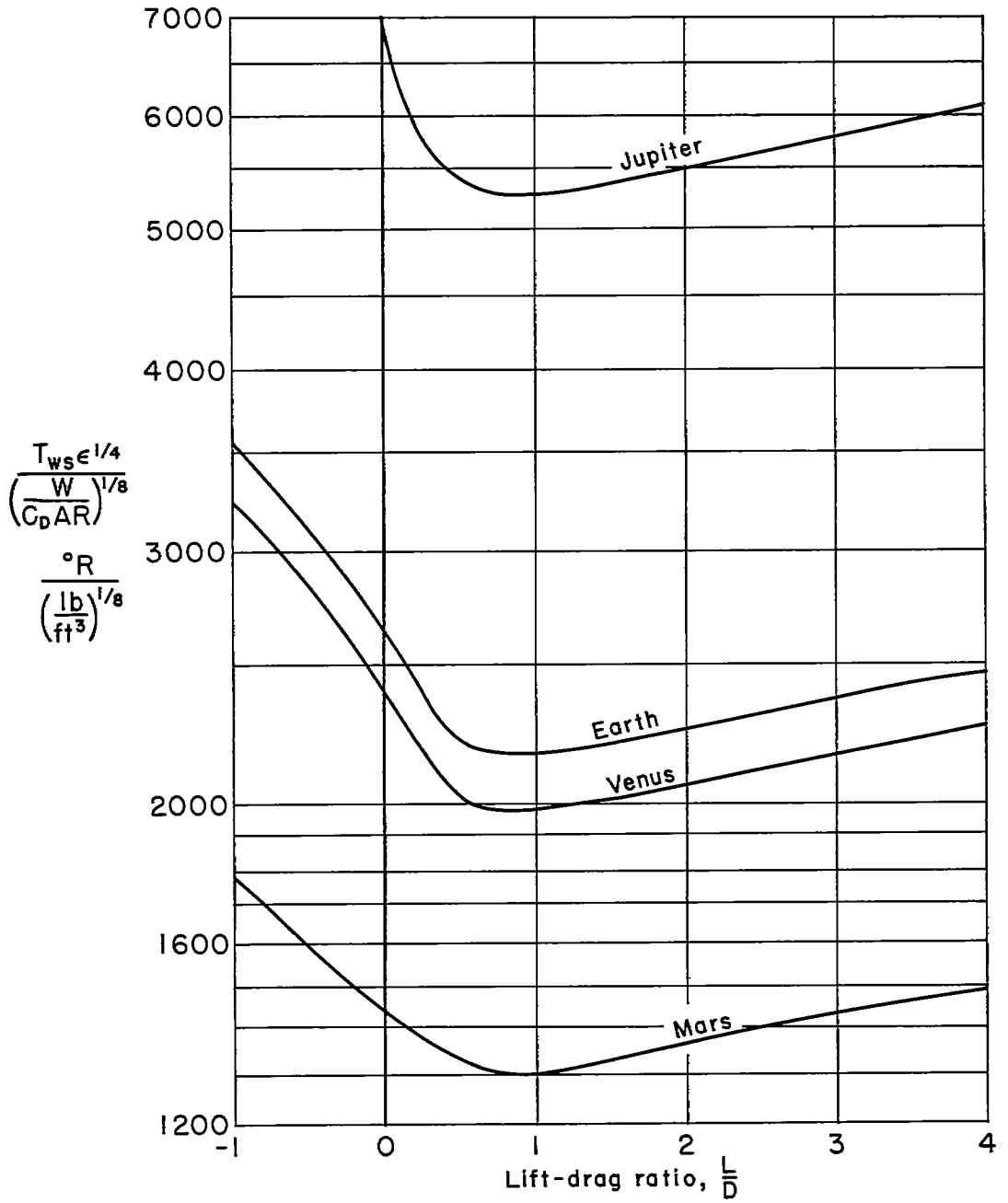

Figure 17.- Maximum surface temperature for entry into various planets from decaying orbits ($\bar{u}_i = 1$, $\varphi_i = 0$).

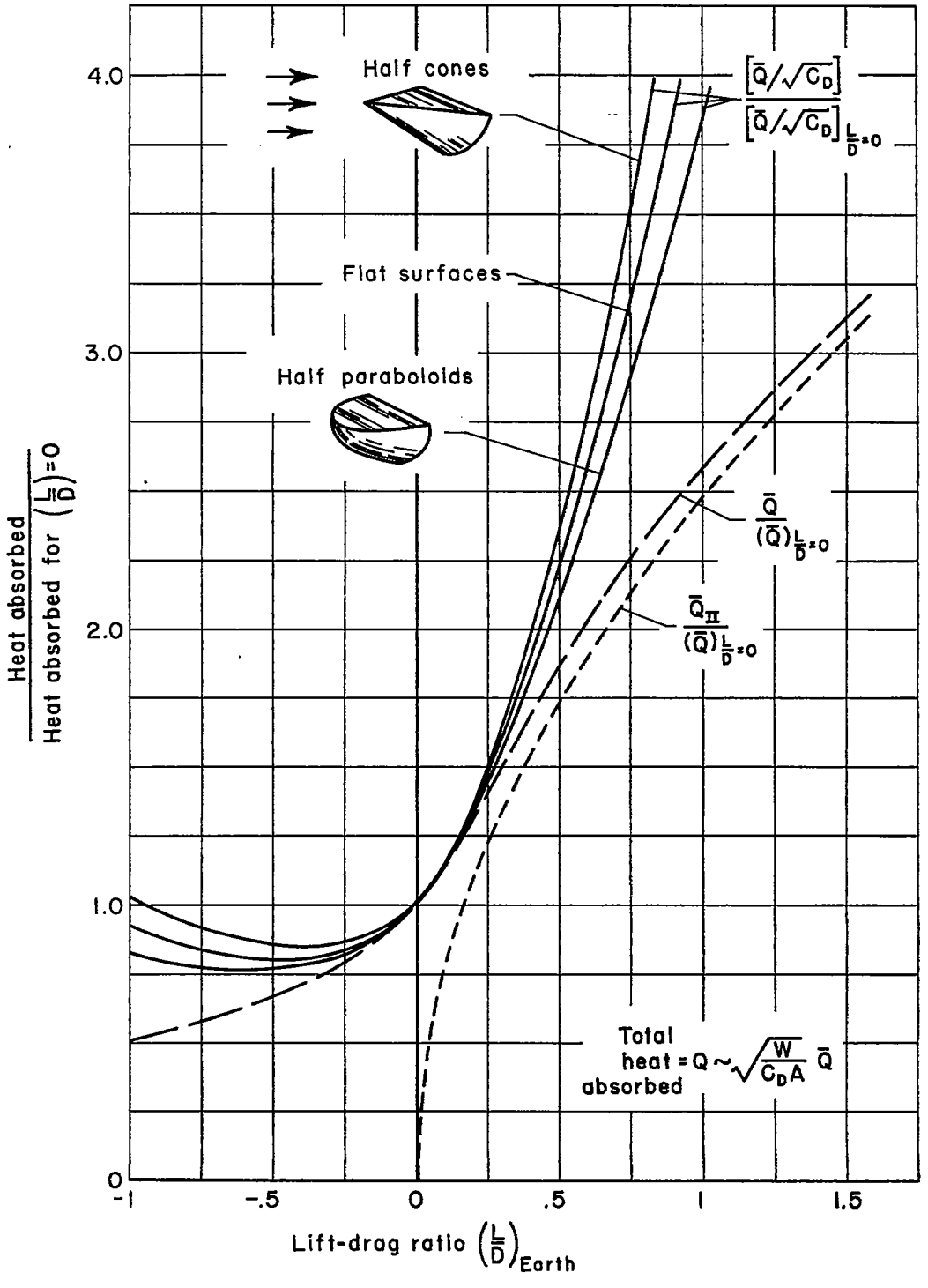

Figure 18.- Effect of lift-drag ratio on total heat absorbed during entry from decaying orbits into Earth atmosphere.

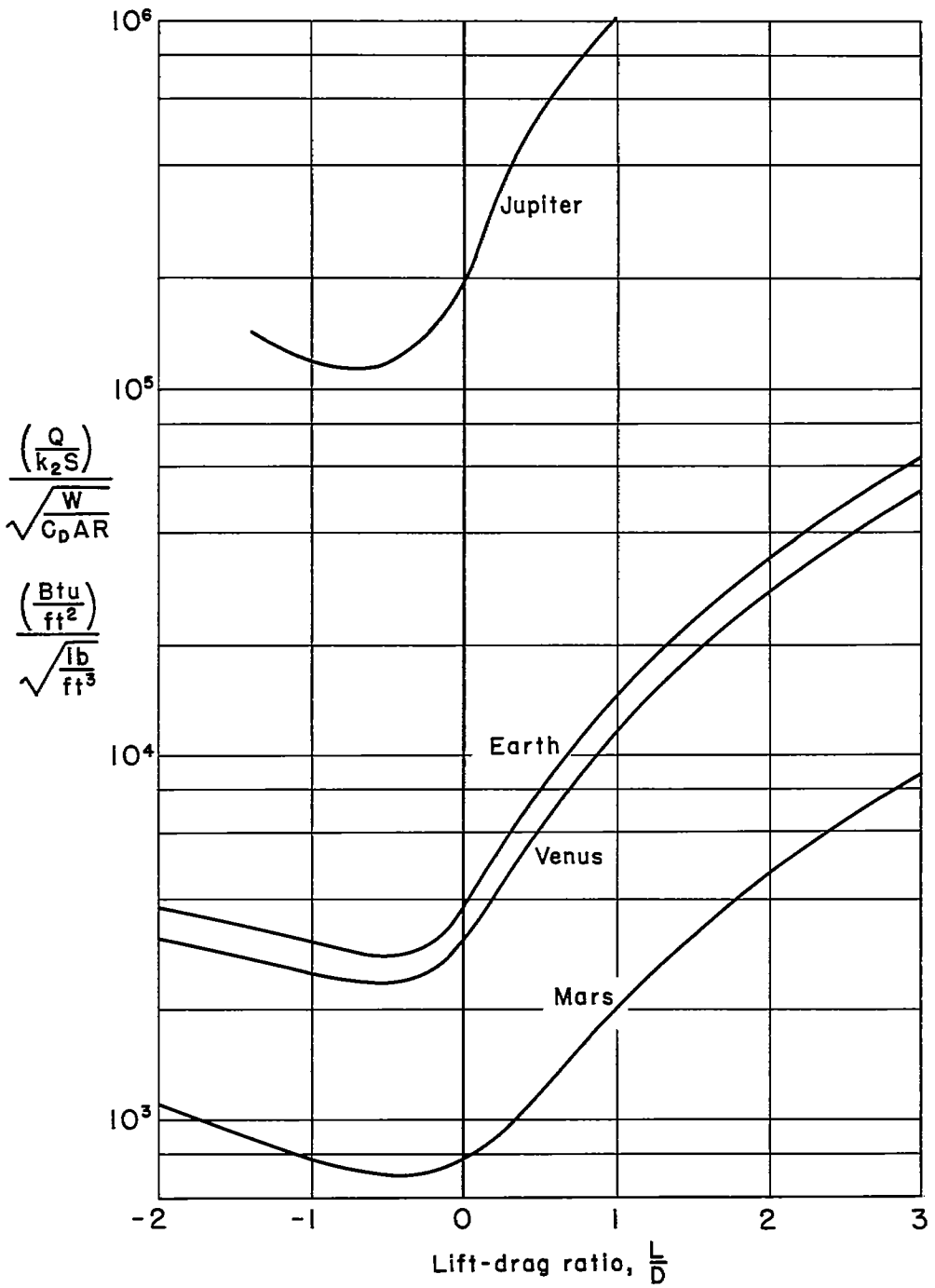

Figure 19.- Total heat absorbed during entry into various planets from decaying orbits ($\bar{u}_i = 1$, $\varphi_i = 0$).

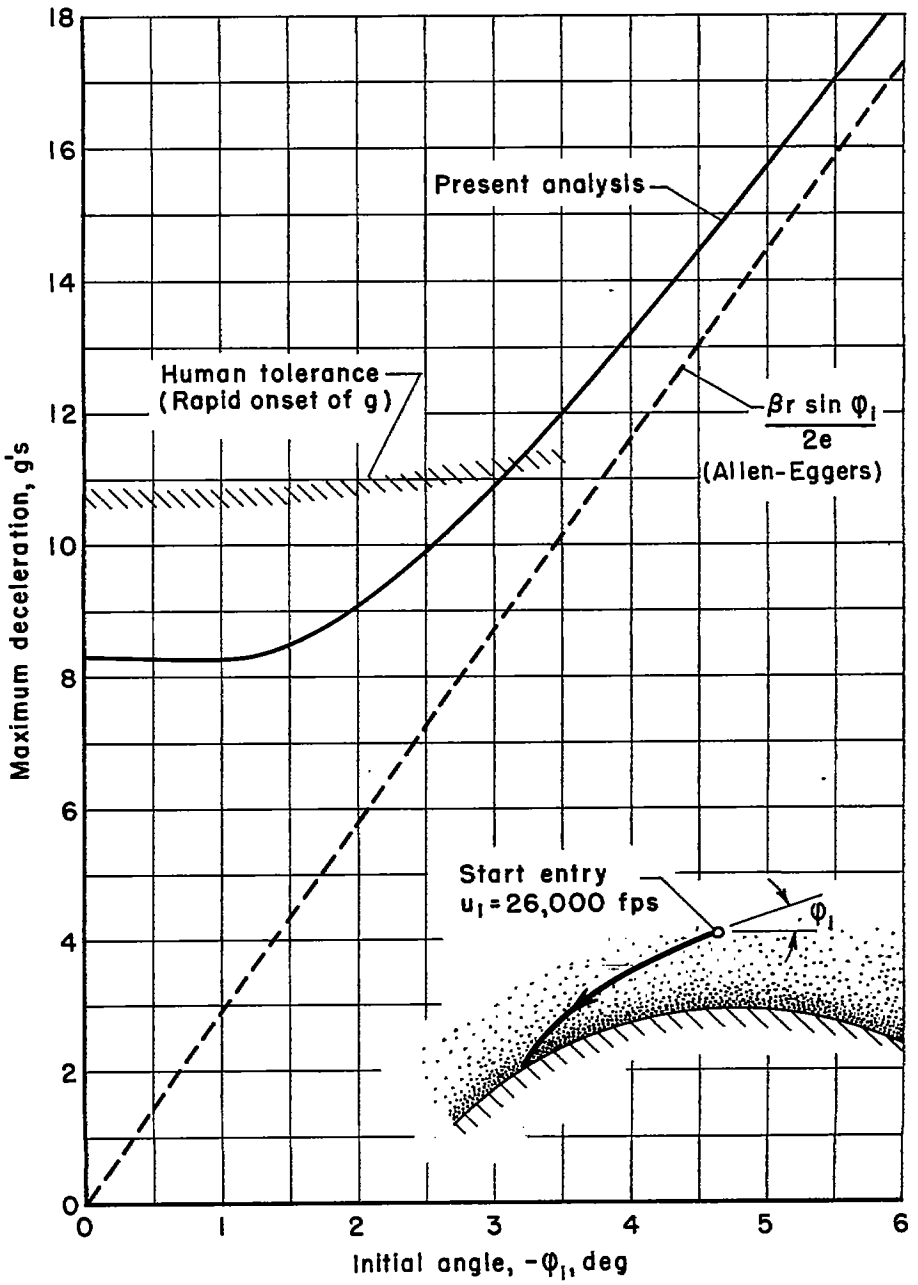

(a) Maximum deceleration.

Figure 20.- Effect of initial angle of entry on deceleration, laminar aerodynamic heating, and range of nonlifting vehicles.

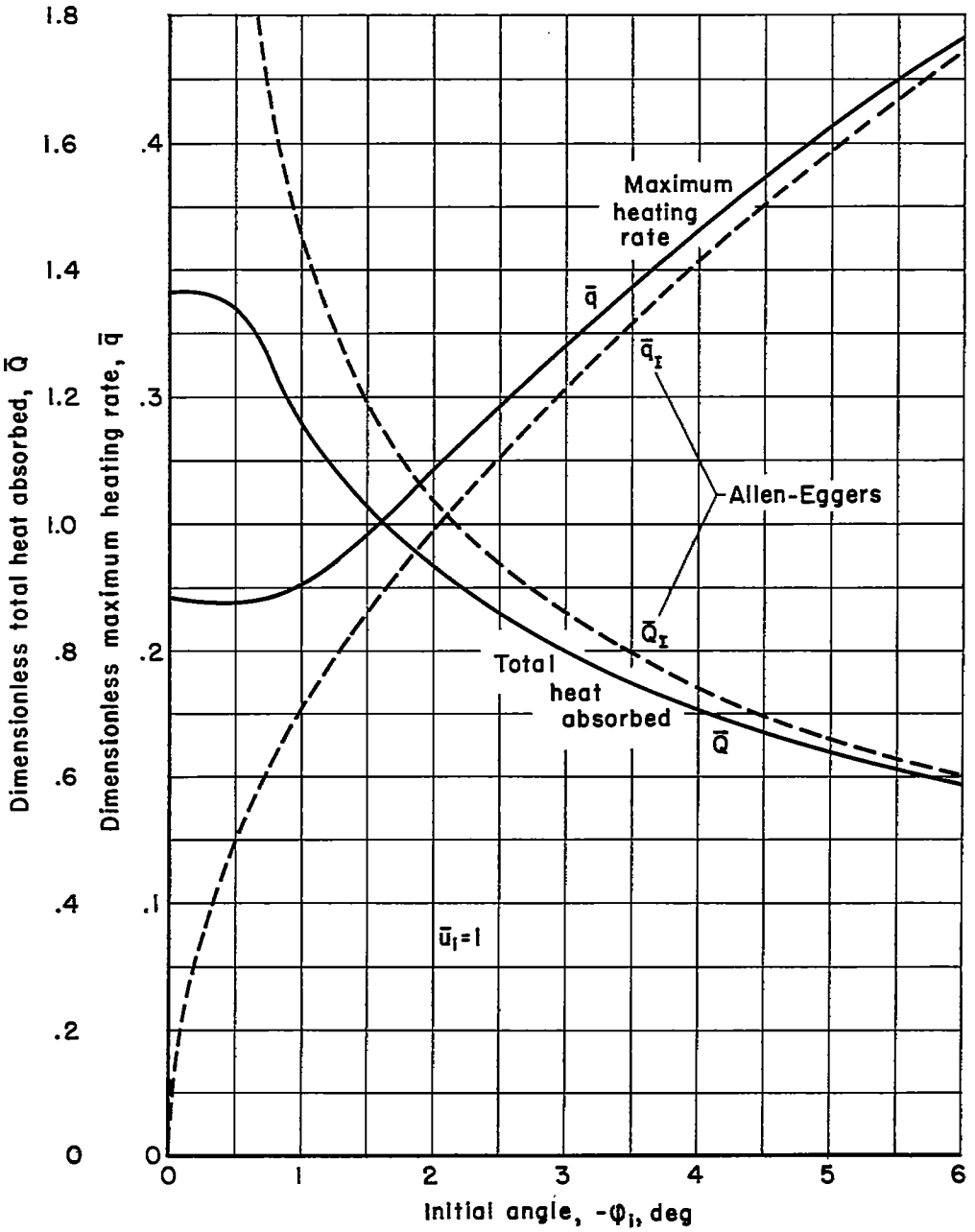

(b) Maximum laminar heating rate and total heat absorbed.

Figure 20.- Continued.

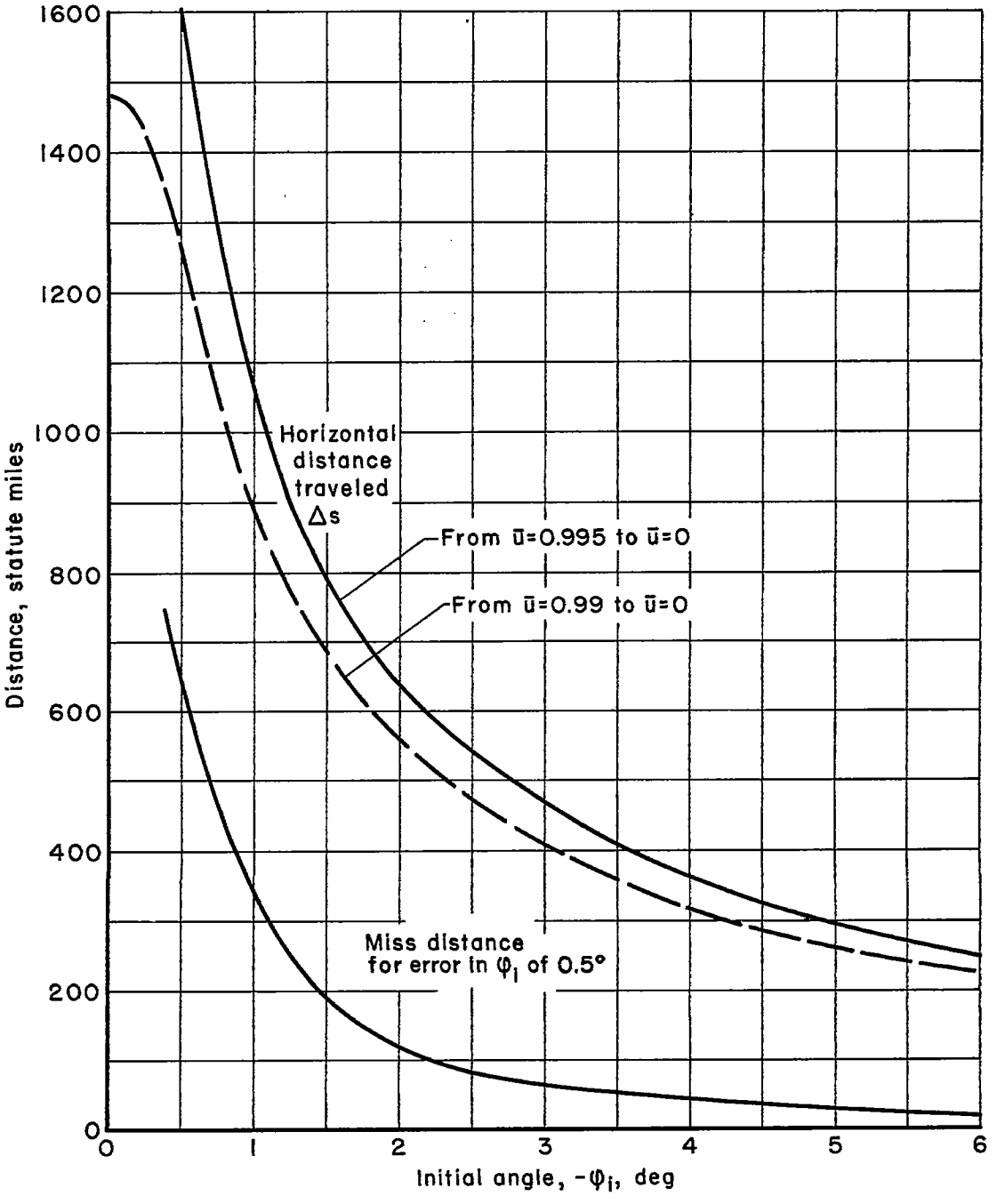

(c) Horizontal distance and horizontal miss distance.

Figure 20.- Concluded.

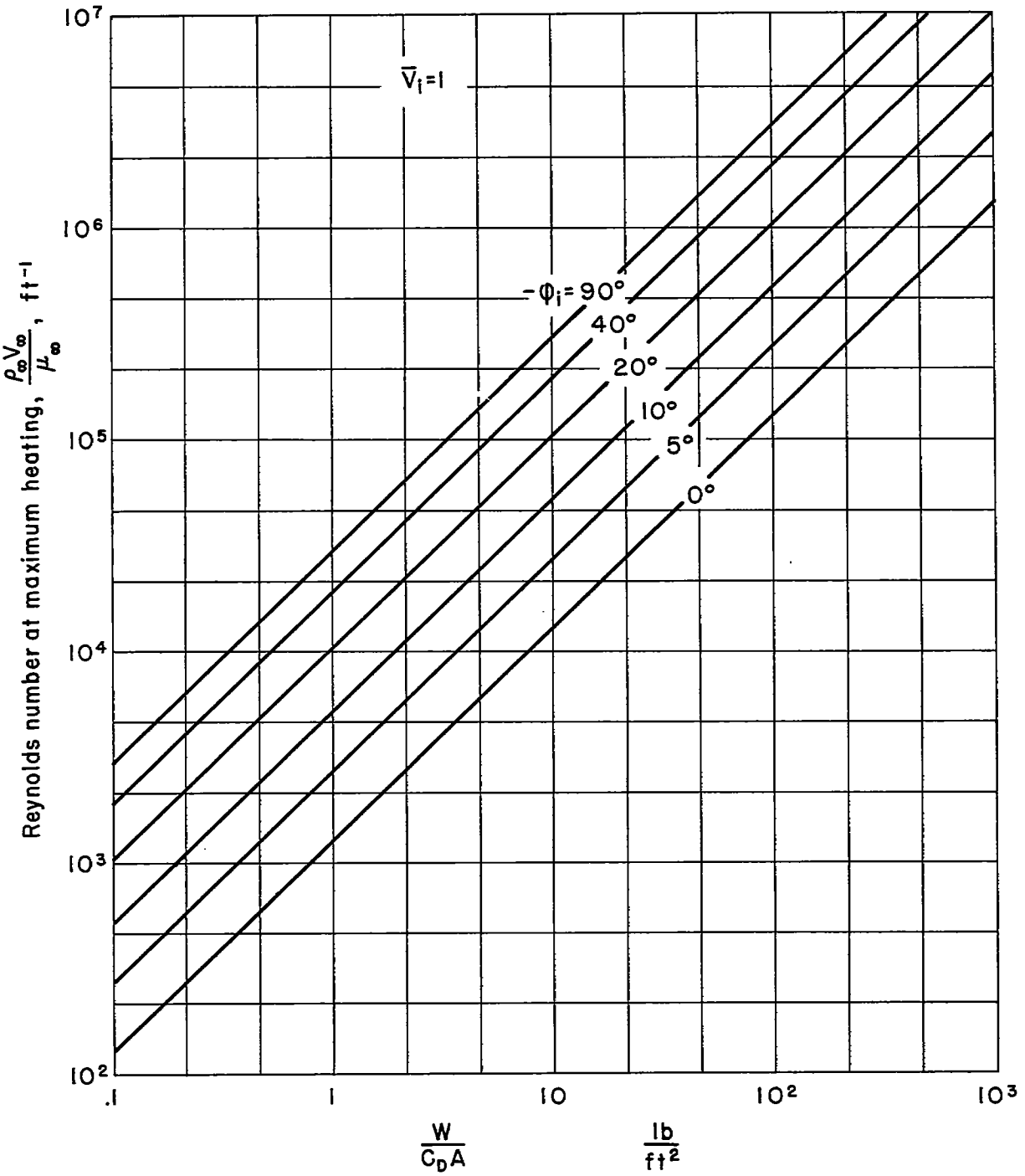

Figure 21.- Reynolds number at peak heating for nonlifting entry from deflected orbits into Earth atmosphere.

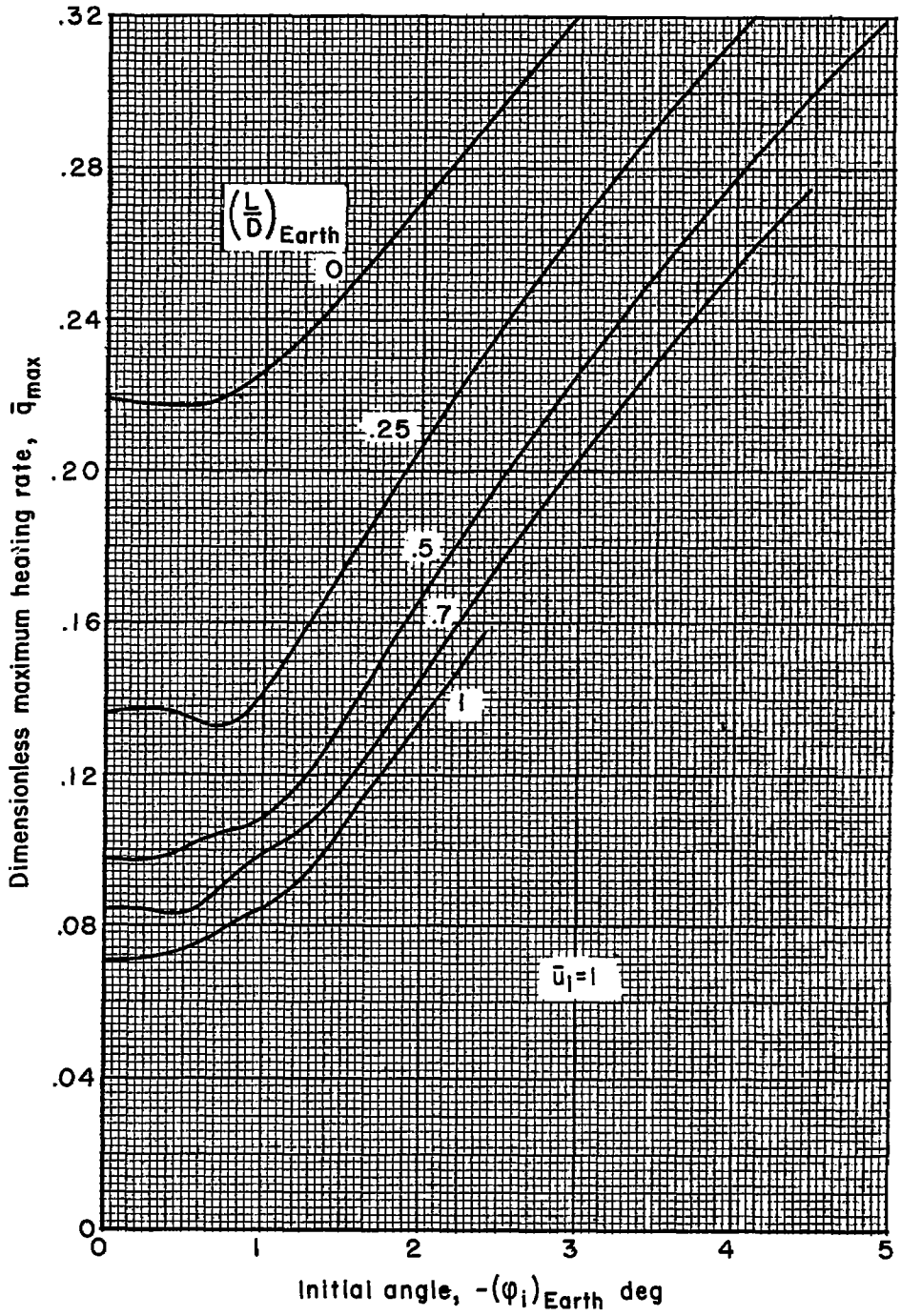

(a) Maximum laminar heating rate.

Figure 22.- Effect of initial angle of entry on laminar aerodynamic heating and range of lifting vehicles.

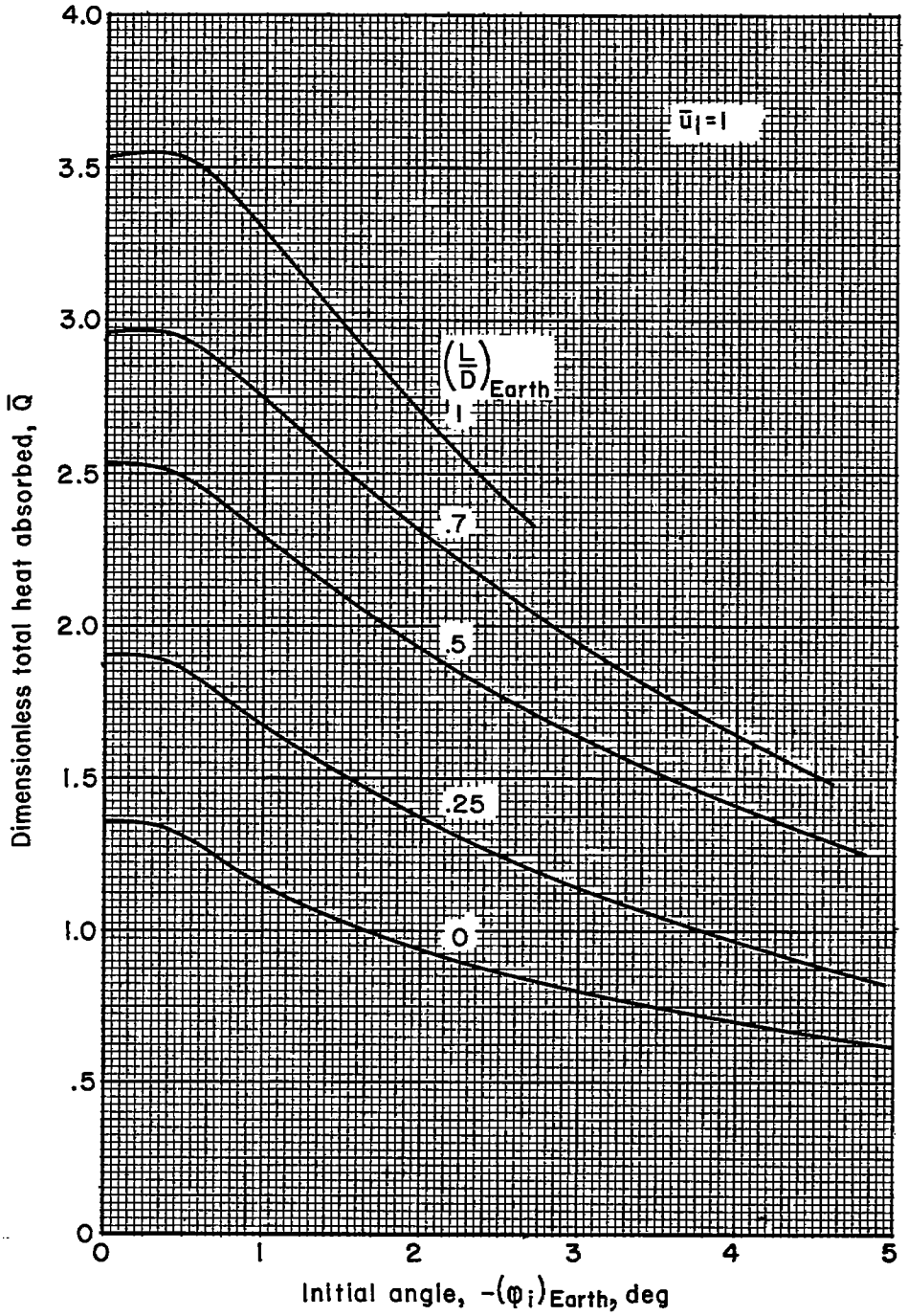

(b) Total laminar heat absorbed from $\bar{u} = 0.99$ to $\bar{u} \cong 0$.

Figure 22.- Continued.

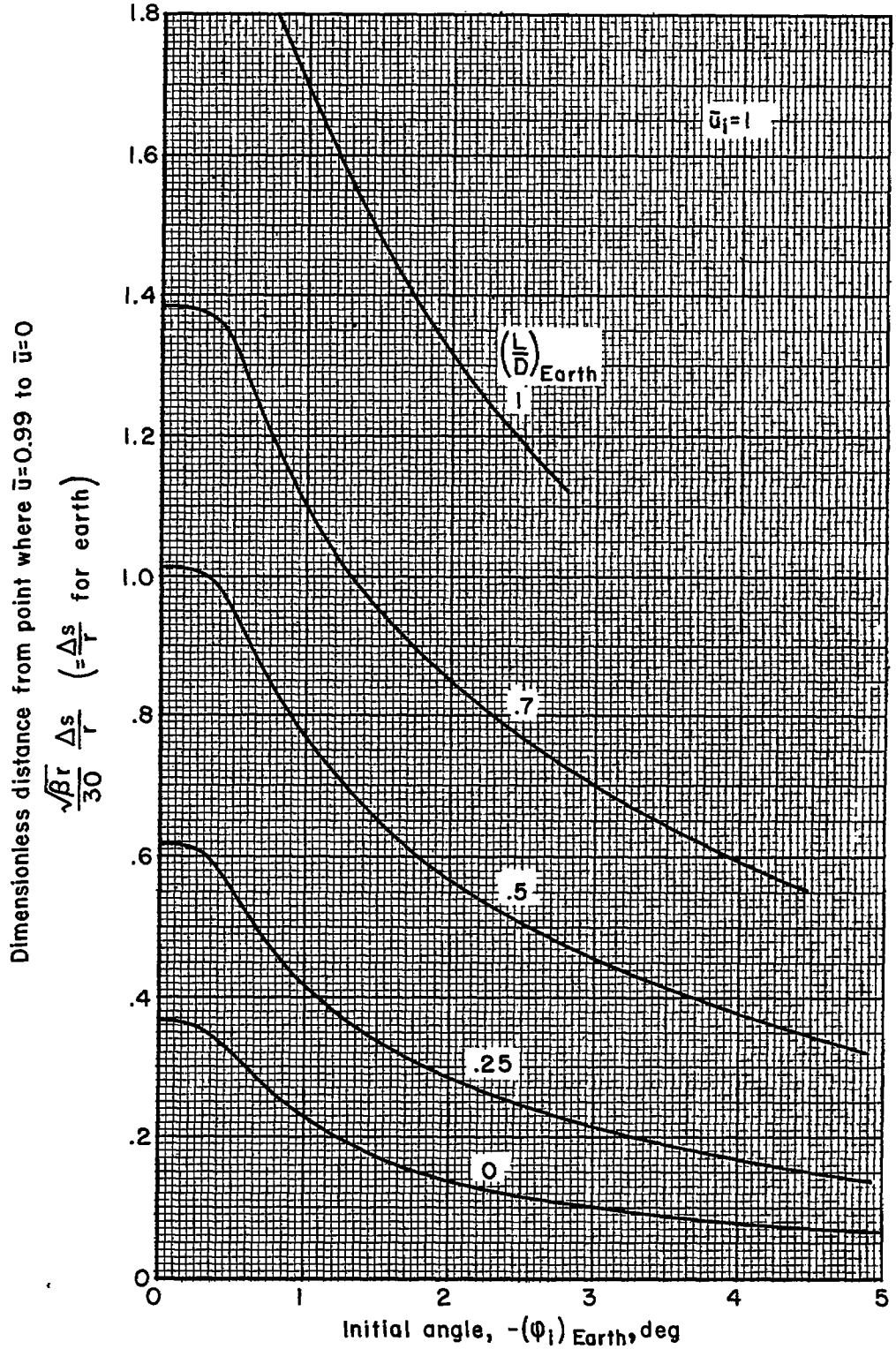

(c) Entry range from $\bar{u} = 0.99$ to $\bar{u} \cong 0$.

Figure 22.- Concluded.

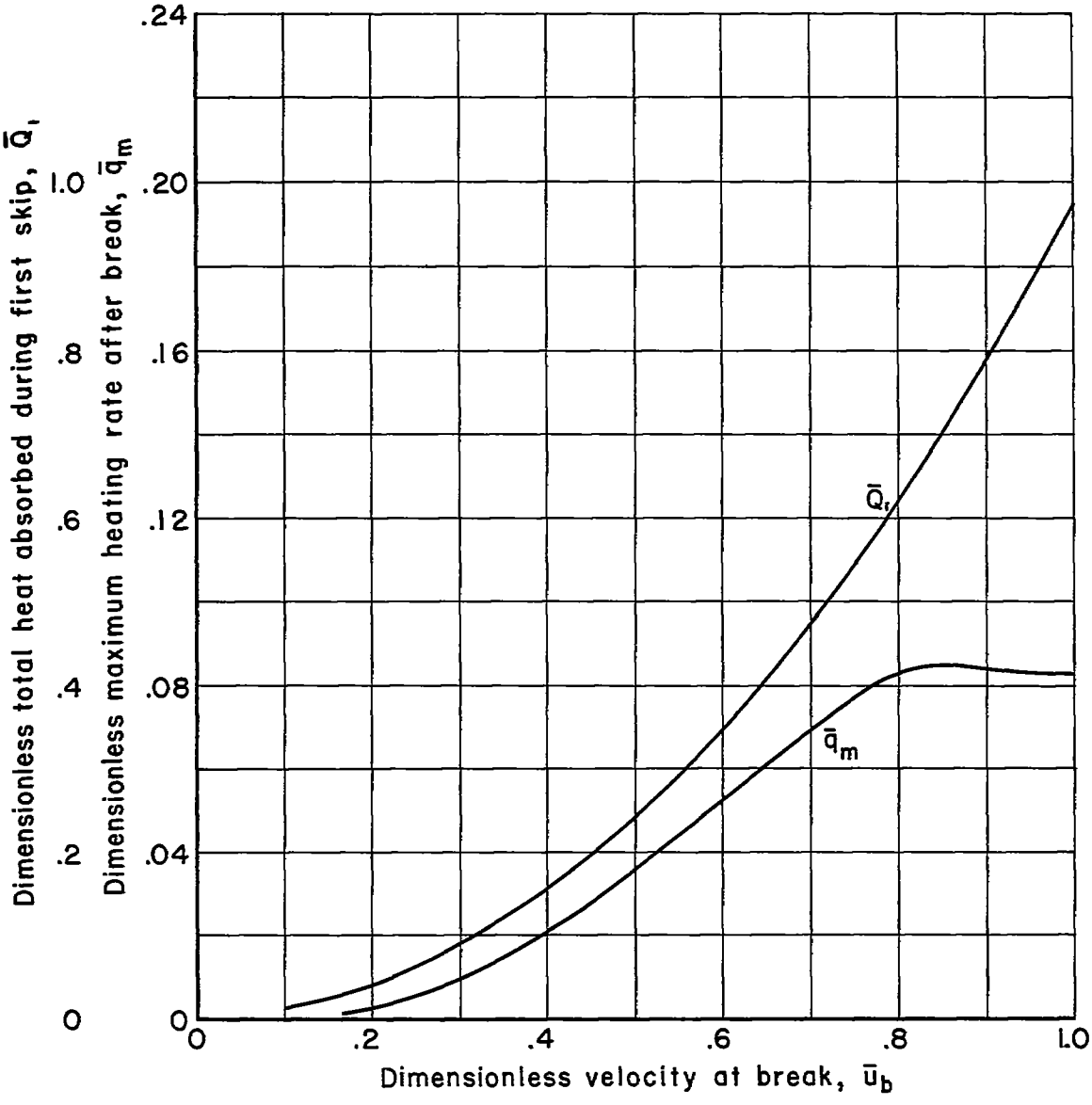

Figure 23.- Dimensionless maximum heating rate and total heat absorbed for a composite entry with $L/D = 0$ down to velocity $\bar{u}_b$, and then $L/D = 0.7$ thereafter.

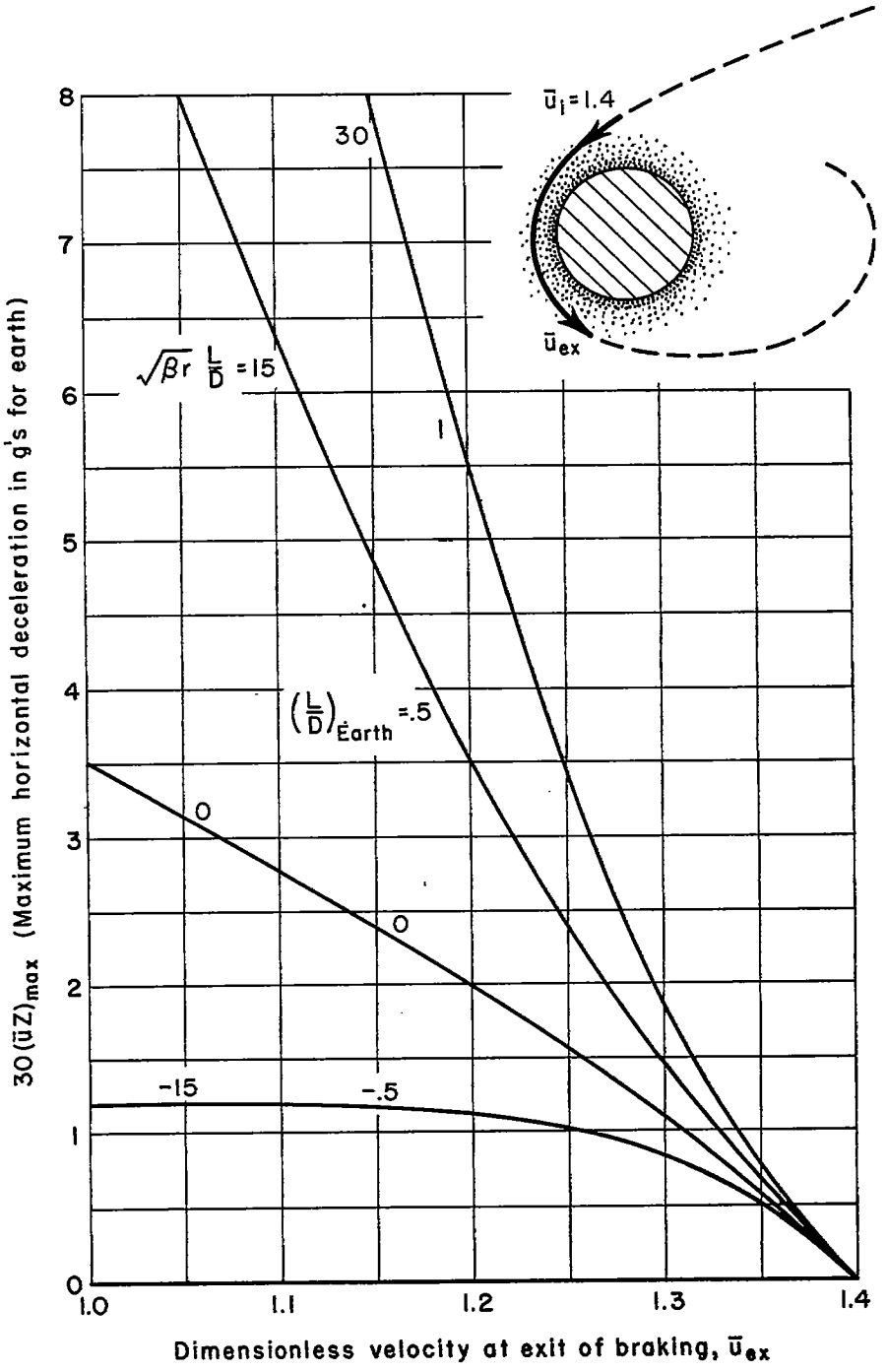

(a) Maximum horizontal deceleration.

Figure 24.- Atmosphere braking for single pass starting with $\bar{u}_i = 1.4$.

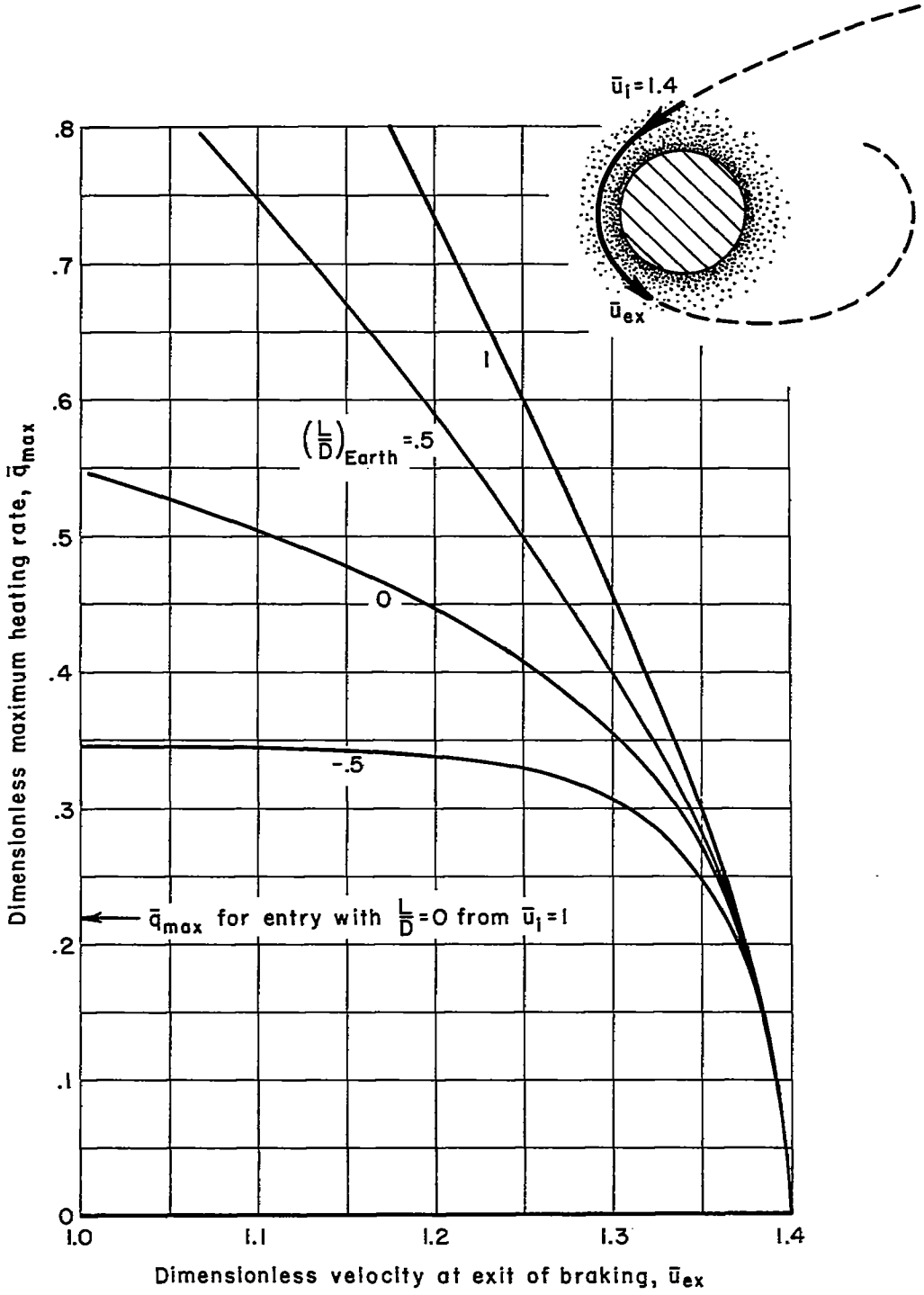

(b) Maximum heating rate.

Figure 24.- Continued.

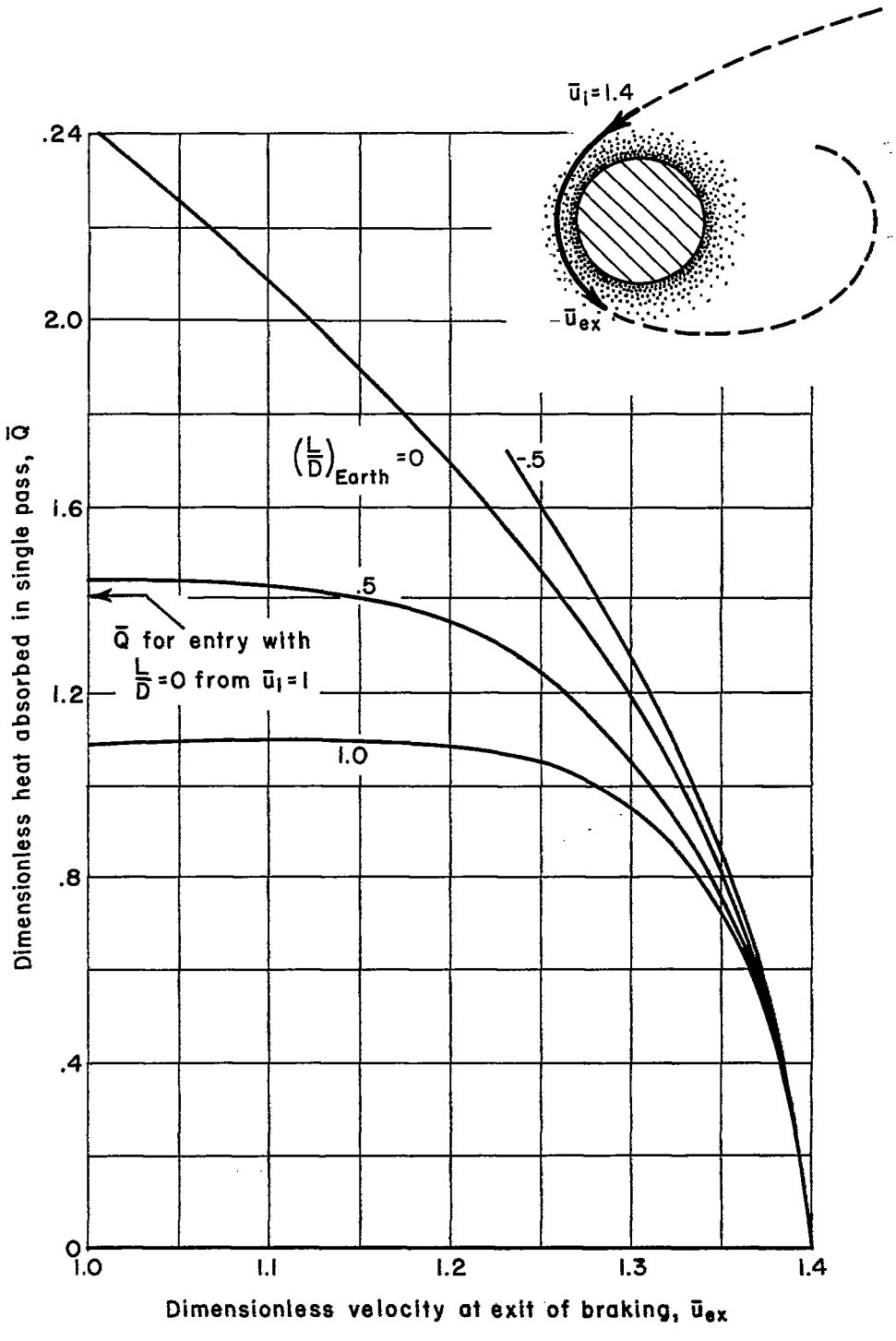

(c) Heat absorbed in single pass.

Figure 24.- Concluded.

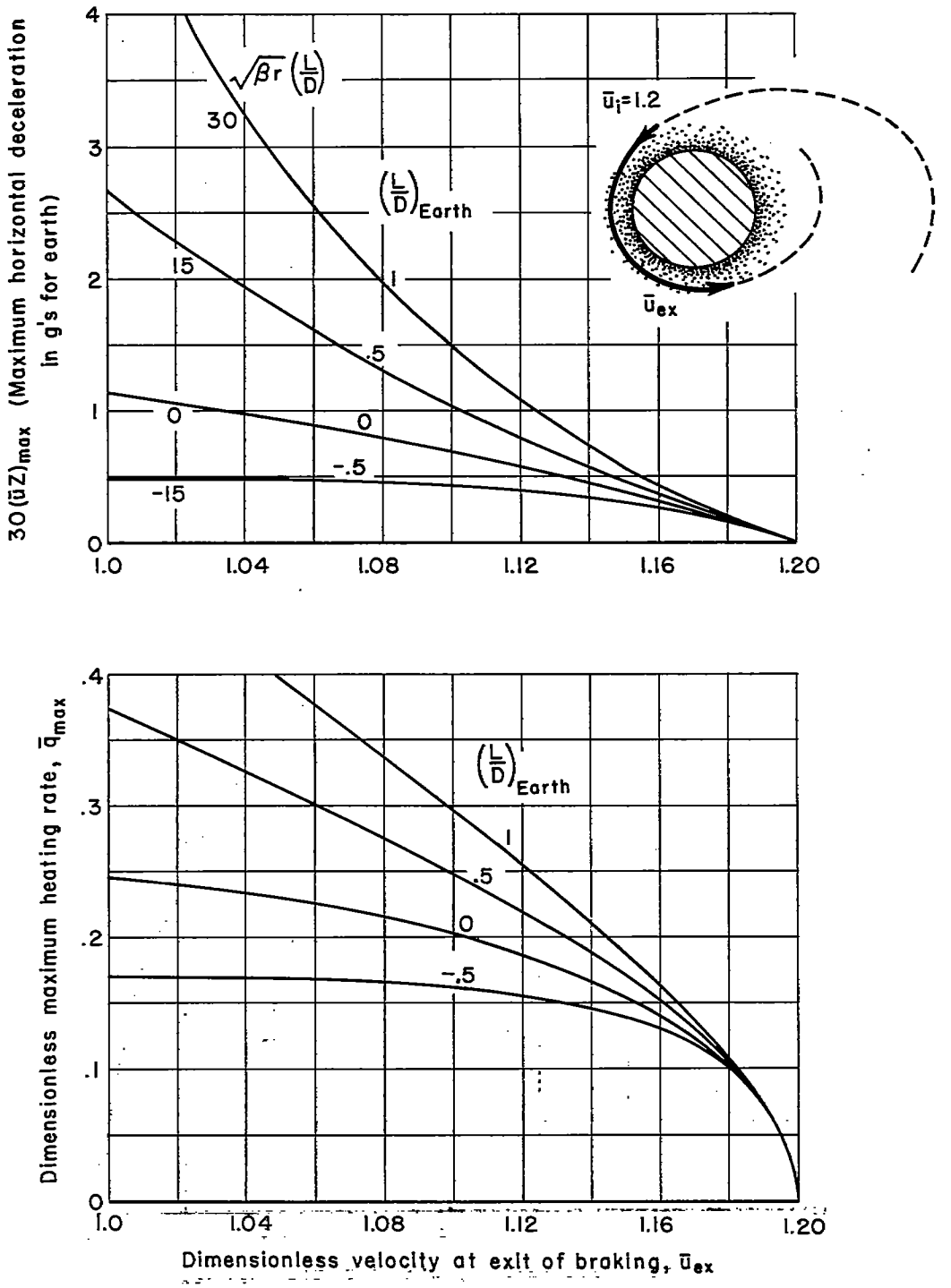

(a) Maximum horizontal deceleration and maximum heating rate.

Figure 25.- Atmosphere braking for single pass starting with $\bar{u}_i = 1.2$.

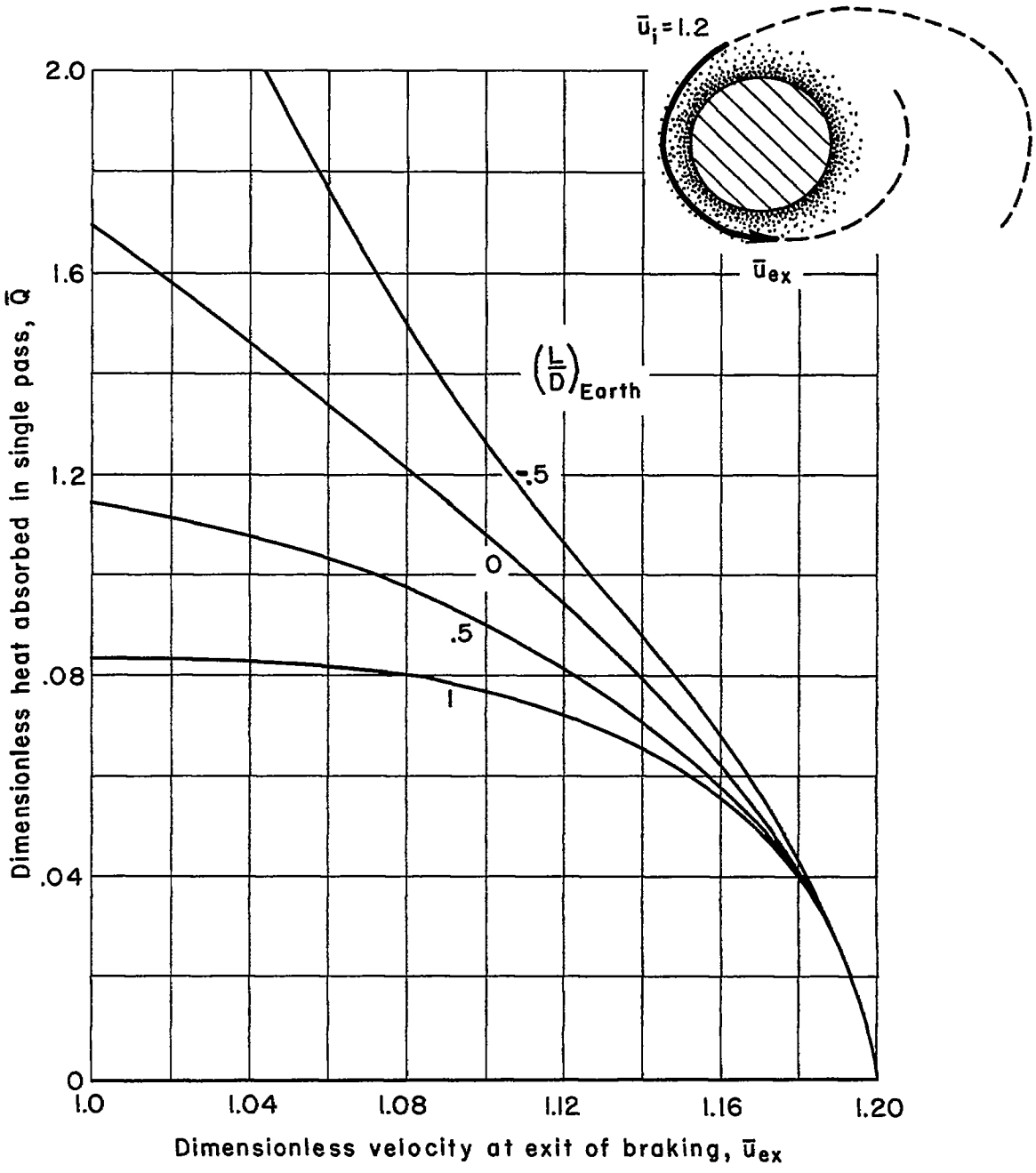

(b) Heat absorbed in single pass.

Figure 25.- Concluded.

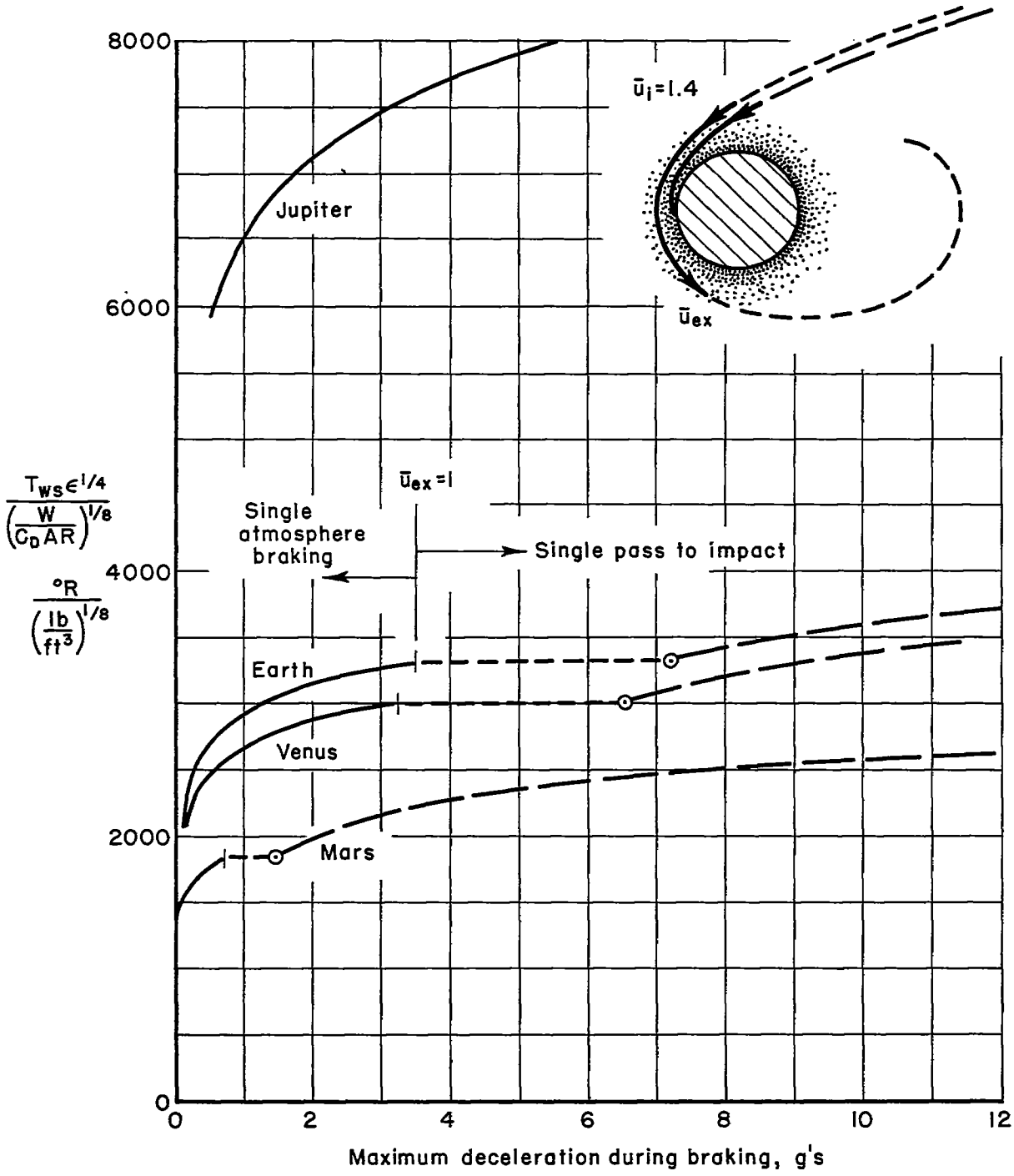

Figure 26.- Maximum temperature during single atmosphere braking pass starting with $\bar{u}_i = 1.4$.

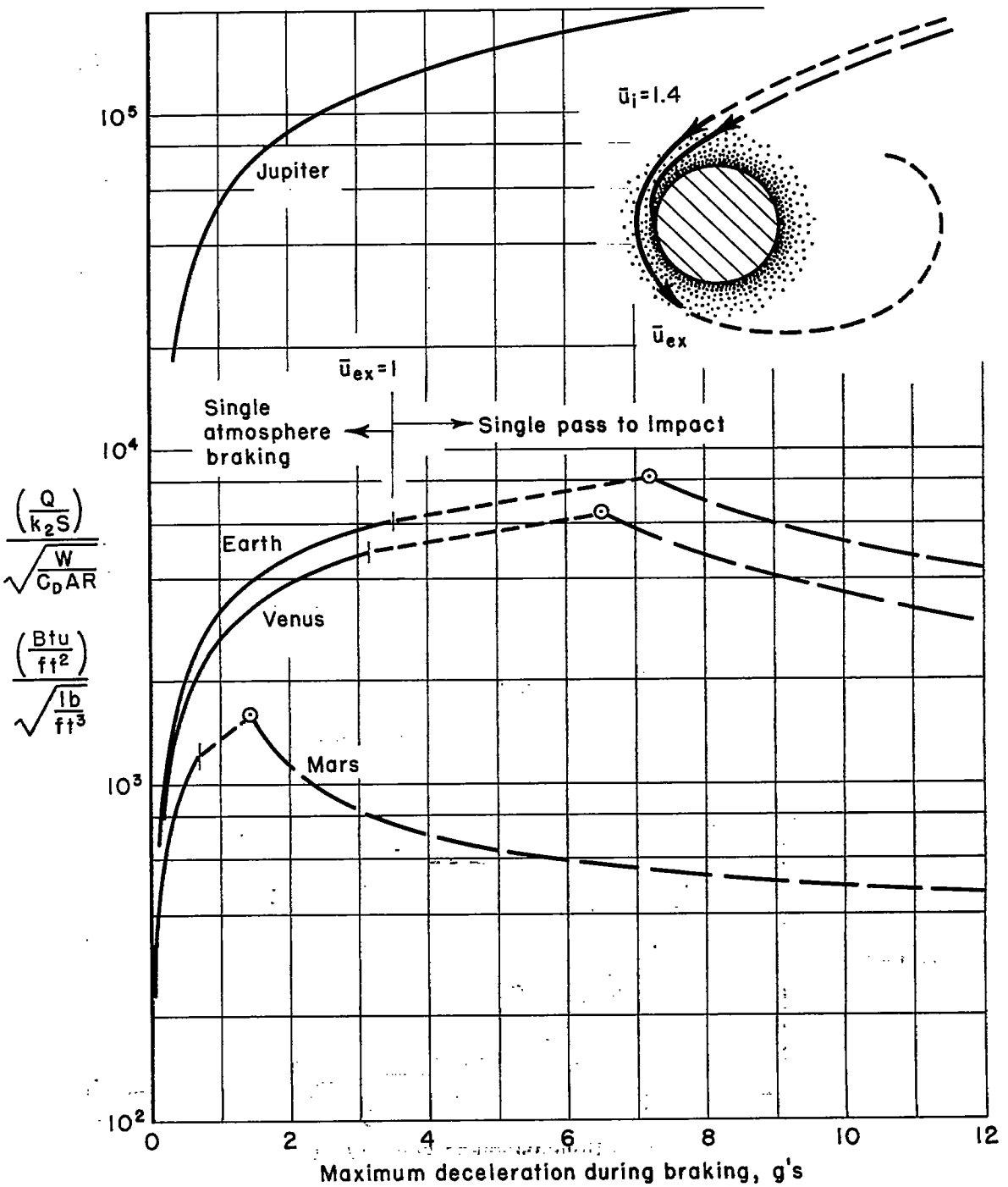

Figure 27.- Heat absorbed during single atmosphere braking pass starting with $\bar{u}_i = 1.4$.

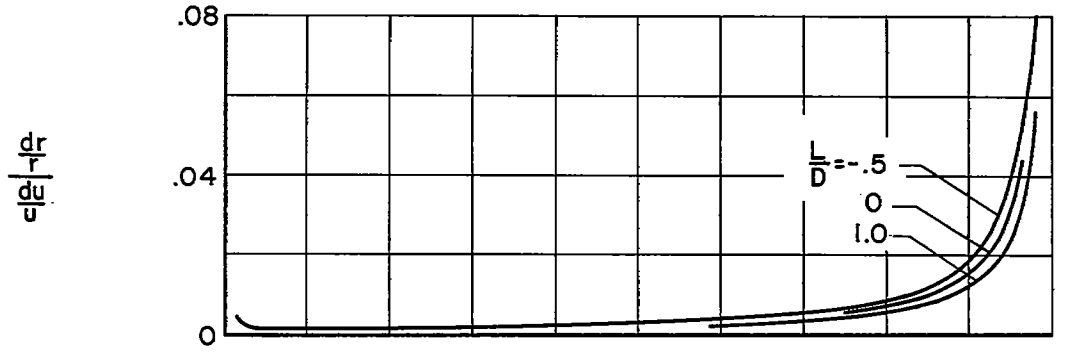

(a) Approximation (a) for various L/D.

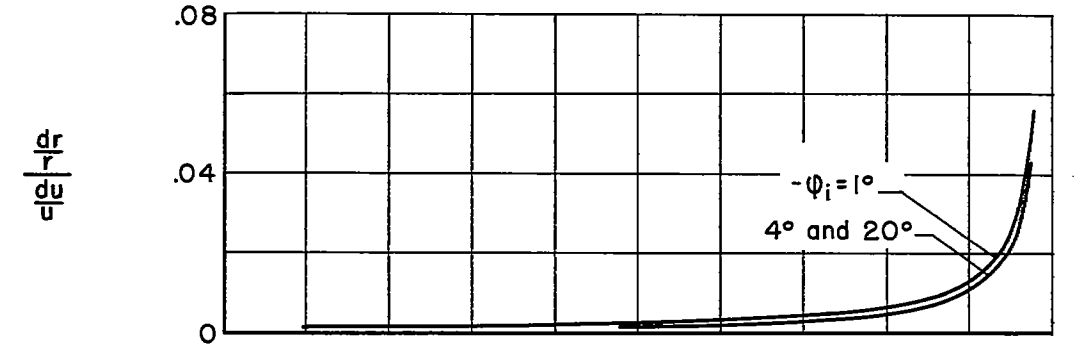

(b) Approximation (a) for various φ_i.

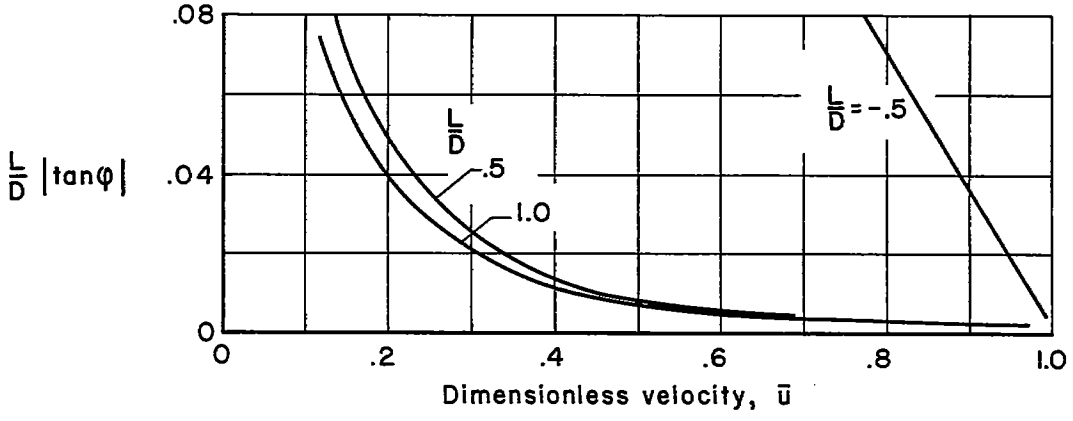

(c) Approximation (b).

Figure 28.- Check on approximations made in analysis.